DAM-RESERVOIR INTERACTION EFFECT ON THE SEISMIC RESPONSE OF CONCRETE GRAVITY DAMS

BY

MOHSEN GHAEMIAN AMIRKOLAI, B. Sc., M.Eng.

A Thesis

Submitted to the School of Graduate Studies

in Partial Fulfilment of the Requirements

for the Degree of

Doctor of Philosophy

McMaster University

DAM-RESERVOIR INTERACTION EFFECT ON THE SEISMIC RESPONSE OF CONCRETE GRAVITY DAMS

DOCTOR OF PHILOSOPHY (1997) McMaster University

(Civil Engineering) Hamilton, Ontario

Title: Dam-reservoir interaction effect on the seismic response of concrete gravity dams

Author: Mohsen Ghaemian Amirkolai,

B.Sc. Sharif University of Technology, Tehran, Iran.

M.Eng. McMaster University, Hamilton, Ontario, Canada.

Supervisor: Dr. A. Ghobarah

Number of pages: xxiv,194

TO MY FAMILY

ABSTRACT

A study was conducted to investigate the dam-reservoir interaction effect on the linear and nonlinear seismic response of concrete gravity dams. A mathematical approach was developed for the solution of the coupled dam-reservoir interaction problem which can be implemented in the nonlinear seismic analysis of concrete gravity dams. Two methods of staggered solution procedures are proposed for the dam-reservoir interaction. Using Routh-Hurwitz criteria, both methods are shown to be unconditionally stable when the two differential equations of the fluid and structure include damping terms. The staggered pressure method was modified for use when the equation of motion includes a lumped (diagonal) mass matrix.

A finite element program was developed to include the staggered solution schemes for seismic analysis of concrete gravity dams. The program considers the dam-reservoir interaction. The reservoir can be considered as infinite in which an appropriate boundary condition can be applied at the desired distance from the upstream face of the dam. The finite reservoir condition is also an option that can be included in the analysis. The effect of the travelling wave where nonuniform earthquake ground motion is applied to the boundary of the reservoir can be evaluated. The nonlinear analysis of the concrete gravity dam was considered based on nonlinear fracture mechanics crack propagation criterion.

Seismic response of a concrete gravity dam subjected to travelling seismic excitation

is investigated. The analysis is applied to the case of a gravity dam with infinite and finite reservoirs of different lengths to evaluate the effect of the travelling seismic wave on the dam crest displacement. Various wave speeds representing the speed of wave travel in the reservoir foundation, are used in the analysis. Earthquake waves are considered to travel in the upstream or the downstream directions.

The nonlinear seismic fracture response of the Pine Flat dam is investigated under the effect of reservoir interaction. Smeared crack analysis model based on a nonlinear fracture mechanics crack propagation criterion was used to study the cracking behaviour of a concrete gravity dam. The staggered method is used to solve the dam-reservoir interaction problem and results of the analysis were compared with the case when the added mass was used to represent the interaction effects.

An experimental program was conducted on small scale models of the concrete dam. A loading mechanism with two actuators was designed to apply four concentrated loads on the upstream face of the dam model. Dynamic load was applied cyclically by an actuator to represent the effects of the earthquake loadings. The static load which represent the hydrostatic pressure was kept constant. The material properties of the model was maintained the same as the prototype. In the proposed approach, the stress distribution at the top part of the dam model and prototype of the same material properties are found to be in close agreement.

ACKNOWLEDGEMENT

I would like to express my sincere appreciation to my supervisor Dr. A. Ghobarah for his guidance, assistance and encouragement at every stage of this research. I am deeply grateful for his effort on reviewing and making remarkable comments on the working draft of the thesis.

Financial support of the Ministry of Culture and Higher Education of Iran is greatly appreciated.

Special thanks are due to Dr. M. R. Kianoush and Dr. M. Dokainish, members of my supervisory committee, for their valuable comments and suggestions.

I would like to thank David Perrett, Peter Koudys and Moe Forget at Applied Dynamic Laboratory (ADL) at McMaster University for their assistance in completing the experimental work.

I am greatly indebted to Mr. M. H. Yassini for his support and concern throughout my graduate studies.

Above all, I wish to express my gratitude to my family for their unfailing support, love and encouragement.

TABLE OF CONTENTS

		Page
ABSTRACT		v
ACKNOWLEDGEMENT		vii
TABLE OF CONTENTS		viii
LIST OF TABLES		xiii
LIST OF FIGURES		xiv
LIST OF SYMBOLS		xix
CHAPTER ONE		
INTRODUCTION		
1.1	OVERVIEW	1
1.2	SEISMIC ANALYSIS OF CONCRETE DAMS	4
1.3	NONLINEAR ANALYSIS OF CONCRETE DAMS	8
1.4	EXPERIMENTAL STUDIES ON CONCRETE DAMS	10
1.5	OBJECTIVES OF THE RESEARCH	12
1.6	ORGANIZATION OF THE THESIS	12
CHAPTER TWO		
STAGGERED SOLUTION SCHEMES FOR DAM-RESERVOIR INTERACTION		
2.1	INTRODUCTION	16
2.2	THE COUPLED DAM-RESERVOIR PROBLEM	18

2.3 FINITE ELEMENT MODELLING OF THE RESERVOIR 19

2.4 TRUNCATED BOUNDARY AT THE FAR END OF THE RESERVOIR 22

2.5 COUPLING MATRIX OF THE DAM-RESERVOIR 24

2.6 TIME STEPPING SCHEME OF THE COUPLED EQUATIONS 27

2.7 STAGGERED DISPLACEMENT METHOD 29

2.8 STABILITY OF THE STAGGERED DISPLACEMENT METHOD 30

2.9 STAGGERED PRESSURE METHOD 35

2.10 STABILITY OF THE STAGGERED PRESSURE METHOD 36

2.11 MODIFIED STAGGERED PRESSURE METHOD 39

2.12 ACCURACY OF THE SOLUTION SCHEME 40

2.13 NUMERICAL RESULTS 40

2.14 CONCLUSIONS 43

CHAPTER THREE

TRAVELLING WAVE EFFECT ON THE RESPONSE OF CONCRETE GRAVITY DAMS

3.1 INTRODUCTION 52

3.2 APPROACH TO TRAVELLING WAVE EXCITATION 54

3.3 HYDRODYNAMIC FORCES ON RIGID DAMS 56

3.3.1 Horizontal Earthquake Ground Motion 58

3.3.2 Vertical Earthquake Ground Motion 60

3.4 TRAVELLING WAVE EFFECT ON THE DAM RESPONSE 61

3.4.1 Horizontal Earthquake Ground Motion 63

3.4.2 Vertical Earthquake Ground Motion 64

3.5 HYDRODYNAMIC FORCES ON FLEXIBLE AND RIGID DAMS 65

3.6 CONCLUSIONS 66

3.6.1 Effect of Travelling Wave on the Hydrodynamic Pressure Response 66

3.6.2 Effect of Travelling Wave on the Dam Crest Response 67

CHAPTER FOUR

NONLINEAR SEISMIC RESPONSE OF CONCRETE GRAVITY DAMS WITH DAM-RESERVOIR INTERACTION

4.1 INTRODUCTION 93

4.2 DISCRETIZATION OF THE COUPLED DAM-RESERVOIR EQUATIONS USING THE α-METHOD 100

4.3 FRACTURE MODEL 103

4.4 SEISMIC ENERGY BALANCE 103

4.5 NUMERICAL RESULTS 105

4.5.1 Linear Analysis 106

4.5.2 Nonlinear Analysis 107

4.6 CONCLUSIONS 110

CHAPTER FIVE

EXPERIMENTAL STUDY OF SMALL SCALE DAM MODELS

5.1 INTRODUCTION 122

5.2 DIMENSIONAL ANALYSIS AND SIMILITUDE REQUIREMENTS 127

5.3 EFFECT OF GRAVITY ON SMALL SCALE MODELLING 129

5.4 EXPERIMENTAL APPROACH 131

5.5 MODELLED DAM 133

5.6 TEST SET-UP AND INSTRUMENTATION 134

5.7 SUMMARY 137

CHAPTER SIX

BEHAVIOUR OF THE DAM MODEL

6.1 INTRODUCTION 151

6.2 TESTING PROGRAM 152

6.3 ANALYSIS 155

6.3.1 Effect of Gravity on the Dam Model 155

6.3.2 Static Response of the Model and Prototype 156

6.3.3 Dynamic response of the Dam-Reservoir System 157

6.4 CONCLUSIONS 158

CHAPTER SEVEN

CONCLUSIONS AND RECOMMENDATIONS

7.1	INTRODUCTION	173
7.2	CONCLUSIONS	173
7.3	RECOMMENDATIONS	176

REFERENCES 179

LIST OF TABLES

Table	Title	Page
5.1	Results of cylinder testing (MPa)	134
5.2	Characteristics of the actuators	135
5.3	Mechanical properties of Sikadur injection gel	136

LIST OF FIGURES

Figure	Title	Page
1.1	Organization of the thesis	15
2.1	Interface element on the dam-reservoir interaction boundary	44
2.2	Finite element model of the dam-reservoir system in example 1	45
2.3	Finite element model of the dam-reservoir system in example 2	46
2.4	First ten seconds of the horizontal component S00E of the May 18, 1940 Imperial Valley earthquake, El Centro record	47
2.5	Dam crest displacement	48
2.6	Hydrodynamic pressure time history near the bottom of the dam	49
2.7	Accuracy of the proposed method with different time steps in example 1	50
2.8	Accuracy of the proposed method with different time step in example 2	51
3.1	First ten seconds of the May 18, 1940 Imperial Valley earthquake, El Centro record	68
3.2	Finite element model of reservoir with rigid dam	69
3.3	Lateral force time history on the upstream face of the rigid dam (Horizontal ground motion, L/h=5)	70
3.4	Lateral force time history on the upstream face of the rigid dam (Horizontal ground motion, L/h=10)	71

3.5 Lateral force time history on the upstream face of the rigid dam (Horizontal ground motion, L/ h=15) 72

3.6 Lateral force time history on the upstream face of the rigid dam (Horizontal ground motion, v=±1500 m/sec., L/h=10) 73

3.7 Response parameters of the lateral force on upstream face of the rigid dam (Horizontal ground motion) 74

3.8 Lateral force time history on the upstream face of the rigid dam (Vertical ground motion, L/h=5) 75

3.9 Lateral force time history on the upstream face of the rigid dam (Vertical ground motion, L/h=10) 76

3.10 Lateral force time history on the upstream face the rigid dam (Vertical ground motion, L/h=15) 77

3.11 Comparison of lateral force time history on the upstream face the rigid dam (Vertical ground motion, L/h=5) 78

3.12 Response parameters of the lateral force on upstream face of the rigid dam (Vertical ground motion) 79

3.13 Finite element model of the dam-reservoir system 80

3.14 Comparison of the dam crest displacement 81

3.15 Dam crest displacement time history, (Horizontal ground motion, L/h=5) 82

3.16 Dam crest displacement time history, (Horizontal ground motion, L/h=10) 83

3.17 Dam crest displacement time history, (Horizontal ground motion, L/h=15) 84

3.18 Maximum dam crest displacement response under the horizontal earthquake 85

3.19 Dam crest displacement time history, (Vertical ground motion, L/h=5) 86

3.20 Dam crest displacement time history, (Vertical ground motion, L/h=10) 87

3.21 Dam crest displacement time history, (Vertical ground motion, L/h=15) 88

3.22 Maximum dam crest displacement response under the vertical earthquake 89

3.23 Hydrodynamic forces on flexible and rigid dams
(Horizontal ground motion, L/h=5) 90

3.24 Hydrodynamic forces on flexible and rigid dams
(Horizontal ground motion, L/h=10) 91

3.25 Hydrodynamic forces on flexible and rigid dams
(Horizontal ground motion, L/h=15) 92

4.1 Finite element model of the dam-reservoir system 111

4.2 First ten seconds of the horizontal S69E component of the July 21,
1952 Taft Lincoln earthquake, Kern County site record, 112

4.3 Dam crest displacement- linear analysis 113

4.4 Dam crest displacement- nonlinear analysis 114

4.5 Dam crest displacement response 115

4.6 Crack profiles of the Pine Flat dam including dam-reservoir interaction 116

4.7 Crack profiles of the Pine Flat dam using added mass 118

4.8 Energy response and energy balance error in the dam-reservoir interaction 120

4.9 Energy response and energy balance error in the added mass approach 121

5.1 Configuration of Pine Flat concrete gravity dam (Donlon and Hall, 1991) 139

5.2 Specimen wooden form 140

5.3 Maximum dynamic load distribution due to Taft earthquake record 141

5.4 Deflection of the dam due to distributed and concentrated loads (Case of hydrostatic and maximum load due to the Taft earthquake record) 142

5.5 Loading mechanism for static and dynamic loads 143

5.6 Loading mechanism 144

5.7 Attachment of U-shaped channel to the specimen 145

5.8 Test set-up 146

5.9 Dam model on foundation platform 147

5.10 Schematic view of MTS control unit connections 148

5.11 Location of the strain gages, displacement transducers and load cells on the dam model 149

5.12 Specimen instrumentation 150

6.1 Distribution of applied static load in the first test 159

6.2 Variation of base strain in the first test 160

6.3 Strain variation at different locations in the first test (strain × 10^6) 161

6.4 Applied static and dynamic loads in the second test 162

6.5 Variation of base strain and displacement in the second test 163

6.6 Crest displacement in the second test 164

6.7 Strain variation at different locations in the second test (strain × 10^6) 165

6.8 Variation of base strain in the third test 166

6.9 Crest displacement in the third test 167

6.10 Strain variation at different locations in the third test (strain × 10^6) 168

6.11 Comparison of strains obtained from experiment and finite element analysis static load=-70 kN, dynamic load=100 kN 169

6.12 Comparison of strains obtained from experiment and finite element analysis static load=-70 kN, dynamic load=-100 kN 170

6.13 Maximum principal tensile stress contours obtained from finite element analysis using proposed experimental approach, MPa static load=-70 kN, dynamic load= ±100 kN 171

6.14 Maximum principal tensile stress contours (MPa) obtained from dynamic analysis of the prototype under the Taft earthquake ground motion scaled to PGA of 0.242g, (Hydrostatic pressure=0.69735 full hydrostatic pressure) 172

LIST OF SYMBOLS

a_0, a_1, a_2, a_3 and a_4	coefficients of the characteristic equation
$a_n(x,y,t)$	component of acceleration on the boundary along the direction of the inward normal n
A	area of the finite element
A^m	area of the model at the base
c	equivalent of [C] in SDF system
[C]	damping matrix of the structure
c′	equivalent of [C'] in SDF system
[C']	damping matrix of the reservoir
[D]	matrix representing truncation of the far end boundary of the reservoir
e	a superscript refers to the element on the dam-reservoir interface
E	modulus of elasticity
ED	the viscous damping energy
EE	stored elastic energy
EF	energy dissipated due to fracture EF (EF= ER-EE)
EH	work done by the hydrodynamic pressure
EI	input energy EI
EK	absolute kinetic energy

EP	work of pre-seismic applied force
EQ	absolute seismic input energy is EQ
ER	nonlinear restoring work
fx_i and fy_i	forces at node i of the interface element along the global X and Y coordinates, respectively
f'_c	compressive strength of concrete
f_{sp}	tensile strength of concrete (obtained from split cylinder test)
$\{f_1\}$	vector of body force and hydrostatic force
$\{f\}^e$	force vector of an interface element
$\{F\}$	vector defined in equations (2.6) and (2.9)
$\{F_1\}$	vector defined in equation (2.1)
$\{F_2\}$	vector defined in equation (2.2)
$\{FF_1\}$	component of the force vector due to acceleration at the boundaries of the dam-reservoir and reservoir-foundation
$\{FF_2\}$	component of the force vector due to truncation at the far boundary
F_d	hydrodynamic lateral force
F_s	hydrostatic lateral force
g	equivalent of [G] in SDF system
[G]	mass matrix of the reservoir
h	height of the reservoir
h^m	base length of the model

[H]	matrix of coefficients $=[G]+\beta\Delta t^2[K']+\gamma\Delta t[C']$
i	time interval
I	force response parameter
k	equivalent of [K] in SDF system
[K]	stiffness matrices of the structure
k′	equivalent of [K'] in SDF system
[K']	stiffness matrix of the reservoir
L	reservoir length
Li	limestone powder
ℓ^e_T	side of the element on the truncated boundary
m	equivalent of [M] in SDF system
M	mineral oil AK-10
[M]	mass matrix of the structure
n	reservoir unit inward normal vector
N_i	element shape function of the structure at node i
N_i^f	shape function of the fluid at node i of the interface element
P	plaster binder
Pb	lead powder
P^m	weight of the model
P(x,y,t)	hydrodynamic pressure in excess of hydrostatic pressure
{P}	vector of hydrodynamic pressures

$\{P\}^e$	hydrodynamic pressure vector of an element on the dam-reservoir interface
$\{P\}_{i+1}$ and $\{P\}_{i+1}$	vectors defined in equation (2.27) and (2.28)
$\{P\}^*_{i+1}$	vector defined in equation (2.47)
$\{P\}^p_{i+1}$,	
$\{U\}^p_{i+1}$ and $\{U\}^p_{i+1}$	defined in equations (2.25), (2.26) and (2.28)
q	equivalent of [Q] in SDF system
[Q]	coupling matrix
$[Q]^e$	coupling matrix of an element on the dam-reservoir interface
r	an index that represents the ratio of the parameters in the prototype and model
R	rubber crumbs
s	prescribed length along the boundary of the elements
S	stress (or pressure)
t	time in second
T	total time of the earthquake ground motion
u and v	displacements along the global X and Y coordinates of the interface element
u_i and v_i	displacements at node i of the interface element along the global X and Y coordinates, respectively
U_n	values of the normal displacement along the element interface

$\{U\}$	vector of displacements
$\{U\}_{i+1}$ and $\{U\}_{i+1}$,	vectors defined in equation (2.25) and (2.26)
$\{\ddot{U}_g\}$	vector of ground acceleration
$\{\ddot{U}\}^*_{i+1}$	vector defined in equation (2.31)
v	earthquake wave velocity
V	velocity of pressure wave in water
W	mixing water
x, y	cartisian coordinates
X, Y	global coordinates
z	z-transformation of $\mu=(1+z)/(1-z)$
α, β and γ	parameters of integrations
Δt	time increment
ϵ	strain
η and β	absolute values of the normal vector on the boundary in the global directions of X and Y, respectively
θ	slope of the far boundary of the reservoir
$\{\delta\}$	displacement vector of an interface element
μ	scalar used in equations (2.35) and (2.36)
ρ	mass density
σ_g	stress due to the gravity term
σ_{ng}	stress due to the non-gravity term (external loading)

σ^{true}	true value of the stress at the base
σ^{expl}	extrapolated value of the stress at the base
σ^{m} and σ^{mg}	total stress and stress due to gravity in the model

CHAPTER ONE

INTRODUCTION

1.1 OVERVIEW

Earthquake analysis of concrete dams has received much attention from researchers during the past decade because of concern for dam safety during earthquakes. Before the development of dynamic analysis procedures, the traditional design of dams used equivalent horizontal static load to represent the earthquake effects (Chopra, 1987). The design criteria allowed no tensile stresses in the dam with a safety factor against overturning moment and a safety factor for shear resistance to sliding.

The development of the finite element technique and its application to the seismic analysis of concrete dams generated extensive research in this area. The problem of seismic analysis of dams is fairly complex due to the dam-reservoir-foundation interaction and the nature of the boundary effects. The complexity of the subject has made it both attractive and challenging for researchers.

The early modelling of dams approximated the dam-water interaction using Westergaard's added mass representation (Westergaard, 1933). This procedure is applicable to the case of concrete dams of vertical upstream face with infinite reservoir length. A closed

form solution was developed for the reservoir for the case of gravity dams with infinite reservoir length (Hall and Chopra, 1982; Fenves and Chopra, 1984b). In this case, the equation of the reservoir can be solved to obtain the pressure at the upstream face of the dam. Then, the calculated pressure is included as an applied force in the finite element model of the dam structure.

The finite element modelling of the reservoir involves the truncation of the of the infinite reservoir. The truncation effect in the finite element model of the reservoir was investigated by several researchers (Hall and Chopra, 1979; Sharan, 1986 and 1987; Tsai and Lee 1990). The idea was to find a proper transmitting boundary condition that can absorb the outgoing wave at the truncated far end of the reservoir. Based on the method of analysis which could be in the time or the frequency domains, the boundary conditions may differ. Implementation of the transmitting boundary in the finite element model of the reservoir simplified the model and made the three dimensional analysis of dams possible. Most of the seismic analysis modelling of concrete gravity dams has been two dimensional and applied to a single monolith. This assumption is realistic for the case of concrete gravity dams with straight or grouted contraction joints. The assumption is also valid for keyed contraction joint in case of severe ground motion. The case of arch dams requires a rigorous 3-D analysis of the structure.

In seismic analysis of concrete dams, the input earthquake ground motion is assumed uniform. This assumption may not be realistic given the large size of the dam-reservoir system. Due to the limited speed of the seismic wave travel, the dam-reservoir system will be subjected to different ground motions. Ground motion is also affected by coherency and

local site conditions. Spatial variation of the earthquake ground motion mainly affects the hydrodynamic pressure on the upstream face of the dam. Few researchers studied the effect of finite velocity of the wave propagation on the hydrodynamic pressure on dams (Flores Victoria et al., 1969). The analytical method implemented to obtain the hydrodynamic pressure is capable of considering vertical earthquake excitations. Using the finite element method for the reservoir fluid with proper analysis for dam-reservoir system, it is possible to consider different wave velocities for the horizontal and vertical components of the earthquake. The flexibility of dams may be an important parameter in their response when subjected to travelling earthquake waves. The reservoir length affects the dam response for the case of finite reservoir length. The effect of travelling wave has not been studied in the case of finite reservoir length.

Recently most of the research in the seismic analysis of dams has been directed towards the nonlinear response of concrete gravity dams. The concept of fracture mechanics is used in nonlinear analysis of the dams by either smeared crack approach or discrete crack approach. Different constitutive models were used to monitor the crack propagation in dams when subjected to earthquake loading (Bhattacharjee and Leger, 1992). In nonlinear seismic response analysis of concrete gravity dams, several parameters are normally used. The values of these parameters remain to be measured. There is a shortage of data on the nonlinear seismic behaviour of the dam concrete material. The nonlinear analysis of arch dams is mainly concerned with modelling the opening and closing of the joints (Kuo, 1982; Fenves et al., 1992). There is a need for a nonlinear constitutive model which can properly represent 3-D behaviour of concrete. In most of the nonlinear analysis approaches, an added mass is

used to represent the reservoir interaction effects on the dam. Nonlinear analysis of concrete gravity dams indicates that dam-reservoir interaction is an important effect that must be included in the analysis. A major concern of researchers is that the developed sophisticated nonlinear analysis tools have not been subjected to verification by actual response data. This is due to the lack of data measurements of the actual performance of dams during earthquakes and the difficulty by which simple small scale tests are conducted. Representative modelling of concrete dams in small scale experimental study is extremely difficult. Nevertheless, portrait of some aspects of the model behaviour may represent a specific case of performance of the actual dam.

1.2 SEISMIC ANALYSIS OF CONCRETE DAMS

The dam-reservoir-foundation interaction is a phenomenon which requires complex mathematical modelling in the seismic analysis of concrete gravity dams. The dam-reservoir system can be categorized as a coupled field system in which two physical systems of fluid and structure interact only at the domains' interface. In such a problem, the presence of interaction implies that the time response of both subsystems must be evaluated simultaneously. Different approaches to the solution of coupled field problem exist (Felippa and Park., 1980). Field elimination, simultaneous solution and partitioned solution are the three classes of solutions of the coupled field system.

An analytical procedure for the seismic analysis of concrete gravity dams based on the substructure method was presented by (Fenves and Chopra, 1984b). The substructure

system equations for dam, impounded water and foundation rock were combined to obtain the frequency domain equation for the complete system. The dynamic response of the dam to earthquake ground motion was obtained by solving the frequency domain equation for the complex-valued frequency response functions of the generalized coordinates. The response history of the generalized coordinates was determined using fourier synthesis techniques. Their analysis used the assumption of vertical upstream face for the dam. The hydrodynamic pressure in the impounded reservoir of infinite length which is governed by the wave equation is due to the horizontal and the vertical accelerations of the upstream face of the dam as well as the vertical acceleration of the reservoir bottom. Motion of thes e two boundaries (upstream face of the dam and reservoir bottom) is related to the hydrodynamic pressure through the boundary conditions. After solving the wave equation, the frequency response functions of the hydrodynamic terms are given as vectors of nodal forces. The response functions are statically equivalent to the pressure functions at the upstream face of the dam and at the reservoir bottom. The frequency doma in equation for the complete system derived from combination of the governing equations in each substructure system, consists of hydrodynamic terms. The main limitation of the frequency domain analysis is that it is not applicable in the case of nonlinear analysis.

For dams with vertical upstream face which are characterized by a rectangular fluid domain of infinite length, the wave equation subjected to the boundary conditions can be solved using standard solution methods for the boundary value problem. However, for dams with inclined upstream face or a reservoir of finite length, numerical methods are required to solve the wave equation. In this case, it is necessary to implement the finite element

technique to model both reservoir and dam structure. The main concern is the effect of truncation of the infinite reservoir that causes reflection of the outgoing waves into the finite element model of the resrvoir. The case of finite reservoir does not require truncation of the reservoir.

In seismic analysis of concrete dams, it is necessary to develop a model to include nonuniform earthquake excitation. In most of the available research, the solution of the wave equation in the reservoir to determine the pressure is based on the assumption of uniform earthquake ground motion. A closed form solution of the wave equation can not be obtained if a nonuniform earthquake excitation is taken as an input ground motion. This also applies for the case of infinite rectangular reservoir. Inclusion of nonuniform excitation in the dynamic analysis is possible if both of the reservoir and the structure are modelled using the finite element technique. A method of analysis is needed to take into account the nonuniform input earthquake excitation for the dynamic analysis of concrete gravity dams.

The available analyses for the nonlinear response of concrete gravity dams represent the dam-reservoir interaction by using the added mass approach. Different techniques have been proposed for simultaneous solution of dam-reservoir interaction using the finite element method. In all of the techniques, displacement was chosen as the response variable for the structure while the pressure can be chosen as a response variable for the fluid. In this case, the equation of motion for the coupled dam-reservoir system is unsymmetric. Another approach is to model the fluid in terms of a potential function of velocity or displacement. This will again result in unsymmetric equation of motion for the coupled dam-reservoir system. The fluid can also be modelled by displacement formulation. In this case, the

equation of motion of the coupled dam-reservoir system is symmetric. The difficulties encountered in applying this method are in the number of variables for the fluid and the effect of spurious vibration mode because of the reduced integration technique. Others mixed approaches have been introduced to model the dam-reservoir interaction.

Fenves and Vargas-Loli (1988) proposed a method for dam-reservoir interaction which is capable of producing a symmetric matrix for the equation of equilibrium of the system. Leger and Bhattacharjee (1992) presented a methodology which can partly represent the dam-reservoir-foundation interaction. The method was proposed for use in nonlinear analysis of concrete gravity dams. The effect of the reservoir is modelled using added mass, damping and spring stiffness matrices. These matrices were chosen based on a comparison with the frequency domain analysis to minimize the difference in structural response. The method is very crude and was found to be time consuming in nonlinear analysis. Modelling of the coupled dam-reservoir problem is quite complex when the nonlinearity of the concrete dam or reservoir are included.

In seismic analysis of concrete gravity dams, a mathematical model that includes the dam-reservoir interaction needs to be developed. The model should overcome the difficulties encountered with available models and be feasible to implement into the nonlinear analysis of concrete dams.

1.3 NONLINEAR ANALYSIS OF CONCRETE DAMS

Nonlinear seismic analysis of concrete dams has been the subject of extensive research during the past decade because of concern over the limitations of the linear analysis. Results of the previous research have shown that most of the concrete gravity dams experience cracking even when subjected to a moderate earthquake ground motion. Therefore, the assumption of linear behaviour may not be appropriate in the analysis of such systems.

Concrete gravity dams can be distinguished from other structure because of their size and their strong interactions with the reservoir and the foundation. The dam-reservoir and dam-foundation interactions are the important aspects of the behaviour that need to be properly modelled in nonlinear analysis of concrete dams. It is a difficult task to develop a comprehensive model to include both nonlinearities and interaction effect in the analysis. These are the major challenges that most ongoing research is facing.

Two classes of solution can be found in the nonlinear study of concrete gravity dams. Discrete crack approach is the first class of the solution which is based on the variable mesh approach. Two methods of linear fracture mechanics and nonlinear fracture mechanics can be used in this approach. The other class of solution is the continuum model in which a fixed finite element mesh is used. Smeared crack model and damage mechanics are the two methods of solution in this class. In the investigation of the nonlinear behaviour of concrete dams, different approaches with different material modelling were attempted.

To understand the nonlinear behaviour of concrete dams, mechanical modelling of the damage is pursued. Bazant and Oh (1983) proposed a fracture mechanics theory of the

smeared crack band. The strain-softening of the material was considered based on the fracture parameters, fracture energy, uniaxial tensile strength and crack band width. Fracture energy could be determined from the stress-strain curve. Formulas were derived to give the fracture parameters. Borst and Nauta (1985) presented a nonlinear method with rotating crack instead of fixed-crack model. Inclusion of shrinkage and plasticity in the nonlinear analysis was made due to decomposition of strain increment into crack strain and concrete strain increments. They found that the reduced integration technique is not suitable in fracture analysis. Bhattacharjee and Leger (1992) presented a state-of-the-art article on constitutive models of concrete gravity dams.

Ghrib and Tinawi (1995b) proposed a continuum model of damage mechanics for predicting the nonlinear response of concrete gravity dams under static loading. The approach to damage mechanics is based on a factor which represent the state of each element. The evolution of the crack is based on the basic properties of the concrete such as compressive strength, tensile strength, and fracture energy. The continuum model uses a fixed mesh which has the advantage of remeshing in discrete crack model. The model can be used for large structures using a reasonable mesh size. Ghrib and Tinawi (1995a) presented anisotropic damage mechanics model for use in the nonlinear seismic analysis of concrete gravity dams. The model represents opening and closing of cracks using the element properties such as compressive strength, tensile strength, and fracture energy. The numerical difficulties due to closing and opening of cracks which introduces a shock wave was overcome by using α-method.

In most of the nonlinear fracture mechanics solutions for the seismic response of a concrete gravity dam, the dam-reservoir interaction is excluded. The dam-reservoir interaction effects are normally approximated by means of added mass approach. Thus a model is needed for including the dam-reservoir interaction in the nonlinear fracture mechanics analysis to study the cracking behaviour of concrete dams.

1.4 EXPERIMENTAL STUDIES ON CONCRETE DAMS

The dynamic response of dams is a complex problem because of dam-reservoir-foundation interaction effect. Most of the research conducted in the area of dam engineering has been theoretical in nature. Although substantial progress has been achieved in mathematical modelling, many assumptions in the analysis remain to be verified. Due to the complex nature of the problem, the large size of the structure and difficulties in physical modelling, little experimental work has been pursued.

There is a definite need to develop new experimental approaches using small scale model testing of concrete gravity dams to investigate the dynamic response of dams. In such a model, it is important that both material scaling criteria and load representation criteria are met. The results from experimental work would be valuable in verifying the assumptions used in theoretical solutions as well as in calibrating the modelling parameters.

The difficulties in physical modelling of concrete dams are mostly in material modelling and the availability of equipment for testing. Research was conducted to find proper combination of the material in the mixture that can meet the criterias for modelling (Raphael, 1963 ; Yoshida and Baba, 1965). Some of the materials need to construct is hazardous and prone to shrinkage cracking in the process of drying (Donlon and Hall, 1991). Limited testing of small scale dam models using the centrifuge equipment was described by Plizzari et al. (1994), Renzi et al. (1994) and Valente et al. (1994). In the testing procedure, the hydrostatic water pressure on the dam model was simulated. The pressure was increased to cause failure of the dam. This represents the case of a dam subjected to overflow loads due to flooding. The main interest in the test was to simulate the crack propagation in the dam model. Due to difficulties in physical modelling, a new approach to dam experimental research is needed to properly model even some limited aspects of the behaviour of the concrete gravity dam prototype.

1.5 OBJECTIVES OF THE RESEARCH

The objectives of this research program are to:

- Develop a mathematical approach for the solution of the coupled dam-reservoir interaction problem which can be implemented in the nonlinear analysis of the dynamic response of concrete gravity dams. The developed approach may be applied to evaluate the effect of the travelling seismic wave on the response of concrete gravity dam.

- Develop a small scale experimental approach to model some aspects of the behaviour of the concrete dam-reservoir system.

1.6 ORGANIZATION OF THE THESIS

Organization of the thesis is shown in flow chart format in figure 1.1. In Chapter 2, two methods of staggered solution procedure for the dam-reservoir interaction are proposed. The first method, staggered displacement method, is based on the approximation of the displacement from the structure equation of motion. The second method, is based on the approximation of pressure from the fluid equation of motion. Using Routh-Hurwitz criteria, both methods are shown to be unconditionally stable when the two differential equations of the fluid and structure include damping terms. The staggered pressure method was modified for use when the equation of motion includes a lumped (diagonal) mass matrix. Two

different configurations of concrete gravity dams are used to investigate the accuracy and the stability of the staggered displacement method and the modified staggered pressure method.

The seismic response of a concrete gravity dam subjected to travelling seismic excitation is evaluated in Chapter 3. The method of staggered displacement analysis for the coupled dam-reservoir system is used in the analysis. The proposed method of analysis is simple and easy to apply. The analysis is applied to the case of a gravity dam with infinite and finite reservoirs of different lengths to evaluate the effect of the travelling seismic wave on the dam crest displacement. Various wave speeds representing the speed of wave travel in the reservoir foundation, are used in the analysis. Earthquake ground motions are considered to travel in the upstream or the downstream directions. In the case of the horizontal ground motion, the results are compared with the benchmark case of infinite reservoir length in which the far end of the reservoir is truncated at length equal to 15 times the dam height. In the analysis, a uniform earthquake is considered at the dam foundation while a nonuniform ground motion is considered at the reservoir boundaries.

The nonlinear seismic fracture response of the Pine Flat dam under the effect of reservoir interaction is included in Chapter 4. Smeared crack analysis model based on a nonlinear fracture mechanics crack propagation criterion is used to study the cracking behaviour of the dam. The staggered method of numerical analysis was used to solve the dam-reservoir interaction problem. Results of the analysis are compared with the case when the added mass approach was used to represent the interaction. The foundation is assumed rigid and no absorption is considered at the reservoir bottom.

Small scale experimental investigation of the concrete dam including specimen

design, test set-up, concrete properties and instrumentation are presented in Chapter 5. A loading mechanism with two actuators designed to apply four concentrated loads at the upstream face of the dam model is described. Reversed cycling loading was applied by an actuator to represent the dynamic effects of the earthquake. A constant static load which represents the hydrostatic pressure was also applied to the specimens. The material properties of the model was the same as the prototype.

Experimental data measurements and analysis of the results are presented in Chapter 6. Finally the conclusions and recommendations for future research are presented in Chapter 7.

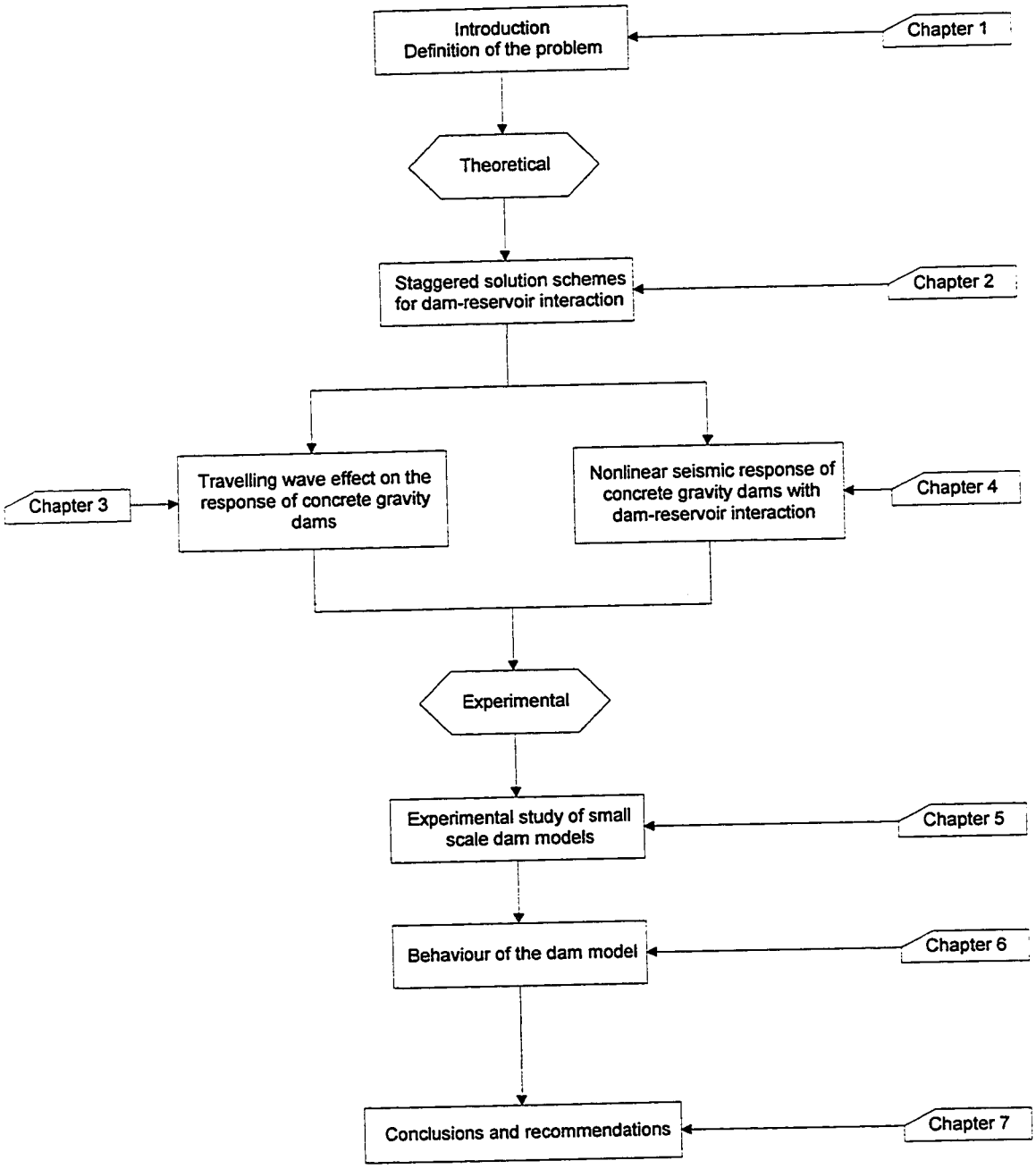

Figure 1.1 Organization of the thesis

CHAPTER TWO

STAGGERED SOLUTION SCHEMES FOR DAM-RESERVOIR INTERACTION

2.1 INTRODUCTION

The dam-reservoir system can be categorized as a coupled field system in which two physical domains of fluid and structure interact only at their interface. In such a problem, the presence of interaction implies that the time response of both subsystems must be evaluated simultaneously (Felippa and Park,1980). Different approaches to the solution of the coupled field problem exist. Field elimination, simultaneous solution and partitioned solution are the three classes of solutions for the coupled field system. The advantages and disadvantages of each method were addressed by Felippa and Park (1980). The field elimination approach is not feasible in the case of nonlinear problems. The reduced system of equations has high order derivatives which cause some difficulties in applying the initial conditions. The simultaneous solution is time consuming and involves many operations, especially when a large number of elements is used. This method contains matrices with a large bandwidth and consequently requires a large amount of memory especially for the cases when the existing matrices are not symmetric. In addition, the main disadvantage of the first two classes of solution arises from the difficulties encountered in using available software while the

partitioned solution has the capability of using existing software for each subsystem. Staggered solution was described by Felippa and Park (1980) as a partitioned solution procedure that can be organized in terms of sequential execution of single-field analyser.

Most of the physical systems are made of subsystems which interact with each other. These physical systems which are referred to as coupled systems, have been investigated by several researchers. Methods of solution vary depending on the governing differential equations of the subystems and may lead to different degrees of accuracy and stability of the solution (Park, 1980; Park and Felippa, 1980). Coupled problems and their numerical solutions were addressed by Felippa and Park (1980); Park and Felippa (1980, 1984); Zienkiewicz and Taylor (1989); Zienkiewicz (1984); and Zienkiewicz and Chan (1989). Zienkiewicz and Chan (1989) proposed an unconditionally stable method for staggered solution of soil-pore fluid interaction problem. Huang (1995) proposed two unconditionally stable methods for the analysis of soil-pore fluid problem. The methods were named pressure correction method and displacement correction method. Zienkiewicz and Chan (1989) presented an unconditionally stable method for staggered solution procedure for the fluid-structure interaction problem. Their method was proved to be unconditionally stable when no damping term was included in the equations of the fluid and the structure. However, when the damping term is included in the equation of the subsystems the proposed method may not be unconditionally stable. The problem of solutions instability when the damping term is included in the differential equation, was recognized by Wood (1990). Most of the staggered solution applications in the field of fluid-structure interaction were conducted using a method which is not unconditionally stable (Zienkiewicz and Newton, 1969; Paul

et al. 1981).

In this study, two methods of staggered solution procedure are applied to the dam-reservoir interaction problem. Both methods are shown to be unconditionally stable when the two differential equations of the fluid and structure include damping terms. The accuracy of the solution using both of the proposed methods, is investigated. Two different configurations of concrete gravity dams are analysed to illustrate the application of the proposed procedure and to compare the solution with available finite element solutions.

2.2 THE COUPLED DAM-RESERVOIR PROBLEM

The dam-reservoir interaction is a classic coupled problem which contains two differential equations of the second order. The equations of the dam structure and the reservoir can be written in the following form:

$$\begin{aligned}[M]\{\ddot{U}\} + [C]\{\dot{U}\} + [K]\{U\} &= \{f_1\} - [M]\{\ddot{U}_g\} + [Q]\{P\} \\ &= \{F_1\} + [Q]\{P\}\end{aligned} \tag{2.1}$$

$$\begin{aligned}[G]\{\ddot{P}\} + [C']\{\dot{P}\} + [K']\{P\} &= \{F\} - \rho\,[Q]^T(\{\ddot{U}\} + \{\ddot{U}_g\}) \\ &= \{F_2\} - \rho\,[Q]^T\{\ddot{U}\}\end{aligned} \tag{2.2}$$

where [M], [C] and [K] are mass, damping and stiffness matrices of the structure and [G], [C'] and [K'] are matrices representing mass, damping and stiffness of the reservoir, respectively. Detailed definitions of the [G], [C'] and [K'] matrices and vector {F}, are

presented in the following sections. [Q] is the coupling matrix; $\{f_1\}$ is the vector of body force and hydrostatic force; and {P} and {U} are the vectors of hydrodynamic pressures and displacements. $\{\ddot{U}_g\}$ is the ground acceleration and ρ is the density of the fluid. The dot represents the time derivative.

2.3 FINITE ELEMENT MODELLING OF THE RESERVOIR

The hydrodynamic pressure distribution in the reservoir is governed by the pressure wave equation. Assuming that water is linearly compressible and neglecting its viscosity, the small amplitude irrotational motion of water is governed by the two-dimensional wave equation:

$$\nabla^2 P(x,y,t) = \frac{1}{V^2} \ddot{P}(x,y,t) \qquad (2.3)$$

where P(x,y,t) is the hydrodynamic pressure in excess of hydrostatic pressure, V is the velocity of pressure wave in water and x and y are the coordinate axes.

The hydrodynamic pressure in the impounded water governed by equation (2.3), is due to the horizontal and the vertical accelerations of the upstream face of the dam, the reservoir bottom as well as the far end of the reservoir in the case of finite reservoir length. The motion of these boundaries is related to the hydrodynamic pressure by the boundary conditions.

For earthquake excitation, the condition at the boundaries of the dam-reservoir, reservoir-foundation and the reservoir-far-end are governed by the equation:

$$\frac{\partial P(x,y,t)}{\partial n} = -\rho\, a_n(x,y,t) \tag{2.4}$$

where ρ is density of water and $a_n(x,y,t)$ is the component of acceleration on the boundary along the direction of the inward normal n. No wave absorption is considered at the boundaries of the reservoir.

Neglecting the free surface wave, the boundary condition at the free surface is written as:

$$P(x,h,t) = 0 \tag{2.5}$$

where h is the height of the reservoir.

Using finite element discretization of the fluid domain and the discretized formulation of equation (2.3), the wave equation can be written in the following matrix form:

$$[G]\ \{\ddot{P}\} + [H]\ \{P\} = \{F\} \tag{2.6}$$

where $G_{ij} = \Sigma G_{ij}^e$, $H_{ij} = \Sigma H_{ij}^e$ and $F = \Sigma F_i^e$.

The coefficient G_{ij}^e, H_{ij}^e and F_i^e for an individual element are determined using the following expressions:

$$G_{ij}^{e} = \frac{1}{V^2} \int_{A_e} N_i \, N_j \, dA \tag{2.7}$$

$$H_{ij}^{e} = \int_{A_e} \left(\frac{\partial N_i}{\partial x} \frac{\partial N_j}{\partial x} + \frac{\partial N_i}{\partial y} \frac{\partial N_j}{\partial y} \right) dA \tag{2.8}$$

$$F_i^{e} = \int_{s_e} N_i \frac{\partial P}{\partial n} \, ds \tag{2.9}$$

where N_i is the element shape function, A_e is the element area and s_e is the prescribed length along the boundary of the elements. In the above formulation, matrices [H] and [G] are constant during the analysis while the force vector {F} and the pressure vector {P} and its derivatives are the variable quantities in equation (2.6).

2.4 TRUNCATED BOUNDARY AT THE FAR END OF THE RESERVOIR

In order to determine the hydrodynamic pressure on the dam due to horizontal ground motion under the assumption of infinite reservoir, the reservoir must be truncated at a reasonable distance. Sommerfeld boundary condition is the most commonly used approach which is based on the assumption that at a far distance from the dam face, the outgoing wave can be considered as plane wave. Hanna and Humar (1982), Humar and Roufaiel (1983) and Sharan (1985a,b; 1986; 1987) used a radiation condition which adequately models the loss of the outgoing wave over a wide range of excitation frequencies. In the present analysis, the Sharan (1986) radiation boundary condition was used. This boundary condition is the most suitable one for the time domain analysis. Other transmitting boundary conditions (Yang et al. 1993) are more accurate than Sharan's, however, the simplicity of the selected boundary condition is a major advantage.

The Sharan boundary condition at the far-end truncated boundary can be written as:

$$\frac{\partial P}{\partial n} = - \frac{\pi}{2h} P - \frac{1}{V} \dot{P} \qquad (2.10)$$

Implementation of the truncated boundary condition in the finite element model, can be done by separating the force vector {F} in equation (2.6) into two components:

$$\{F\} = \{FF_1\} + \{FF_2\} \qquad (2.11)$$

where $\{FF_1\}$ is the component of the force due to acceleration at the boundaries of the dam-

reservoir and reservoir-foundation while $\{FF_2\}$ is due to truncation at the far boundary and can be written as:

$$\{FF_2\} = -\frac{\pi}{2h}[D]\{P\} - \frac{1}{V}[D]\{\dot{P}\} \tag{2.12}$$

where $D_{ij}=\Sigma D_{ij}^e$ and D_{ij}^e is defined as:

$$D_{ij}^e = \int_{\ell_T^e} N_i N_j \, d\ell_T \tag{2.13}$$

In equation (2.13), ℓ_T^e is the side of the element on the truncated boundary. Substituting equations (2.11) and (2.12) into equation (2.6) results in:

$$[G]\{\ddot{P}\} + \frac{1}{V}[D]\{\dot{P}\} + \left([H] + \frac{\pi}{2h}[D]\right)\{P\} = \{FF_1\} \tag{2.14}$$

Putting equation (2.14) in the format of equation (2.2) the following relationships are obtained:

$$\begin{aligned} [C'] &= \frac{1}{V}[D] \\ [K'] &= [H] + \frac{\pi}{2h}[D] \\ \{F_2\} - \rho[Q]^T\{\ddot{U}\} &= \{FF_1\} \end{aligned} \tag{2.15}$$

2.5 COUPLING MATRIX OF THE DAM-RESERVOIR

The coupling matrix relates the pressure of the reservoir and the forces on the dam-reservoir interface as following:

$$[Q]\ \{ P \} = \{ f \} \tag{2.16}$$

where {f} is the force vector acting on the structure due to the hydrodynamic pressure.

Figure 2.1 shows a line element on the interaction boundary of the dam-reservoir. The work done by the hydrodynamic pressure on the interaction surface of the structure must be equal to the work of the equivalent nodal forces on the interface boundary of an element. Thus, for unit thickness elements as shown in figure 2.1, the following expression can be written:

$$\int_{s_e} P\ U_n\ ds = \{ f \}^{e^T} \{ \delta \} = \{ fx_1 \quad fy_1 \quad fx_2 \quad fy_2 \} \begin{Bmatrix} u_1 \\ v_1 \\ u_2 \\ v_2 \end{Bmatrix} \tag{2.17}$$

where P and U_n are the values of the hydrodynamic pressure and normal displacement along the element interface, respectively. {δ} and $\{f\}^e$ are the displacement and force vector of an interface element. u_i and v_i (fx_i and fy_i) are the displacements (forces) at node i of the interface element along the global X and Y coordinates, respectively. The integration is performed along each element on the dam-reservoir interface. The superscript and subscript 'e' refer to the element on the dam-reservoir interface. Writing u and v, displacements along

the global X and Y coordinates of the interface element, in terms of structure shape functions, then:

$$u = u_1 N_1 + u_2 N_2 \qquad v = v_1 N_1 + v_2 N_2 \tag{2.18}$$

where N_i is the structure shape function at node i of the interface element. For the normal displacement along the element surface, U_n, we have:

$$U_n = u_n + v_n = \eta u_1 N_1 + \eta u_2 N_2 + \beta v_1 N_1 + \beta v_2 N_2 \tag{2.19}$$

In equation (2.19), η and β are the absolute values of the normal vector on the boundary in the global directions of X and Y, respectively. Equation (2.19) can be written in the following form:

$$U_n = \left\{ \eta N_1 \;\; \beta N_1 \;\; \eta N_2 \;\; \beta N_2 \right\} \{ \delta \} = \{ N_n^s \}^T \{ \delta \} \tag{2.20}$$

The hydrodynamic pressure can be expressed as shape function of the fluid in the form:

$$P = \{ N^f \} \{ P \}^e = \{ N_1^f \;\; N_2^f \} \{ P \}^e \tag{2.21}$$

where N_i^f is the fluid shape function at node i of the interface element. Combining equations (2.17), (2.20) and (2.21), there is obtained:

$$\{ f \}^e = \int_{s_e} \{ N_n^s \} \{ N^f \}^T ds \;\; \{ P \}^e = [Q]^e \{ P \}^e \tag{2.22}$$

where $[Q]^e$ and $\{P\}^e$ are the coupling matrix and hydrodynamic pressure vector of an element

on the dam-reservoir interface. The total coupling matrix [Q] is obtained by assembling all element coupling matrices. From equation (2.22), $[Q]^e$ is written as:

$$[Q]^e = \int_{s_e} \{N_n^s\} \{N^f\}^T \, ds \tag{2.23}$$

For an interface element as shown in figure 2.1, then:

$$[Q]^e = \int_{s_e} \begin{bmatrix} \eta N_1 N_1^f & \eta N_1 N_2^f \\ \beta N_1 N_1^f & \beta N_1 N_2^f \\ \eta N_2 N_1^f & \eta N_2 N_2^f \\ \beta N_2 N_1^f & \beta N_2 N_2^f \end{bmatrix} ds \tag{2.24}$$

2.6 TIME-STEPPING SCHEME OF THE COUPLED EQUATIONS

Direct integration scheme is used to find the displacement and hydrodynamic pressure at the end of the time increment i+1 given the displacement and hydrodynamic pressure at time i. The Newmark-β method is used for discretization of both equations (implicit-implicit method). In this method $\{\dot{U}\}_{i+1}$, $\{U\}_{i+1}$, $\{\dot{P}\}_{i+1}$ and $\{P\}_{i+1}$ can be written as follows:

$$\begin{aligned} \{\dot{U}\}_{i+1} &= \{\dot{U}\}^{p}_{i+1} + \gamma\Delta t\ \{\ddot{U}\}_{i+1} \\ \{\dot{U}\}^{p}_{i+1} &= \{\dot{U}\}_{i} + (1-\gamma)\Delta t\ \{\ddot{U}\}_{i} \end{aligned} \tag{2.25}$$

$$\begin{aligned} \{U\}_{i+1} &= \{U\}^{p}_{i+1} + \beta\Delta t^{2}\ \{\ddot{U}\}_{i+1} \\ \{U\}^{p}_{i+1} &= \{U\}_{i} + \Delta t\ \{\dot{U}\}_{i} + (0.5-\beta)\ \Delta t^{2}\ \{\ddot{U}\}_{i} \end{aligned} \tag{2.26}$$

$$\begin{aligned} \{\dot{P}\}_{i+1} &= \{\dot{P}\}^{p}_{i+1} + \gamma\ \Delta t\ \{\ddot{P}\}_{i+1} \\ \{\dot{P}\}^{p}_{i+1} &= \{\dot{P}\}_{i} + (1-\gamma)\ \Delta t\ \{\ddot{P}\}_{i} \end{aligned} \tag{2.27}$$

$$\begin{aligned} \{P\}_{i+1} &= \{P\}^{p}_{i+1} + \beta\Delta t^{2}\ \{\ddot{P}\}_{i+1} \\ \{P\}^{p}_{i+1} &= \{P\}_{i} + \Delta t\ \{\dot{P}\}_{i} + (0.5-\beta)\ \Delta t^{2}\ \{\ddot{P}\}_{i} \end{aligned} \tag{2.28}$$

where γ and β are the integration parameters.

The governing field equations at time i+1 can be written as follows:

$$[M]\ \{\ddot{U}\}_{i+1} + [C]\ \{\dot{U}\}_{i+1} + [K]\ \{U\}_{i+1} = \{F_1\}_{i+1} + [Q]\ \{P\}_{i+1} \tag{2.29}$$

$$[G]\ \{\ddot{P}\}_{i+1} + [C']\ \{\dot{P}\}_{i+1} + [K']\ \{P\}_{i+1} = \{F_2\}_{i+1} - \rho\ [Q]^T\ \{\ddot{U}\}_{i+1} \tag{2.30}$$

The coupled field equations (2.29) and (2.30) can be solved using the staggered solution scheme. The procedure can be started by guessing $\{P\}_{i+1}$ in equation (2.29) to solve for $\{U\}_{i+1}$ and its derivatives. Then equation (2.30) can be solved to find $\{P\}_{i+1}$. This method can not guarantee the unconditional stability of the solution. Similarly, guessing $\{\ddot{U}\}_{i+1}$ at first to calculate $\{P\}_{i+1}$ from equation (2.30) and then calculating $\{U\}_{i+1}$ from equation (2.29) can not provide unconditionally stable procedure.

In the following sections, two methods of staggered solution are proposed which are shown to be unconditionally stable.

2.7 STAGGERED DISPLACEMENT METHOD

In this method, equation (2.29) can be approximated as following:

$$[M]\ \{\ddot{U}\}^{*}_{i+1} = \{F_1\}_{i+1} + [Q]\ \{P\}^{p}_{i+1} - [C]\ \{\dot{U}\}^{p}_{i+1} - [K]\ \{U\}^{p}_{i+1} \tag{2.31}$$

Combining equations (2.31) and (2.29) gives:

$$\begin{aligned}[M]\ \{\ddot{U}\}_{i+1} =& [M]\ \{\ddot{U}\}^{*}_{i+1} + \beta\Delta t^2\ [Q]\ \{\ddot{P}\}_{i+1} \\ &- \gamma\Delta t\ [C]\ \{\ddot{U}\}_{i+1} - \beta\Delta t^2\ [K]\ \{\ddot{U}\}_{i+1}\end{aligned} \tag{2.32}$$

Taking advantage of the lumped mass which results in a diagonal mass matrix, equation (2.32) can be modified as:

$$[M]\ \{\ddot{U}\}_{i+1} = [M]\ \{\ddot{U}\}^{*}_{i+1} + \beta\Delta t^2\ [Q]\ \{\ddot{P}\}_{i+1} \tag{2.33}$$

Substituting equation (2.33) into equation (2.30), then:

$$\begin{aligned}&\left([G] + \rho\beta\Delta t^2\ [Q]^T\ [M]^{-1}\ [Q] \right)\ \{\ddot{P}\}_{i+1} + [C']\ \{\dot{P}\}_{i+1} + [K']\ \{P\}_{i+1} = \\ &\{F_2\}_{i+1} - \rho\ [Q]^T\ \{\ddot{U}\}^{*}_{i+1}\end{aligned} \tag{2.34}$$

In equation (2.34), the right hand side terms are known, thus, $\{P\}_{i+1}$ can be obtained. In order to correct the approximation made in equation (2.33), $\{P\}_{i+1}$ can be substituted in equation (2.29) to calculate $\{U\}_{i+1}$ and its derivatives.

Therefore, the procedure of the staggered displacement method can be summarized by the following steps:

1. Solving equation (2.31) to calculate $\{\ddot{U}\}^*_{i+1}$.
2. Substituting $\{\ddot{U}\}^*_{i+1}$ in equation (2.34) to calculate $\{P\}_{i+1}$.
3. Substituting $\{P\}_{i+1}$ in equation (2.29) to calculate $\{U\}_{i+1}$ and its derivatives.

2.8 STABILITY OF THE STAGGERED DISPLACEMENT METHOD

In an unconditionally stable solution method, instability can be attributed to that of structure. While in a conditionally stable method, the stability may be due to numerical or structural instability. To show that the described method of staggered displacement is unconditionally stable, consider a modally decomposed system with scalar values. In such a system, displacement and the pressure must not grow. Thus for $|\mu|<1$ we have:

$$\{U\}_{i+1} = \mu \{U\}_i \;;\; \{\dot{U}\}_{i+1} = \mu \{\dot{U}\}_i \;;\; \{\ddot{U}\}_{i+1} = \mu \{\ddot{U}\}_i \tag{2.35}$$

$$\{P\}_{i+1} = \mu \{P\}_i \;;\; \{\dot{P}\}_{i+1} = \mu \{\dot{P}\}_i \;;\; \{\ddot{P}\}_{i+1} = \mu \{\ddot{P}\}_i \tag{2.36}$$

Using z-transformation of $\mu=(1+z)/(1-z)$, the condition for stability requires that the real part of z is negative ($Re(z)\leq 0$) and that the Routh-Hurwitz criterion (Wood, 1990; Zienkiewicz and Taylor, 1989) apply. For $\beta=0.25$ and $\gamma=0.5$, equations (2.25), (2.26), (2.27) and (2.28) become:

$$\{\ddot{U}\}_{i+1} = \frac{4\,z^2}{\Delta t^2}\{U\}_{i+1} \quad ; \quad \{\dot{U}\}_{i+1} = \frac{2\,z}{\Delta t}\{U\}_{i+1}$$

$$\{\dot{U}\}^p_{i+1} = \frac{2\,z - z^2}{\Delta t}\{U\}_{i+1} \quad ; \quad \{U\}^p_{i+1} = (1 - z^2)\{U\}_{i+1} \tag{2.37}$$

$$\{\ddot{P}\}_{i+1} = \frac{4\,z^2}{\Delta t^2}\{P\}_{i+1} \quad ; \quad \{\dot{P}\}_{i+1} = \frac{2\,z}{\Delta t}\{P\}_{i+1}$$

$$\{\dot{P}\}^p_{i+1} = \frac{2\,z - z^2}{\Delta t}\{P\}_{i+1} \quad ; \quad \{P\}^p_{i+1} = (1 - z^2)\{P\}_{i+1} \tag{2.38}$$

Rewriting equation (2.29) without the force term, then:

$$[M]\{\ddot{U}\}_{i+1} + [C]\{\dot{U}\}_{i+1} + [K]\{U\}_{i+1} - [Q]\{P\}_{i+1} = 0 \tag{2.39}$$

Combining equations (2.32) and (2.34) and substituting them into equation (2.30) without the force term, gives:

$$[G]\{\ddot{P}\}_{i+1} + [C']\{\dot{P}\}_{i+1} + [K']\{P\}_{i+1} +$$
$$\rho\,[Q]^T[M]^{-1}([M] + \gamma\Delta t\,[C] + \beta\Delta t^2\,[K])\{\ddot{U}\}_{i+1} = 0 \tag{2.40}$$

The modally decomposed system is represented by a single degree of freedom equation. The single degree of freedom equivalent of equations (2.39) and (2.40) will be obtained by substituting the mass, damping and stiffness values m, c and k instead of [M], [C] and [K] in equation (2.39) and g, c′ and k′ instead of [G], [C′] and [K′] in equation (2.40). The coupling matrix [Q] would be represented by scalar quantity q. The characteristic equation of the coupled field can be written by substituting equations (2.37) and (2.38) into equations (2.39) and (2.40) as follows:

$$\begin{vmatrix} m\frac{4z^2}{\Delta t^2} + c\frac{2z}{\Delta t} + k & -q \\ \frac{\rho q}{m}\left(m + \frac{\Delta t}{2}c + \frac{\Delta t^2}{4}k\right)\frac{4z^2}{\Delta t^2} & g\frac{4z^2}{\Delta t^2} + c'\frac{2z}{\Delta t} + k' \end{vmatrix} = 0 \qquad (2.41)$$

or

$$a_0 z^4 + a_1 z^3 + a_2 z^2 + a_3 z + a_4 = 0 \qquad (2.42)$$

where:

$$a_0 = \frac{16\ m\ g}{\Delta t^4} \quad ; \quad a_1 = \frac{8\ m\ c'}{\Delta t^3} + \frac{8\ g\ c}{\Delta t^3}$$

$$a_2 = \frac{4\ m\ k'}{\Delta t^2} + \frac{4\ c\ c'}{\Delta t^2} + \frac{4\ g\ k}{\Delta t^2} + \frac{4\ \rho\ q^2}{\Delta t^2} + \frac{2\ \rho\ q^2\ c}{m\ \Delta t} + \frac{\rho\ q^2\ k}{m} \qquad (2.43)$$

$$a_3 = \frac{2\ c'\ k}{\Delta t} + \frac{2\ c\ k'}{\Delta t} \quad ; \quad a_4 = k\ k'$$

The Routh-Hurwitz conditions for stability are:

$$a_0 > 0 \quad ; \quad a_1\ ,\ a_2\ ,\ a_3\ ,\ a_4 \geq 0\ ; \quad \begin{vmatrix} a_1 & a_3 \\ a_0 & a_2 \end{vmatrix} > 0\ ; \quad \begin{vmatrix} a_1 & a_3 & 0 \\ a_0 & a_2 & a_4 \\ 0 & a_1 & a_3 \end{vmatrix} > 0 \qquad (2.44)$$

For the structural system of dam and reservoir; m, c, k, g, c' and k' are positive quantities. Therefore, a_0, a_1, a_2, a_3 and a_4 are always positive. The values of the two determinants in equation (2.44) are given as:

$$a_1\ a_2 - a_3\ a_0 =$$

$$\frac{32}{\Delta t^5}\ m^2\ c'\ k' + \frac{32}{\Delta t^5}\ m\ c'^2\ c + \frac{32\ \rho}{\Delta t^5}\ m\ c'\ q^2 + \frac{16\ \rho}{\Delta t^4}\ c'\ q^2\ c$$

$$+ \frac{8\ \rho}{\Delta t^3}\ c'\ q^2\ k + \frac{32}{\Delta t^5}\ g\ c^2\ c' + \frac{32}{\Delta t^5}\ g^2\ c\ k \qquad (2.45)$$

$$+ \frac{32\ \rho}{\Delta t^5}\ g\ c\ q^2 + \frac{16\ \rho}{\Delta t^4}\ g\ c^2\ q^2 + \frac{8\ \rho}{\Delta t^3}\ g\ c\ q^2\ k$$

$$a_1 a_2 a_3 - a_1^2 a_4 - a_3^2 a_0 =$$

$$\frac{64}{\Delta t^6}\left(m k' \sqrt{c c'} - g k \sqrt{c c'} \right)^2 + \frac{64}{\Delta t^6} m c'^3 c k + \frac{64}{\Delta t^6} m c'^2 c^2 k'$$

$$+ \frac{64\,\rho}{\Delta t^6} m c'^2 q^2 k + \frac{64\,\rho}{\Delta t^6} m c' q^2 c k' + \frac{32\,\rho}{\Delta t^5} c'^2 q^2 c k$$

$$+ \frac{32\,\rho}{\Delta t^5} c' q^2 c^2 k' + \frac{16\,\rho}{\Delta t^4} c'^2 q^2 k^2 + \frac{16\,\rho}{\Delta t^4} c' q^2 k c k' \qquad (2.46)$$

$$+ \frac{64}{\Delta t^6} g c^2 c'^2 k + \frac{64}{\Delta t^6} g c^3 c' k' + \frac{64\,\rho}{\Delta t^6} g c q^2 c' k$$

$$+ \frac{64\,\rho}{\Delta t^6} g c^2 q^2 k' + \frac{32\,\rho}{\Delta t^5} g c^2 q^2 c' k + \frac{32\,\rho}{\Delta t^5} g c^3 q^2 k'$$

$$+ \frac{16\,\rho}{\Delta t^4} g c q^2 k^2 c' + \frac{16\,\rho}{\Delta t^4} g c^2 q^2 k k'$$

All the terms in equation (2.45) and (2.46) are positive. Recalling the condition of stability (2.44), then the method of staggered displacement is unconditionally stable.

2.9 STAGGERED PRESSURE METHOD

In this method, the pressure can be approximated using equation (2.30) as following:

$$[G]\ \{\ddot{P}\}^{*}_{i+1} = \{F_2\}_{i+1} - [C']\ \{\dot{P}\}^{p}_{i+1} - [K']\ \{P\}^{p}_{i+1} \tag{2.47}$$

Substituting equation (2.47) into equation (2.30), there is obtained:

$$\begin{aligned}[G]\ \{\ddot{P}\}_{i+1} &= [G]\ \{\ddot{P}\}^{*}_{i+1} - \rho\ [Q]^T\ \{\ddot{U}\}_{i+1} \\ &- \gamma\Delta t\ [C']\ \{\ddot{P}\}_{i+1} - \beta\Delta t^2\ [K']\ \{\ddot{P}\}_{i+1}\end{aligned} \tag{2.48}$$

or:

$$(\ [G] + \beta\Delta t^2\ [K'] + \gamma\Delta t\ [C']\ )\ \{\ddot{P}\}_{i+1} = [G]\ \{\ddot{P}\}^{*}_{i+1} - \rho\ [Q]^T\ \{\ddot{U}\}_{i+1} \tag{2.49}$$

Substituting equation (2.49) into equation (2.29) with $[H]=[G]+\beta\Delta t^2[K']+\gamma\Delta t[C']$, gives:

$$\begin{aligned}(\ [M] + \rho\beta\Delta t^2\ [Q]\ [H]^{-1}\ [Q]^T\ )\ \{\ddot{U}\}_{i+1} + [C]\ \{\dot{U}\}_{i+1} + [K]\ \{U\}_{i+1} = \\ \{F_1\}_{i+1} + [Q]\ (\ \{P\}^{p}_{i+1} + \beta\Delta t^2\ [H]^{-1}\ [G]\ \{\ddot{P}\}^{*}_{i+1})\end{aligned} \tag{2.50}$$

Using equation (2.50), the variable $\{\ddot{U}\}_{i+1}$ can be calculated. Substituting $\{\ddot{U}\}_{i+1}$ into equation (2.29) gives $\{P\}_{i+1}$ and its derivatives.

Therefore, the procedure of staggered pressure method can be summarized by the following steps:

1. Solving equation (2.47) to calculate $\{P\}^*_{i+1}$.
2. Substituting $\{P\}^*_{i+1}$ in equation (2.50) to calculate $\{\ddot{U}\}_{i+1}$.
3. Substituting $\{\ddot{U}\}_{i+1}$ in equation (2.49) to calculate $\{P\}_{i+1}$ and its derivatives.

2.10 STABILITY OF THE STAGGERED PRESSURE METHOD

For stability check, similar procedure as that used in the displacement method can be applied. Rewriting equations (2.29) and (2.30) without the force terms, then:

$$[M]\ \{\ddot{U}\}_{i+1} + [C]\ \{\dot{U}\}_{i+1} + [K]\ \{U\}_{i+1} - [Q]\ \{P\}_{i+1} = 0 \qquad (2.51)$$

$$[G]\ \{\ddot{P}\}_{i+1} + [C']\ \{\dot{P}\}_{i+1} + [K']\ \{\ddot{P}\}_{i+1} + \rho\ [Q]^T\ \{\ddot{U}\}_{i+1} = 0 \qquad (2.52)$$

The characteristic equation of the coupled field for a modally decomposed system with scalar values, can be written by substituting equations (2.37) and (2.38) into equations (2.51) and (2.52):

$$\begin{vmatrix} m\,\frac{4z^2}{\Delta t^2} + c\,\frac{2z}{\Delta t} + k & -q \\ \rho\, q\,\frac{4z^2}{\Delta t^2} & g\,\frac{4z^2}{\Delta t^2} + c'\,\frac{2z}{\Delta t} + k' \end{vmatrix} = 0 \qquad (2.53)$$

or

$$a_0 z^4 + a_1 z^3 + a_2 z^2 + a_3 z + a_4 = 0 \tag{2.54}$$

where:

$$a_0 = \frac{16\ m\ g}{\Delta t^4} \quad ; \quad a_1 = \frac{8\ m\ c'}{\Delta t^3} + \frac{8\ g\ c}{\Delta t^3}$$

$$a_2 = \frac{4\ m\ k'}{\Delta t^2} + \frac{4\ c\ c'}{\Delta t^2} + \frac{4\ g\ k}{\Delta t^2} + \frac{4\ \rho\ q^2}{\Delta t^2} \tag{2.55}$$

$$a_3 = \frac{2\ c'\ k}{\Delta t} + \frac{2\ c\ k'}{\Delta t} \quad ; \quad a_4 = k\ k'$$

The coefficients of the polynomial are all positive. The determinants in the Routh-Hurwitz conditions (equation 2.44), give:

$$a_1\ a_2 - a_3\ a_0 =$$

$$\frac{32}{\Delta t^5} m^2\ c'\ k' + \frac{32}{\Delta t^5} m\ c'^2\ c + \frac{32\ \rho}{\Delta t^5} m\ c'\ q^2 + \tag{2.56}$$

$$\frac{32}{\Delta t^5} g\ c^2\ c' + \frac{32}{\Delta t^5} g^2\ c\ k + \frac{32\ \rho}{\Delta t^5} g\ c\ q^2$$

$$a_1\, a_2\, a_3 - a_1^2\, a_4 - a_3^2\, a_0 =$$

$$\frac{64}{\Delta t^6}\left(m\, k'\sqrt{c\, c'} - g\, k\sqrt{c\, c'}\right)^2 + \frac{64}{\Delta t^6} m\, c'^3\, c\, k + \frac{64}{\Delta t^6} m\, c'^2\, c^2\, k' + \tag{2.57}$$

$$\frac{64\,\rho}{\Delta t^6} m\, c'^2\, q^2\, k + \frac{64\,\rho}{\Delta t^6} m\, c'\, q^2\, c\, k' + \frac{64}{\Delta t^6} g\, c^3\, c'\, k' +$$

$$\frac{64}{\Delta t^6} g\, c^2\, c'^2\, k + \frac{64\,\rho}{\Delta t^6} g\, c^2\, q^2\, k' + \frac{64\,\rho}{\Delta t^6} g\, c\, q^2\, c'\, k$$

These terms are all positive. Therefore, given the stability condition of equation (2.44), the method of staggered pressure is unconditionally stable.

2.11 MODIFIED STAGGERED PRESSURE METHOD

Most of the available nonlinear solutions assume a diagonal mass matrix for the purpose of analysis. The staggered displacement method is the most suitable coupled field problem solution procedure for the case of nonlinear analysis. In the case of the staggered pressure method some difficulties may arise due to added mass effect in equation (2.50) which changes the mass matrix from diagonal to a full matrix. For this reason the staggered pressure method was modified to apply to nonlinear analysis.

The staggered pressure method is modified by rewriting equation (2.50) in the following approximate form:

$$[M]\ \{\ddot{U}\}_{i+1} + [C]\ \{\dot{U}\}_{i+1} + [K]\ \{U\}_{i+1} = \{F_1\}_{i+1} + [Q]\ (\ \{P\}^{p}_{i+1} + \beta\Delta t^2\ [H]^{-1}\ (\ [G]\ \{\ddot{P}\}^{*}_{i+1} - \rho\ [Q]^T\ \{\ddot{U}\}_i)\ ) \tag{2.58}$$

Therefore, the procedure of the modified staggered pressure method can be summarized by the following steps:

1. Solving equation (2.47) to calculate $\{P\}^{*}_{i+1}$.
2. Substituting $\{P\}^{*}_{i+1}$ in equation (2.58) to calculate $\{\ddot{U}\}_{i+1}$.
3. Substituting $\{\ddot{U}\}_{i+1}$ in equation (2.49) to calculate $\{P\}_{i+1}$ and its derivatives.

The modified staggered pressure method does not guarantee unconditional stability of the solution. In the Following analysis, the modified staggered pressure method is used instead of the staggered pressure method and the results are compared with those obtained using the staggered displacement analysis procedure.

2.12 ACCURACY OF THE SOLUTION SCHEME

The accuracy of the staggered solution scheme can be improved by increasing the number of iterations and/or by decreasing the time step. Increasing the number of iterations of the staggering scheme is a time consuming process. The accuracy of the proposed methods is based on the selection of the appropriate time step. In all of the following analyses no iterations have been made for the purpose of improving accuracy. The staggered displacement method and the modified staggered pressure method are compared with the finite element solution of example problems for the purpose of evaluating the accuracy of the analysis.

2.13 NUMERICAL RESULTS

Two cases of concrete gravity dams with different reservoir levels were analysed to demonstrate the applicability and accuracy of the proposed methods. The modulus of elasticity, unit weight and Poisson's ratio of concrete were taken as 3,430 MPa, 2400 kg/m^3 and 0.2, respectively. The selected dam-reservoir system for the two cases of numerical examples are shown in figures 2.2 and 2.3. In the first example, a full reservoir is considered and the structure has a fundamental frequency of 6.837 rad/sec. The second example has a typical configuration of a concrete gravity dam of fundamental frequency of 7.57 rad/sec with partially filled reservoir.

Figure 2.4 shows ten seconds of the horizontal S00E component of the May 18, 1940 Imperial Valley earthquake, El Centro site record, which is selected for the purpose of the

dynamic analysis. The ground motion has peak acceleration of 0.348g. The values of the integration parameters in the Newmark-β method were taken as β=0.25 and γ=0.5. The velocity of pressure wave in water was taken as 1438.66 m/sec.

Results of the analysis using the staggered displacement and modified pressure methods were compared with the dynamic analysis using EAGD-84 (Fenves and Chopra, 1984a) program which assumes infinite reservoir length. In order to determine the hydrodynamic pressure on the dam due to horizontal ground motion under the assumption of infinite reservoir, the reservoir must be truncated at a reasonable distance. The truncated boundary at the far-end should absorb the outgoing waves. In finite element formulation of the reservoir, Sharan boundary condition (Sharan, 1986) which truncates the reservoir, was applied at a distance L=10H from the dam.

The EAGD-84 is a computer code in the frequency domain which gives the steady state response of the system. The presented results from the staggered methods are obtained from the time domain analysis which include the steady state and transient responses of the system. In the case of a typical concrete gravity dam, the transient response is negligible.

Four node isoparametric elements were used to represent the finite elements of the structure and the fluid domains. Stiffness proportional damping (Rayleigh damping) is used. To minimize the effect of the round-off errors on the accuracy of the solution, double precision arithmetic is used.

Figure 2.5 shows the results of the analysis for the dam crest displacement of the two dam examples. For a time step dt= 0.001 sec, excellent agreement is found between the response obtained from two proposed methods and the EAGD-84 solution.

The hydrodynamic pressure time histories on the upstream face near the bottom of the dams in the two examples are shown in figure 2.6. Results of the staggered displacement method and the staggered pressure method coincide.

Figures 2.7 and 2.8 show the results of the analysis obtained using different time steps. The figures show that the staggered displacement method is accurate even for the large time step of dt=0.02 sec. In the case of the modified staggered pressure method using time step smaller than 0.004 sec, good results are obtained. Using time steps larger than 0.004 sec in the modified pressure method leads to instability of the solution.

2.14 CONCLUSIONS

Two methods of staggered solution procedure for the dam-reservoir coupled system are introduced. The staggered displacement method, is based on the approximation of the displacement from the structure equation of the motion. The staggered pressure method is based on the approximation of the pressure from the fluid equation of motion. Using Routh-Hurwitz criteria, both methods are proved to be unconditionally stable when the two differential equations of the fluid and structure include damping terms. The method of displacement which is feasible for nonlinear analysis is used in the solution of numerical examples. The staggered pressure method was modified for use when the equation of the motion includes a lumped (diagonal) mass matrix. The modified staggered pressure method is also used to solve the same examples for comparison. Two cases of concrete gravity dams are analysed to investigate the accuracy and stability of the staggered displacement method. The method is found to be accurate when compared with the finite element solution. No instability is observed in the analysis in the case of displacement method. However, in case of modified staggered pressure, numerical instability is observed for large time steps. It is concluded that the displacement method gives stable solution with accurate results even for a large time step. The method is found to be less time consuming than the finite element analysis. The staggered pressure method is applicable where in problems with full mass matrix.

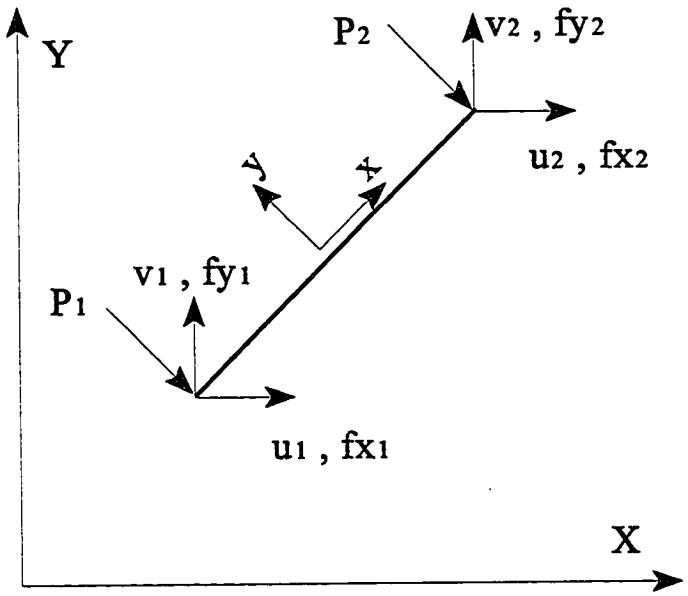

Figure 2.1 Interface element on the dam-reservoir interaction boundary

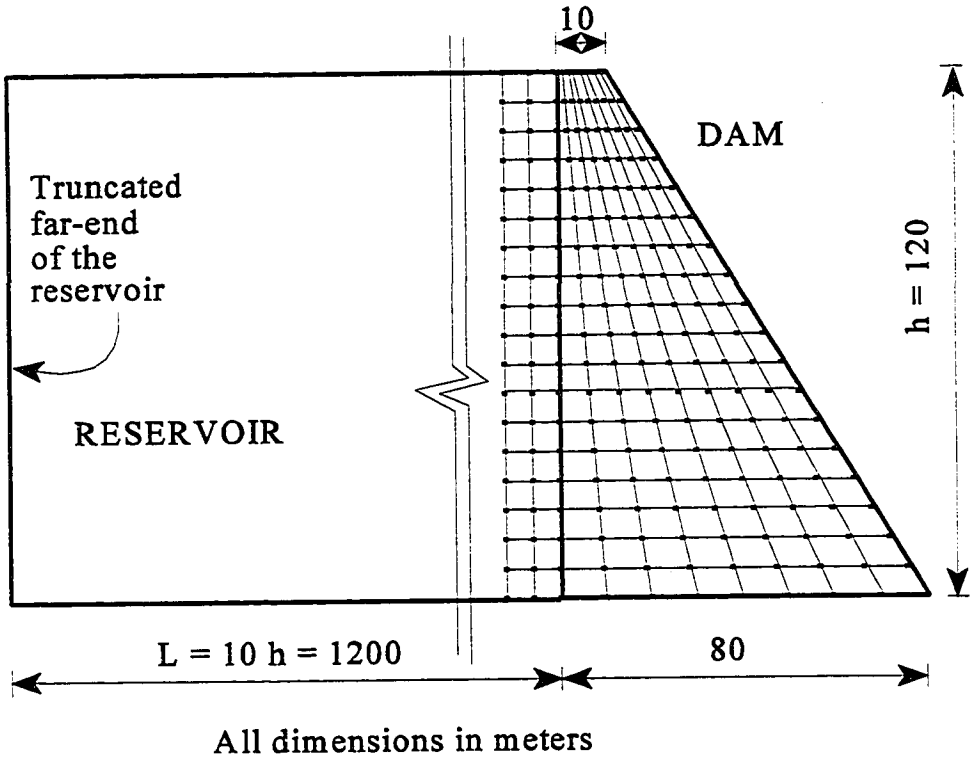

Figure 2.2 Finite element model of the dam-reservoir system in example 1

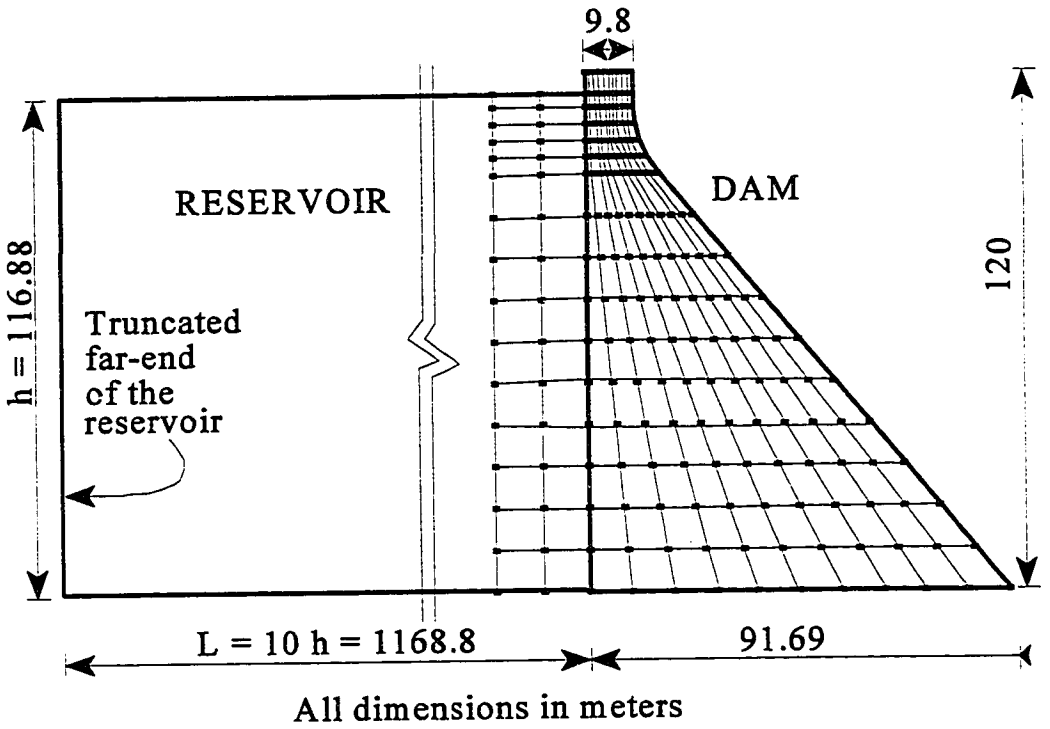

Figure 2.3 Finite element model of the dam-reservoir system in example 2

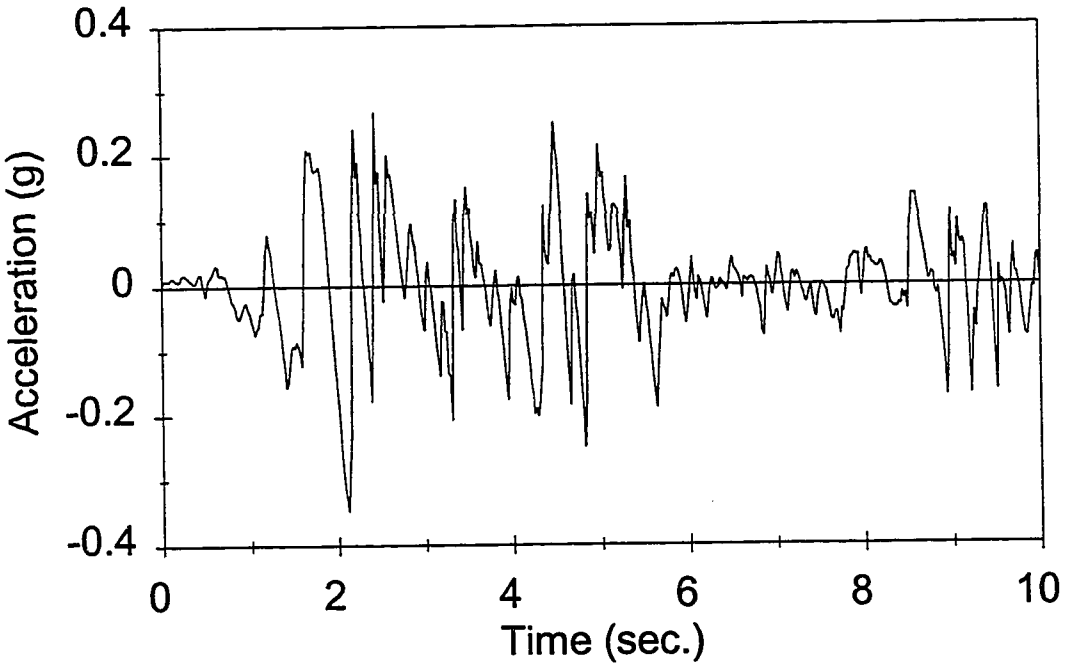

Figure 2.4 First ten seconds of the horizontal component S00E of the May 18, 1940 Imperial Valley earthquake, El Centro record

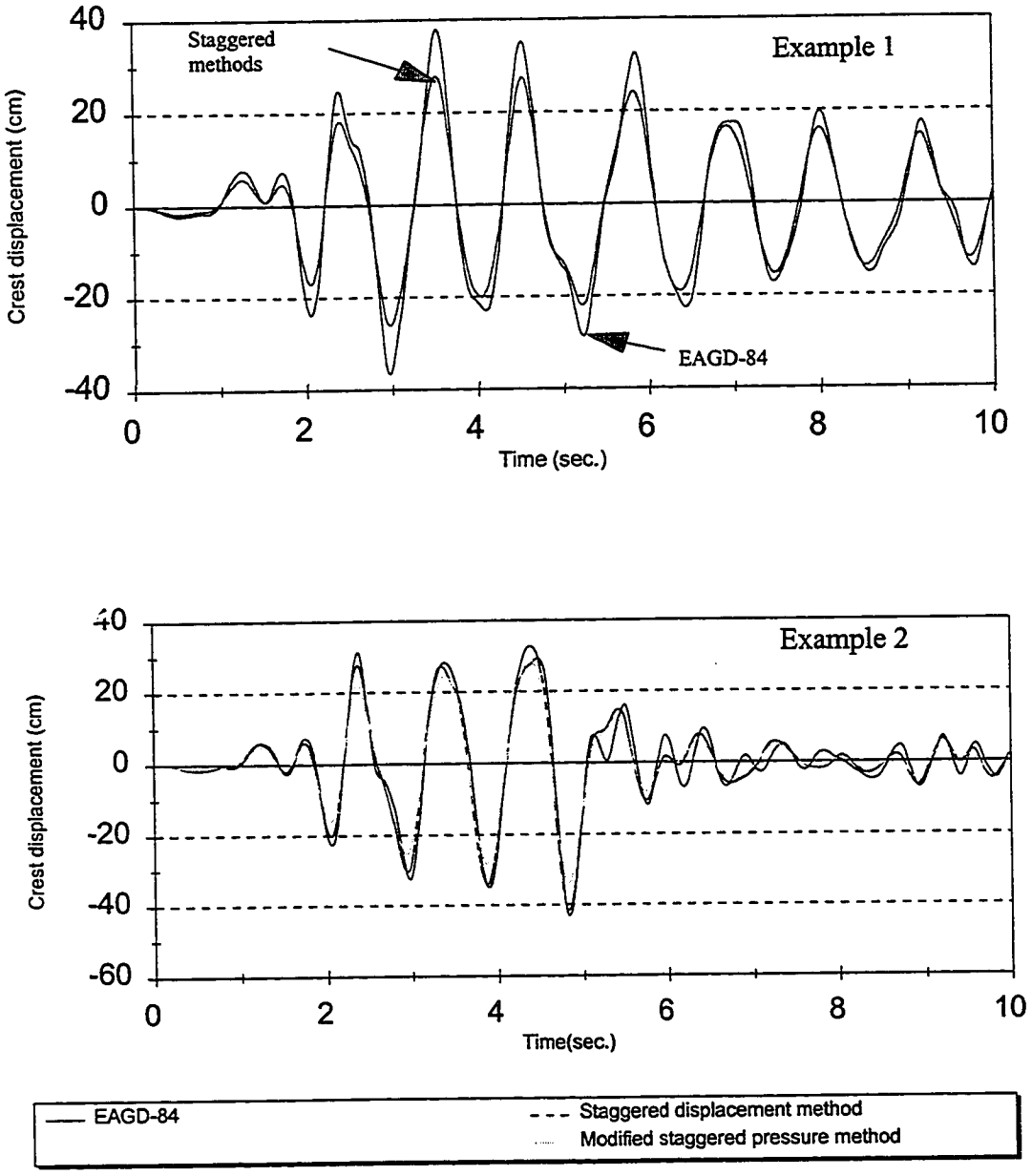

Figure 2.5 Dam crest displacement

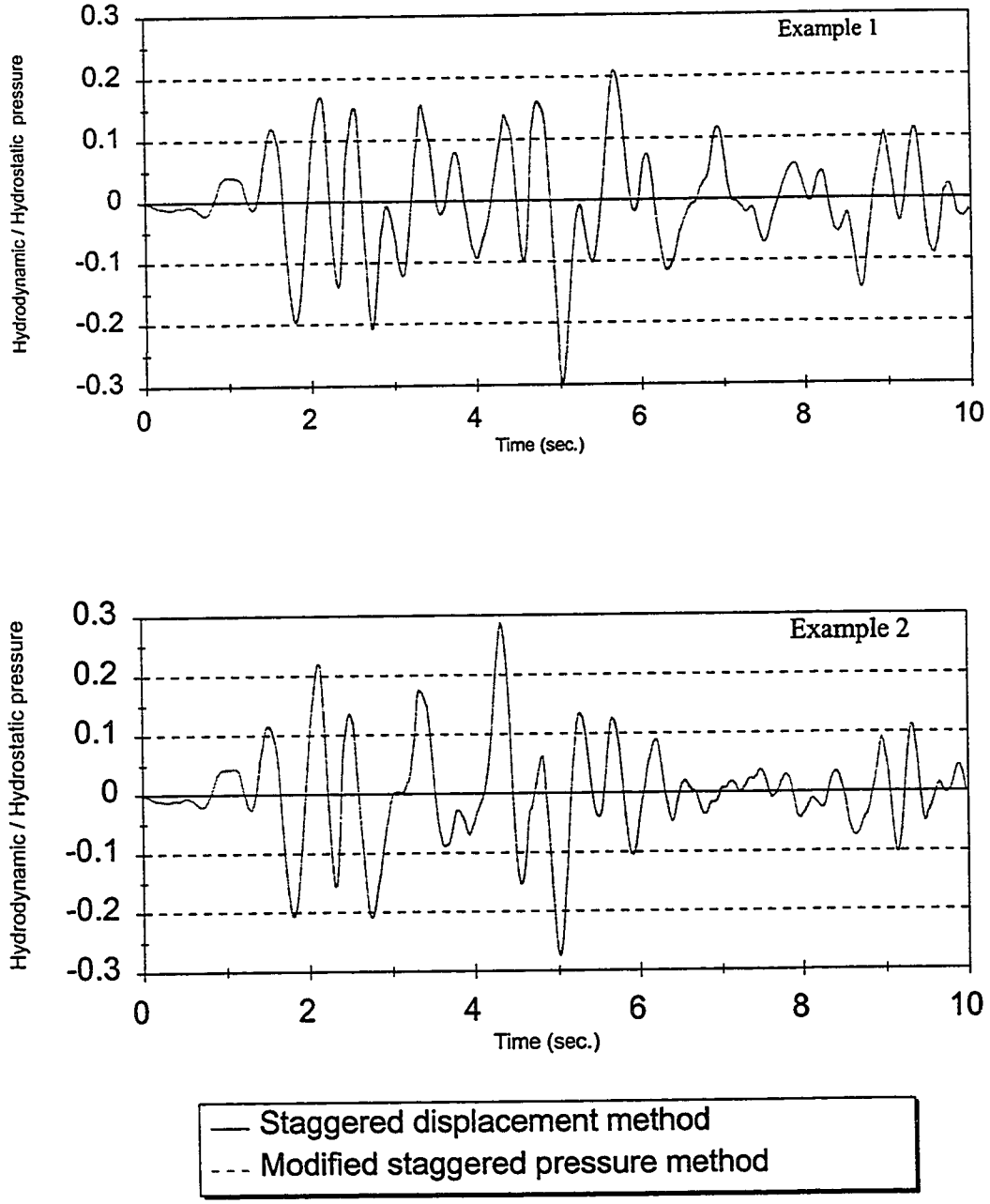

Figure 2.6 Hydrodynamic pressure time history near the bottom of the dam

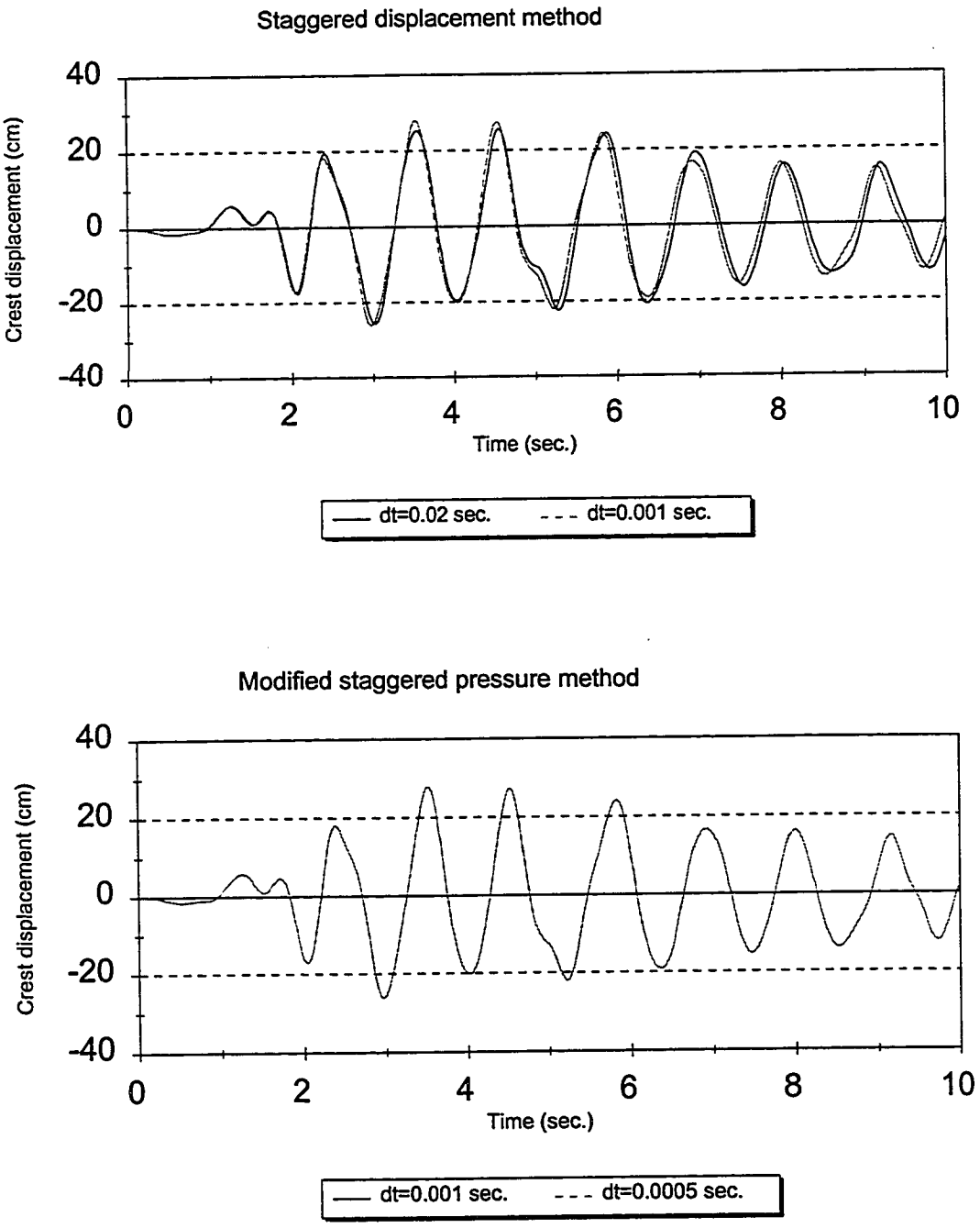

Figure 2.7 Accuracy of the proposed method with different time steps in example 1

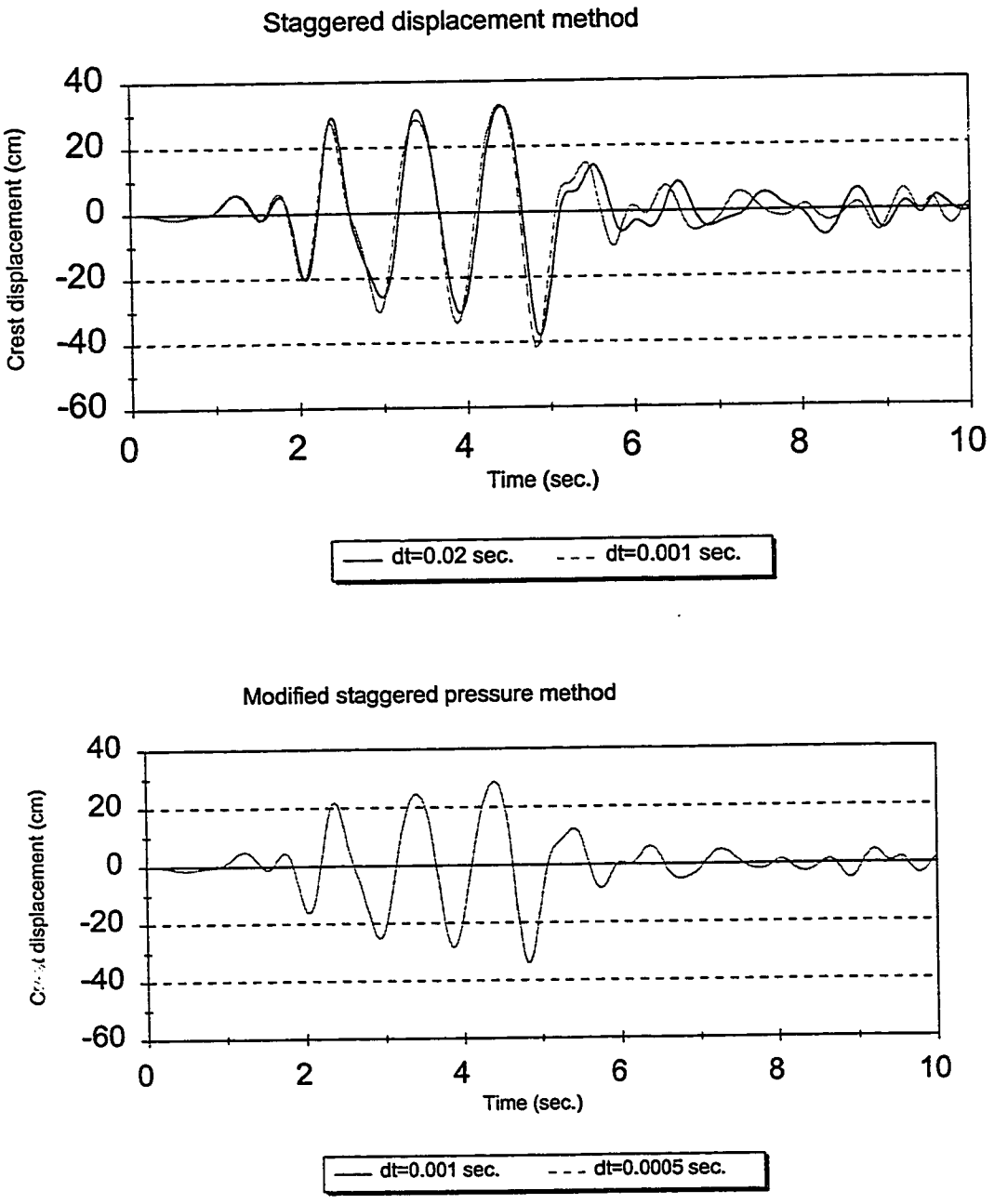

Figure 2.8 Accuracy of the proposed method with different time step in example 2

CHAPTER THREE

TRAVELLING WAVE EFFECT ON THE RESPONSE OF CONCRETE GRAVITY DAMS

3.1 INTRODUCTION

Since Westergaard's (1933) classic work on the prediction of the water pressure on dams during an earthquake, much research has been undertaken on the hydrodynamic forces on concrete gravity dams. A closed form solution for the hydrodynamic pressure was presented by Chopra (1967) for the case of a rigid dam with vertical up-stream face under horizontal and vertical ground motions. Analytical solutions of the wave equation for the dam-reservoir interaction were developed and extensive work was conducted on the finite element analysis of the dam-reservoir system.

The truncated boundary for the finite element and boundary element modelling of the infinite reservoir were studied by several researchers (Zienkiewicz and Newton 1969; Hall and Chopra 1979; Hanna and Humar 1982; Humar and Roufaiel 1983; Sharan 1985a and b; Sharan 1986; Sharan 1987; Yang et al. 1991). Yang et al. (1993) investigated the hydrodynamic pressure on a dam with suitable transmitting boundary condition at the far field of the fluid domain. A state-of-the-art article on the subject of hydrodynamic pressure

on dams was presented by Tsai and Lee (1990).

The horizontal and vertical earthquake ground motions are expected to vary from one end of the reservoir to the other. The assumption of nonuniform ground motion is a more realistic representation of the earthquake input than the uniform motion assumption. Spatial variation of the earthquake ground motion is expected to have an important effect on the response of large dams. In most of the available research, uniform earthquake ground motion was considered to act on the dam, along the reservoir bottom length and at the far end for the case of finite reservoir. The effect of nonuniform excitation of the dam-foundation-reservoir system on the hydrodynamic pressure is an important aspect of the evaluation of design forces on dams that needs to be investigated. Flores Victoria et al. (1969) studied the effect of finite velocity of propagation of the earthquake on the hydrodynamic pressure on the dam. The vertical component of the earthquake was taken into consideration. Velocity of the earthquake wave was assumed to be greater than the velocity of the pressure wave in water. The reservoir was taken to be of infinite length.

Aviles and Sanchez-Sesma (1989) studied the hydrodynamic pressure on rigid gravity dams with a finite reservoir and incompressible water under horizontal excitation. It was assumed that under harmonic ground motion, the far end of the reservoir can be subjected to out-of-phase motion. Baumber and Ghobarah (1995) studied dam monolith response under horizontal excitation with a phase difference between the dam and far end boundary. Nowak and Hall (1990) investigated the effect of non-uniform earthquake excitation on the response of an arch dam. The earthquake was considered as plane body wave normally incident to the axis of the canyon which was assumed to be of uniform cross section. Kojic and Trifunac

(1991 a and b) presented the analysis of arch dams to nonuniform motion of the canyon walls. Hydrodynamic effect of the reservoir was included as an added mass. Ramadan and Novak (1992) studied dam response to spatially variable seismic ground motion. They considered a joint coherency model which presents spatially incoherent ground motions in both time and frequency domains. They applied the spatially variable ground motion to the dam base in the upstream-downstream direction of the dam. A uniform earthquake ground motion was used to obtain the hydrodynamic pressure on the upstream face of the dam. They found that the effect of the spatially variable ground motion on the response is negligible.

In this Chapter, the effect of nonuniform earthquake ground motion on the response of concrete gravity dams is discussed. The objective is to follow a rational approach to investigate the effect of the travelling earthquake wave on the hydrodynamic forces and dam crest displacement response. Different cases of infinite and finite reservoir lengths assuming compressible water, were studied. For the case of flexible dams, the method of staggered displacement is used for the purpose of the dynamic analysis. The method is simple and suitable for this type of analysis.

3.2 APPROACH TO TRAVELLING WAVE EXCITATION

Concrete gravity dams are large structures with dimension in the hundreds of meters. The reservoir system may measure several kilometers long. Due to limited speed of the travelling seismic wave, it is necessary to evaluate the contribution of the travelling earthquake ground motion to the dynamic analysis of the system. Nonuniform earthquake

ground motion will be applied to the dam and to the reservoir bottom and boundaries.

It has been shown that variation of the earthquake along the upstream-downstream direction of the dam, applied at its base does not influence the dam response significantly (Ramadan and Novak, 1992). Therefore, it may be reasonable to assume a uniform earthquake at the dam base and nonuniform earthquake at the reservoir boundaries.

In the following sections, two series of analyses are carried out to investigate the travelling wave effect on the response of the dam-reservoir system. In the first series, the effect of travelling wave on the hydrodynamic pressure on the dam is studied. For simplicity, a rigid concrete gravity dam are assumed. In the second analysis, the travelling wave effect on a flexible dam response is studied.

A finite element program was developed to analyse the coupled dam-reservoir system. Four node isoparametric elements were used to represent the finite elements of the fluid domain and the structure. The analysis may be conducted for the case of infinite reservoir or finite reservoir with the proper boundary definition. The earthquake ground motion record is applied as input to the analysis and the ground motion at different locations of the boundary are determined based on the wave velocity. For simplicity, no wave absorption is included in the analysis. A uniform earthquake is considered at the dam foundation while nonuniform motion is considered at the reservoir boundary. To minimize the effect of the round-off errors on the accuracy of the solution, double precision arithmetic is used.

Ten seconds of the horizontal S00E and vertical components of the May 18, 1940 Imperial Valley earthquake, El Centro site record, are selected for the purpose of the analysis

(figure 3.1). Only phase difference between the waves at two locations is considered. Spatial coherency of the ground motion is not included. Three seismic wave velocities of 500, 1000 and 1500 m/s are used. These velocities represent a reasonable range of soft and firm soil conditions. The seismic waves are considered to travel in both the upstream and downstream directions of the stream flow. For the purpose of demonstration of the results, the wave speed is considered to be positive when the wave travels towards the upstream side of the reservoir. The practical range for the reservoir length to reservoir height ratios may start from L/h=5 to infinite reservoirs. In this investigation, three different cases of reservoir length to height ratios (L/h=5, 10 and 15) are chosen.

3.3 HYDRODYNAMIC FORCES ON RIGID DAMS

To investigate the effect of travelling wave on hydrodynamic pressure on the upstream face of concrete gravity dams, a rigid gravity dam is considered. In the case of rigid dams, there is no dam-reservoir interaction. Thus, the wave equation of the reservoir (equation (2.2) with $\{\ddot{U}\} = 0.0$) is solved when subjected to the appropriate boundary conditions.

Direct integration scheme is used to solve for the hydrodynamic pressure in the time domain. The α-method (Hughes, 1987; Hilber et al., 1977) is used for discretization of equation (2.2). Using the α-method of integration, the reservoir fluid equation at time i+1 can be written as follows:

$$[G]\{\ddot{P}\}_{i+1} + [C']\{\dot{P}\}_{i+1} + (1+\alpha)[K']\{P\}_{i+1} - \alpha[K']\{P\}_{i} = \{F_2\}_{i+1} \qquad (3.1)$$

Introducing equations (2.27) and (2.28) into equation (3.1) for implicit integration scheme, the pressure vector at time i+1 is obtained in the form:

$$
\begin{aligned}
&([G] + \gamma\, \Delta t\, [C'] + (1+\alpha)\, \beta\, \Delta t^2\, [K'])\ \{P\}_{i+1} = \\
&\quad [G]\ (\{P\}_i + \Delta t\, \{\dot{P}\}_i + \Delta t^2\, (0.5-\beta)\, \{\ddot{P}\}_i) + \\
&\quad [C']\ (\gamma\, \Delta t\, \{P\}_i + \Delta t^2\, (\gamma-\beta)\, \{\dot{P}\}_i + \Delta t^3\, (0.5\gamma-\beta)\, \{\ddot{P}\}_i) + \\
&\quad [K']\ (\alpha\, \beta\, \Delta t^2\, \{P\}_i) + \beta\, \Delta t^2\, \{F_2\}_{i+1}
\end{aligned}
\tag{3.2}
$$

In selecting the time integration parameters α, β and γ, the following conditions for stability must be satisfied (Hilber and Hughes, 1978):

$$
\begin{aligned}
&-\frac{1}{3} \le \alpha \le 0 \\
&\beta = \frac{(1-\alpha)^2}{4} \\
&\gamma = \frac{1}{2} - \alpha
\end{aligned}
\tag{3.3}
$$

The stability and accuracy of the solution depend on the selected values for the α, β and γ parameters, time step Δt and size of the finite element. When the parameters of the integration are selected as α=0, β=0.25 and γ=0.5, the α-method reduces to the average acceleration method. Here, the values of the integration parameters were taken as α=-0.2, β=0.36 and γ=0.7.

A rigid vertical dam with a rectangular reservoir of height of h=150 m was analysed.

The selected dam-reservoir system is shown in figure 3.2. The velocity of pressure wave in water was taken as 1438.66 m/sec. The lateral hydrodynamic force at the upstream face of the dam was found by integration of the pressure distribution on the face of the dam. The hydrodynamic force is normalized to the hydrostatic force on the upstream face of the dam. The results of the analysis for different ground motion wave velocities and L/h ratios were compared. Two parameters are of interest. These are the maximum absolute hydrodynamic force in addition to a force response parameter I, defined to represent the number of response peaks and their values as follows:

$$I = \frac{1}{0.02\ T} \int_0^T \left(\frac{F_d}{F_s}\right)^2 dt \qquad (3.4)$$

Where F_d and F_s are the hydrodynamic and hydrostatic forces, respectively. T is the total time of the hydrodynamic force time history.

3.3.1 Horizontal Earthquake Ground Motion

Analysis of the dam-reservoir system for a dam of height h=150 m was conducted when the system was subjected to travelling horizontal earthquake ground motion. Results of the analysis of finite reservoirs were compared with the case of an infinite reservoir length. In the case of an infinite reservoir, only the upstream face of the dam was subjected to the earthquake ground motion. The reservoir was truncated at L=15h and the Sharan boundary condition (Sharan, 1986) was applied at the truncated surface.

In the case of finite reservoir, two ground motions were applied at the rigid dam and

the far end of the reservoir. The time lag between the two records of the earthquake depends on the length of the reservoir and the assumed wave velocity. If the ground motion wave is assumed to travel toward the upstream of the reservoir, the actual earthquake is applied to the dam while the phased ground motion was applied at the far-end of the reservoir. Ground motion variations other than the phase difference were ignored.

Results of the analysis for the hydrodynamic lateral force on a dam-reservoir system of L/h=5, 10 and 15 are shown in figures 3.3, 3.4 and 3.5, respectively. In the figures, the negative wave travel velocity represents a wave travelling towards the downstream direction of the dam. The peak of the lateral force time history was found to be near the peak of the earthquake ground motion in the case of infinite reservoir (figures 3.3a, 3.4a and 3.5a). In the case of finite reservoir, the reflection of the out-going wave is superimposed on the wave moving toward the far-end and results in high values of the response parameters (figures 3.3e, 3.4e and 3.5e).

The case of finite-reservoir normally gives higher lateral force on the dam when compared with the case of infinite reservoir. The response parameters for the case of uniform ground motion applied to finite reservoir increase as the reservoir length decreases. Applying uniform ground motion does not result in maximum response in most cases (figures 3.3b to 3.3d and 3.3f to 3.3h).

The hydrodynamic pressure on rigid dams is influenced by the velocity of the travelling horizontal earthquake excitation, direction of the wave propagation, height of the dam and length of the reservoir. The wave velocity and direction of the wave propagation can significantly change the response parameters depending on the reservoir length, as

illustrated by the lateral force response plots in figures 3.3 to 3.5. The direction of the earthquake wave was found to have a significant effect on the hydrodynamic pressure acting on the dam. For the purpose of comparison, two wave velocities of ±1500 m/s in the reservoir system of L/h=10 are considered and the lateral force time history is shown in figure 3.6. From the figure, the negative velocity which represents a wave travelling from the far end boundary to the dam can give higher lateral force response than the wave travelling in the opposite direction.

The behaviour of the force response parameter I, is similar to the variation of the maximum absolute lateral forces on the dam as shown in figure 3.7. An important difference is that the force parameter takes into account the number of peaks as well as their magnitude. This comparison suggests that the I parameter represents a quantitative measure of the forces on the dam. Figure 3.7, indicates that the infinite reservoir solution does not provide conservative design forces.

3.3.2 Vertical Earthquake Ground Motion

The selected dam-reservoir example was analysed when the system was subjected to a travelling vertical earthquake ground motion. The earthquake motion was assumed to vary along the reservoir bottom. Ground acceleration was taken constant over the element length on the bottom boundary.

The variation of the lateral force response with the travel velocity of the wave for the cases of reservoir L/h=5, 10 and 15 are plotted in figures 3.8, 3.9 and 3.10, respectively. From figures 3.8a, 3.9a and 3.10a, it was found that the reservoir length had no effect on the

response of rigid dams for the case of uniform ground motion. For different values of reservoir length, the same response of the pressure was obtained.

For an earthquake wave travel velocity of 500 m/s, results of the response parameters were lower when compared with the case of uniform earthquake excitation. As the wave velocity increases the lateral force response increases (figures 3.8 to 3.10). The observation can also be made that in the case of a negative wave travel velocity (from the far boundary towards the dam direction), the lateral force response may be higher than for the case of wave travelling towards the upstream direction of the reservoir. However, as shown in figure 3.11, the hydrodynamic pressure is less sensitive to the direction of the wave travel when compared to the case of horizontal earthquake excitation.

The force response parameter I, plotted in figure 3.12, correlates well with the variation of the maximum absolute lateral force. In the case of the vertical ground motion component, the lateral force response on the dam is less sensitive to the variation of the reservoir length than in the case of horizontal ground motion.

3.4 TRAVELLING WAVE EFFECT ON THE DAM RESPONSE

The seismic response of a flexible concrete gravity dam subjected to travelling seismic excitation is investigated. The method of staggered displacement is used to solve the coupled dam-reservoir problem. Stiffness proportional damping (Rayleigh damping) is used for the structure, to obtain the time domain response. The values of the integration parameters in the Newmark-β method were taken as β=0.25 and γ=0.5. These values

correspond to the α-method with α=0.0. The velocity of pressure wave in water was taken as 1438.66 m/sec.

A concrete gravity dam with a rectangular reservoir was analysed. The modulus of elasticity, unit weight and Poisson's ratio of concrete were taken as 27,580 MPa, 2400 kg/m^3 and 0.2, respectively. The selected dam-reservoir system is shown in figure 3.13. The dam-reservoir system has the same configuration as dam-reservoir system in figure 2.3. It is a typical configuration of a concrete gravity dam with partially filled reservoir.

The results of the analysis for the case of infinite reservoir (uniform ground motion), using the staggered displacement method were compared with the dynamic analysis using EAGD-84 (Fenves and Chopra, 1984a) program which is a frequency domain solution that assumes infinite reservoir length. The water depth h is taken as 116.88 m in this example. In order to determine the dam response due to horizontal ground motion under the assumption of infinite reservoir, the reservoir is truncated at a distance L=15h from the dam where Sharan boundary condition (Sharan. 1986) is applied.

The horizontal dam crest displacement at the upstream face of the dam was found to be a suitable parameter for the purpose of demonstration. Figures 3.14 shows results of the analysis for the dam crest displacement of the example of the concrete gravity dam. For a time step dt= 0.002 seconds, excellent agreement is found between the response obtained from the staggered displacement method and the EAGD-84 solution. In the following sections the results of the analysis of different horizontal and vertical ground motion wave velocities and L/h ratios were compared.

3.4.1 Horizontal Earthquake Ground Motion

The analysis of the dam-reservoir system was conducted when the system was subjected to travelling horizontal earthquake ground motion. Results of the analysis were compared with the case of infinite reservoir length. The dam crest displacement with the dam-reservoir system of L/h=5, 10 and 15 are shown in figures 3.15, 3.16 and 3.17, respectively. The peak of the dam crest displacement time history is not near the peak of earthquake ground motion in the case of infinite reservoir (figures 3.15a). This may be due to dam-reservoir interaction which shifts the peak of the response away from the peak of the earthquake ground motion. In the case of finite reservoir, the reflection of the out-going wave is superimposed on the wave moving toward the far-end and results in higher values of the dam crest displacement (figures 3.15, 3.16 and 3.17).

The case of finite-reservoir normally gives higher response when compared with the case of infinite reservoir. The effect of travelling wave is more pronounced when the reservoir length is shorter. As the reservoir length increases, the response due to uniform ground motion increases when compared with nonuniform ground motion. The exception to the trend is the case of L/h=15 (figure 3.17f) where the maximum response is not much higher than the case of uniform earthquake (figure 3.18).

The dam crest displacement is influenced by the velocity of the travelling horizontal earthquake excitation, direction of the wave propagation, height of the dam and length of the reservoir. The wave velocity and direction of the wave propagation can significantly change the response depending on the reservoir length, as illustrated by the dam crest displacement plots in figures 3.15 to 3.17. The direction of the earthquake wave was found to have a

significant effect on the dam crest response of the dam. The maximum absolute dam crest displacement is shown in figure 3.18.

3.4.2 Vertical Earthquake Ground Motion

The selected dam-reservoir example was analysed when the system was subjected to a travelling vertical earthquake ground motion. The earthquake motion was assumed to vary along the reservoir bottom. Ground acceleration was taken constant over the element length on the bottom boundary.

The variation of the dam crest response with the travel velocity for the cases of reservoir L/h=5, 10 and 15 are plotted in figures 3.19, 3.20 and 3.21, respectively. From the figures, it was found that, unlike the rigid dam, the reservoir length had an effect on the response of the dam for the case of uniform ground motion. It can be seen that the case of uniform earthquake results in higher response when compared with the case of the nonuniform earthquake.

As shown in figure 3.22, when the wave velocity increases the maximum crest displacement increases. The dam crest displacement is less sensitive to the direction of the wave travel when compared to the case of horizontal earthquake excitation.

3.5 HYDRODYNAMIC FORCES ON FLEXIBLE AND RIGID DAMS

The analysis of the dam-reservoir system shown in figure 3.13, was conducted under the horizontal earthquake ground motion. The results of the hydrodynamic forces on a flexible dam are compared with the case when the dam is assumed to be rigid. Figures 3.23, 3.24 and 3.25 show hydrodynamic forces on the flexible and rigid dams. In the case of infinite reservoir and flexible dam, higher hydrodynamic force were obtained in comparison with the forces on a rigid dam (figure 3.23a). The peak of hydrodynamic force on the flexible dam shifted away from the time of peak ground acceleration which coincides with the peak response in the case of rigid dam.

In the case of finite reservoir of L/h=5, for uniform and nonuniform earthquake ground motion, the peak of the hydrodynamic force response is higher on the rigid dam as compared with the flexible dam (figures 3.23b and c). As the reservoir length increases, the peak of hydrodynamic force response decreases in rigid dams (figures 3.24 and 3.25). The decrease of hydrodynamic forces is more pronounced in nonuniform earthquake excitation (figures 3.24c and 3.25c).

The lateral force comparisons shown in figures 3.23, 3.24 and 3.25 indicate that the flexible dam assumption is necessary.

3.6 CONCLUSIONS

3.6.1 Effect of Travelling Wave on the Hydrodynamic Pressure Response

The effect of travelling earthquake excitation on the hydrodynamic lateral force of the dam-reservoir system was studied. Based on the results of the analysis of a specific dam-reservoir system, it was found that the hydrodynamic pressure on rigid dams is influenced by the direction of wave travel, velocity of the travelling earthquake excitation, and reservoir length to dam height ratio.

Nonuniform horizontal earthquake ground motion results in higher hydrodynamic forces on the dam in comparison with uniform ground motion. In the case of the vertical ground motion component, uniform excitation gives higher hydrodynamic pressure response than nonuniform motion. The earthquake wave velocity is an important factor that affects the response parameters significantly. The inclusion of nonuniform earthquake excitations is necessary in the calculation of the hydrodynamic pressure distribution on dams.

The influence of reservoir length on the hydrodynamic load is significant for the case of horizontal earthquake ground motion. However, in the case of vertical motion the lateral force response on the rigid dam is not sensitive to reservoir length to dam height ratio.

The direction of the earthquake wave propagation in the horizontal direction has a noticeable effect on the hydrodynamic force response on rigid dams. However, the response parameters due to the vertical earthquake excitation are not sensitive to the direction of the wave propagation.

A force response parameter is proposed for quantifying the magnitude as well as the

number of peaks of the hydrodynamic forces on the dam. The parameter takes into consideration a measure of the ground motion duration.

3.6.2 Effect of Travelling Wave on the Dam Crest Response

The effect of travelling earthquake excitation on crest response of a flexible concrete gravity dam was studied. Based on the results of the analysis of a specific dam-reservoir system, it was found that the dam crest response is influenced by the direction of wave travel, velocity of the travelling earthquake excitation, and reservoir length to dam height ratio.

Nonuniform horizontal earthquake ground motion results in higher crest displacement in comparison with uniform ground motion. In the case of the vertical ground motion component, uniform excitation gives higher dam crest displacement response than nonuniform motion. The earthquake wave velocity is an important factor that may affect the dam crest displacement response significantly. The inclusion of nonuniform earthquake excitations is necessary in the calculation of the dam crest displacement pressure distribution on dams.

The influence of reservoir length on the dam response is significant for the case of horizontal earthquake ground motion. However, in the case of nonuniform vertical ground motion the dam crest response is not sensitive to reservoir length to dam height ratio.

The direction of the earthquake wave propagation in the horizontal direction has a noticeable effect on the dam response. However, the dam response to the vertical earthquake excitations is not sensitive to the direction of the wave propagation.

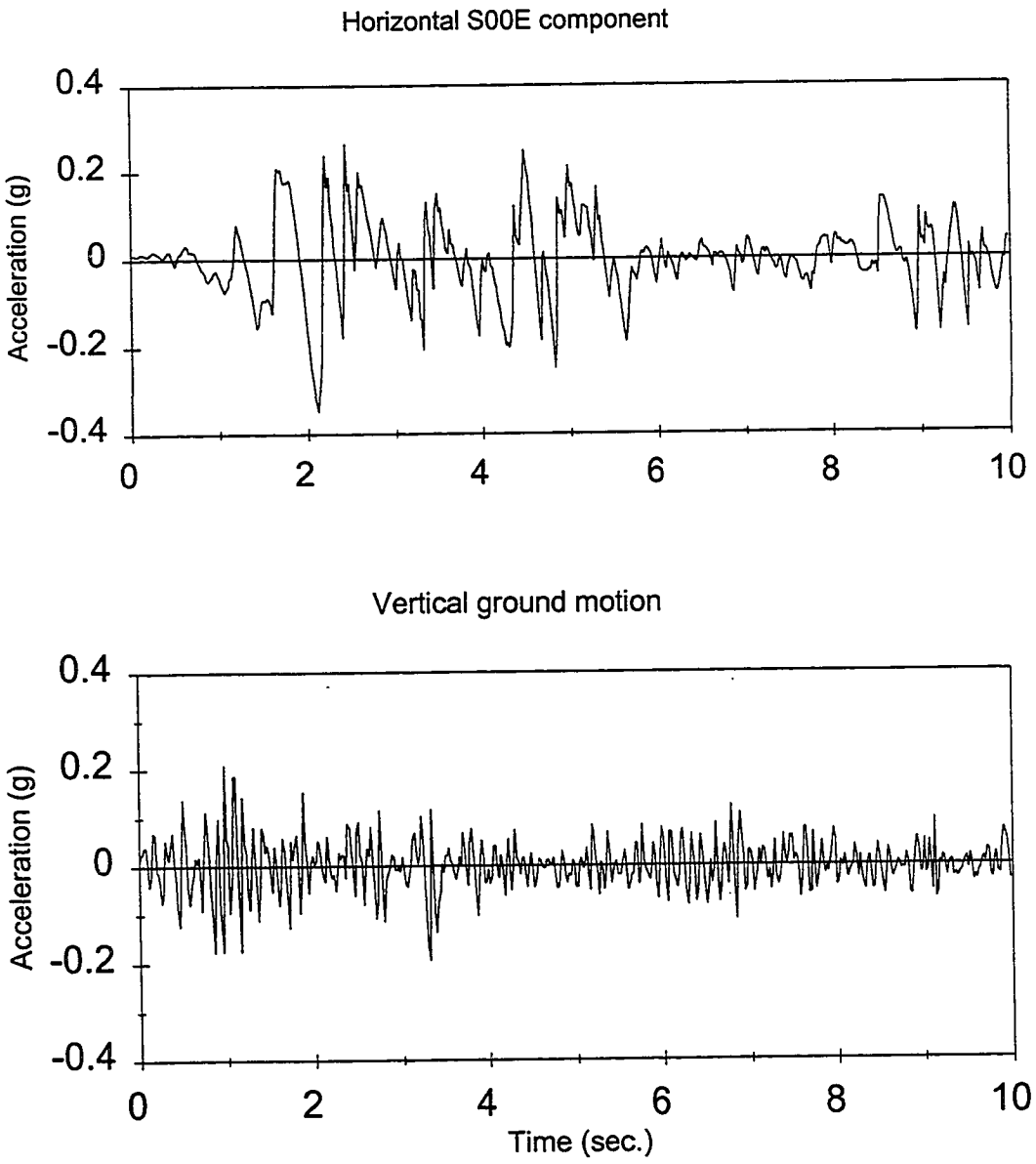

Figure 3.1 First ten seconds of the May 18, 1940 Imperial Valley earthquake, El Centro record

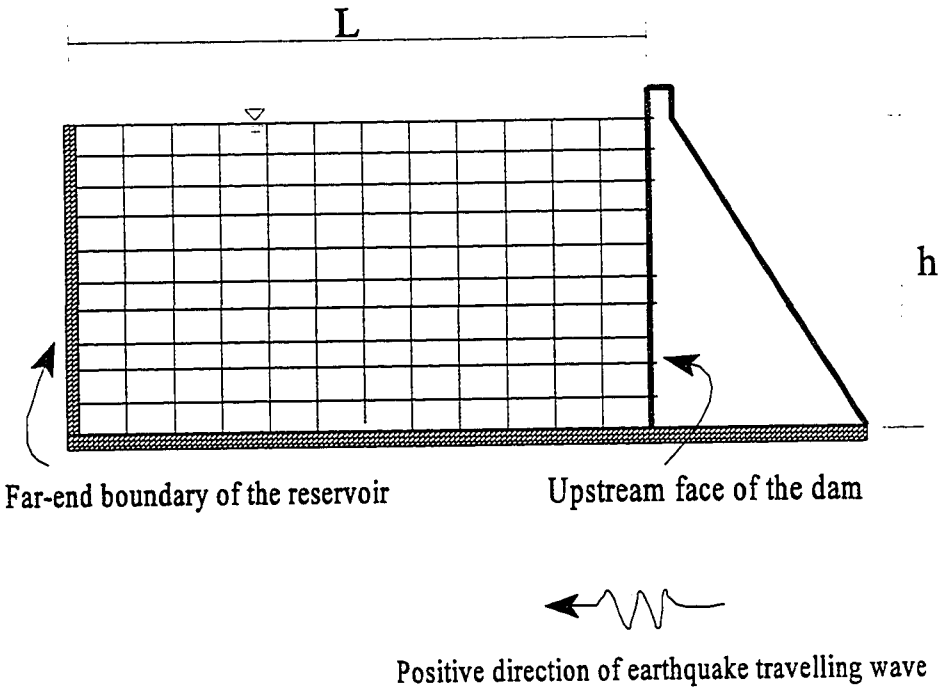

Figure 3.2 Finite element model of reservoir with rigid dam

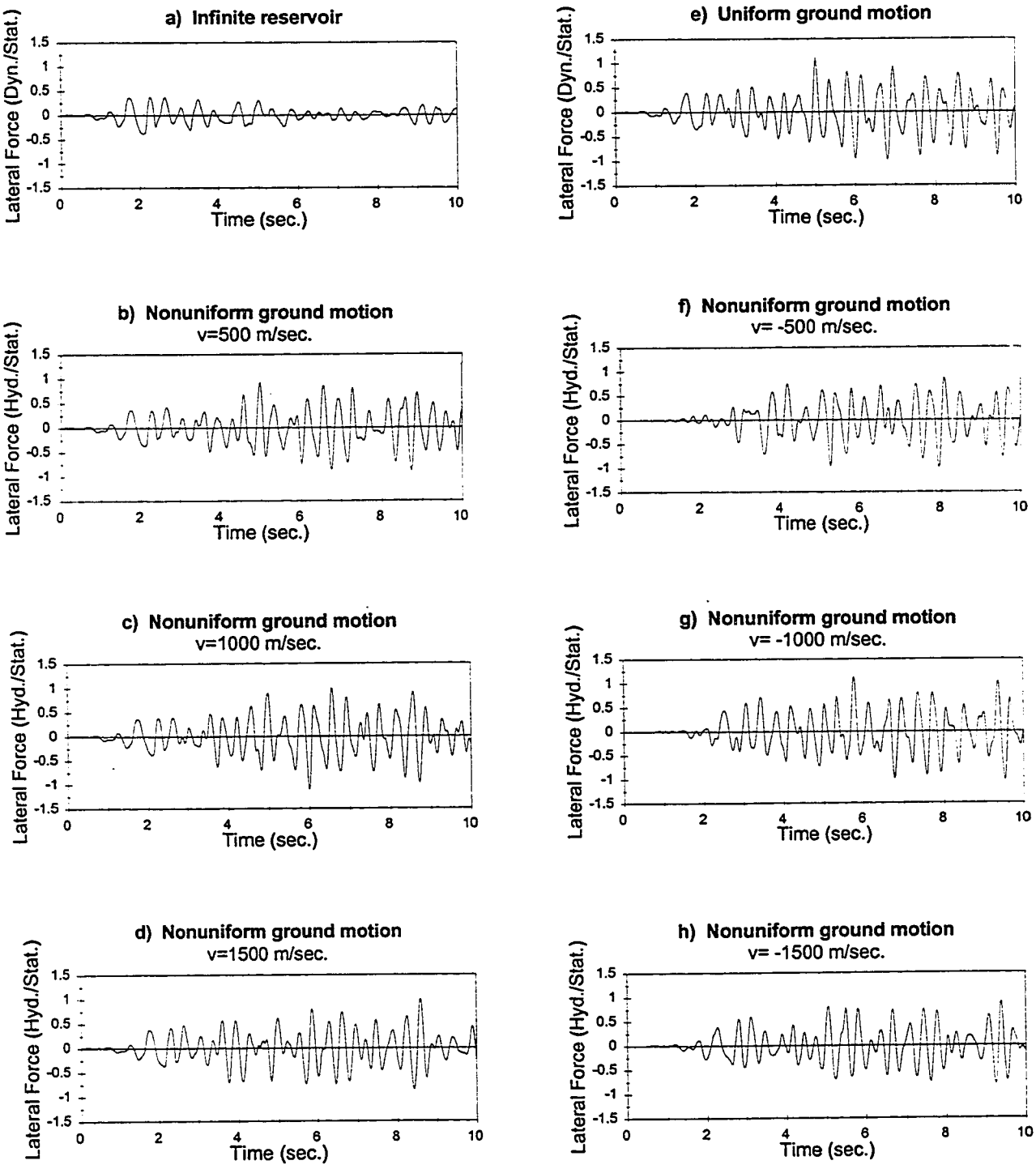

Figure 3.3 Lateral force time history on the upstream face of the rigid dam (Horizontal ground motion, L/h=5)

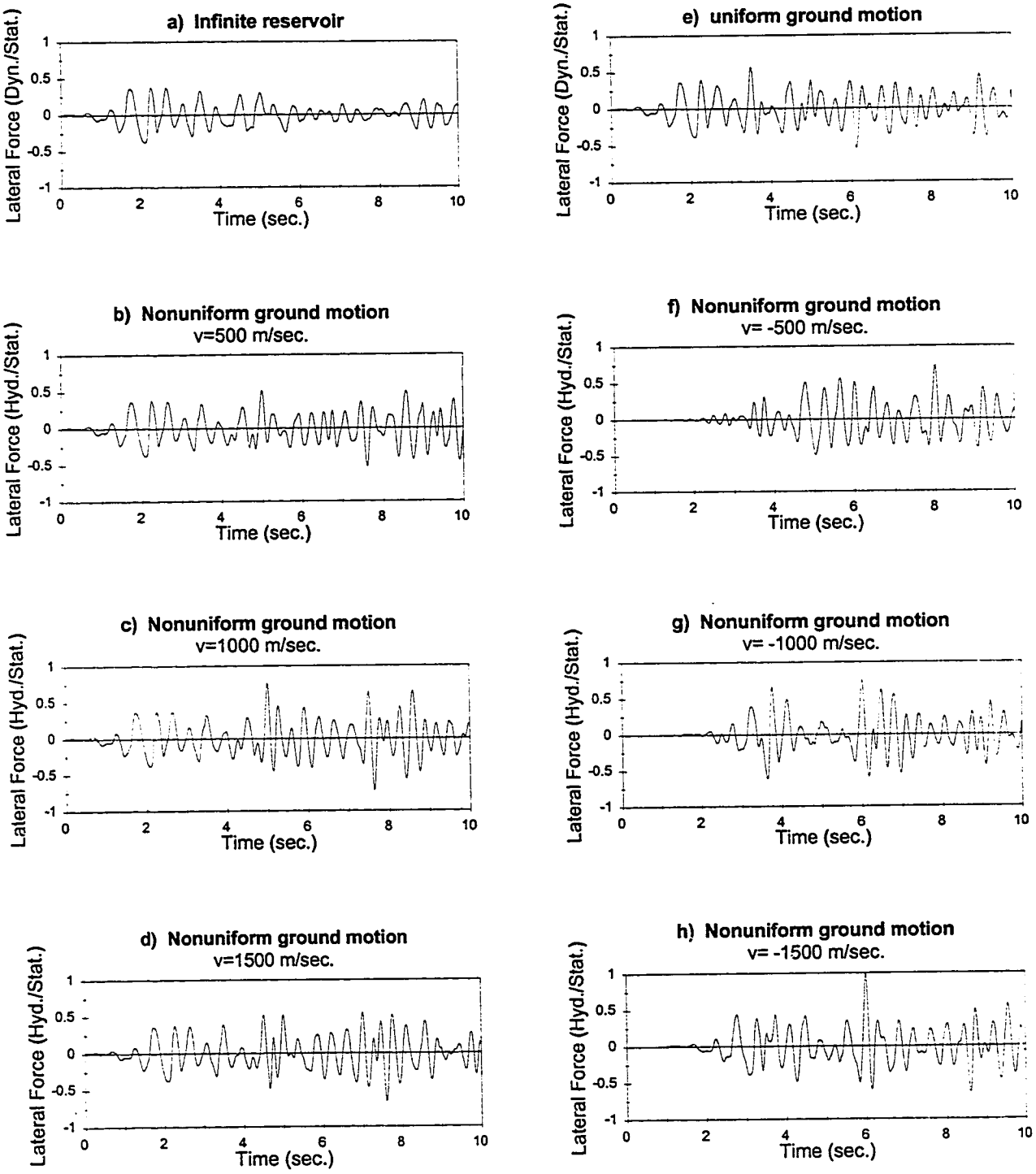

Figure 3.4 Lateral force time history on the upstream face of the rigid dam (Horizontal ground motion, L/h=10)

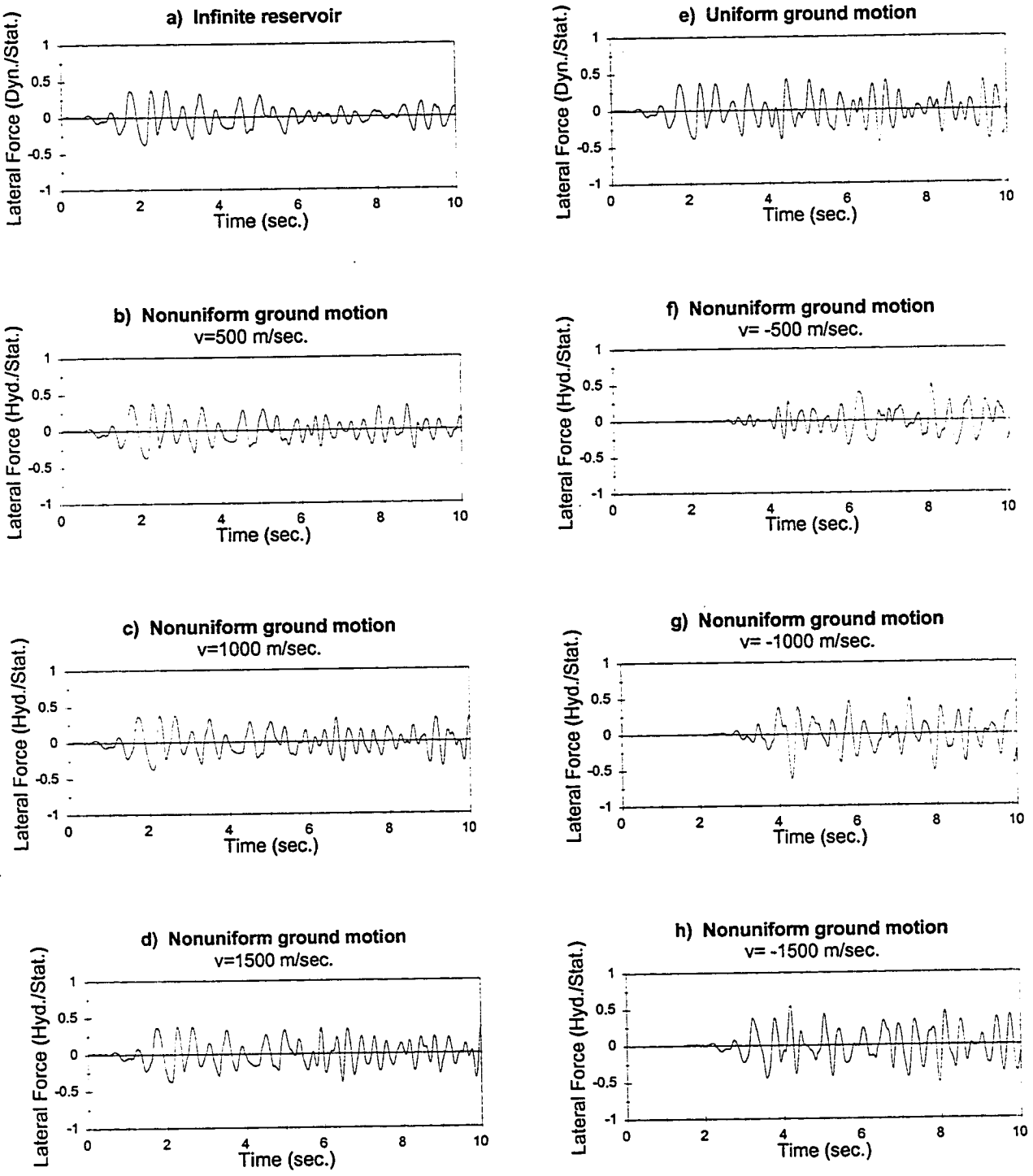

Figure 3.5 Lateral force time history on the upstream face of the rigid dam (Horizontal ground motion, L/ h=15)

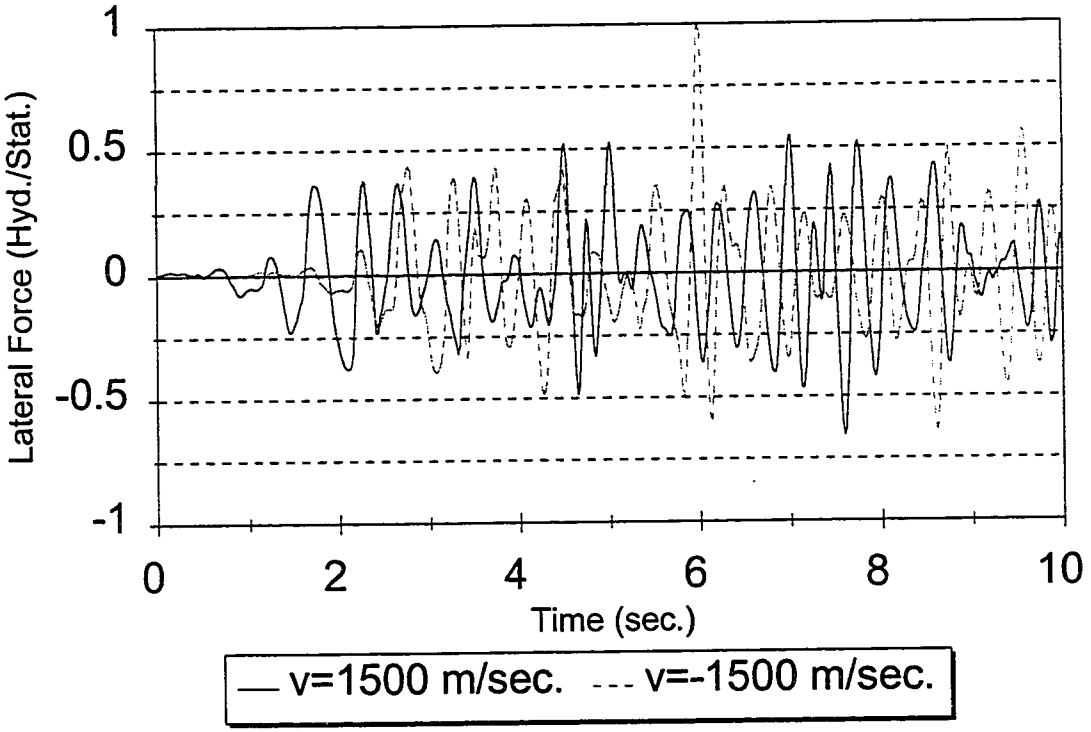

Figure 3.6 Lateral force time history on the upstream face of the rigid dam
(Horizontal ground motion, v=±1500 m/sec., L/h=10)

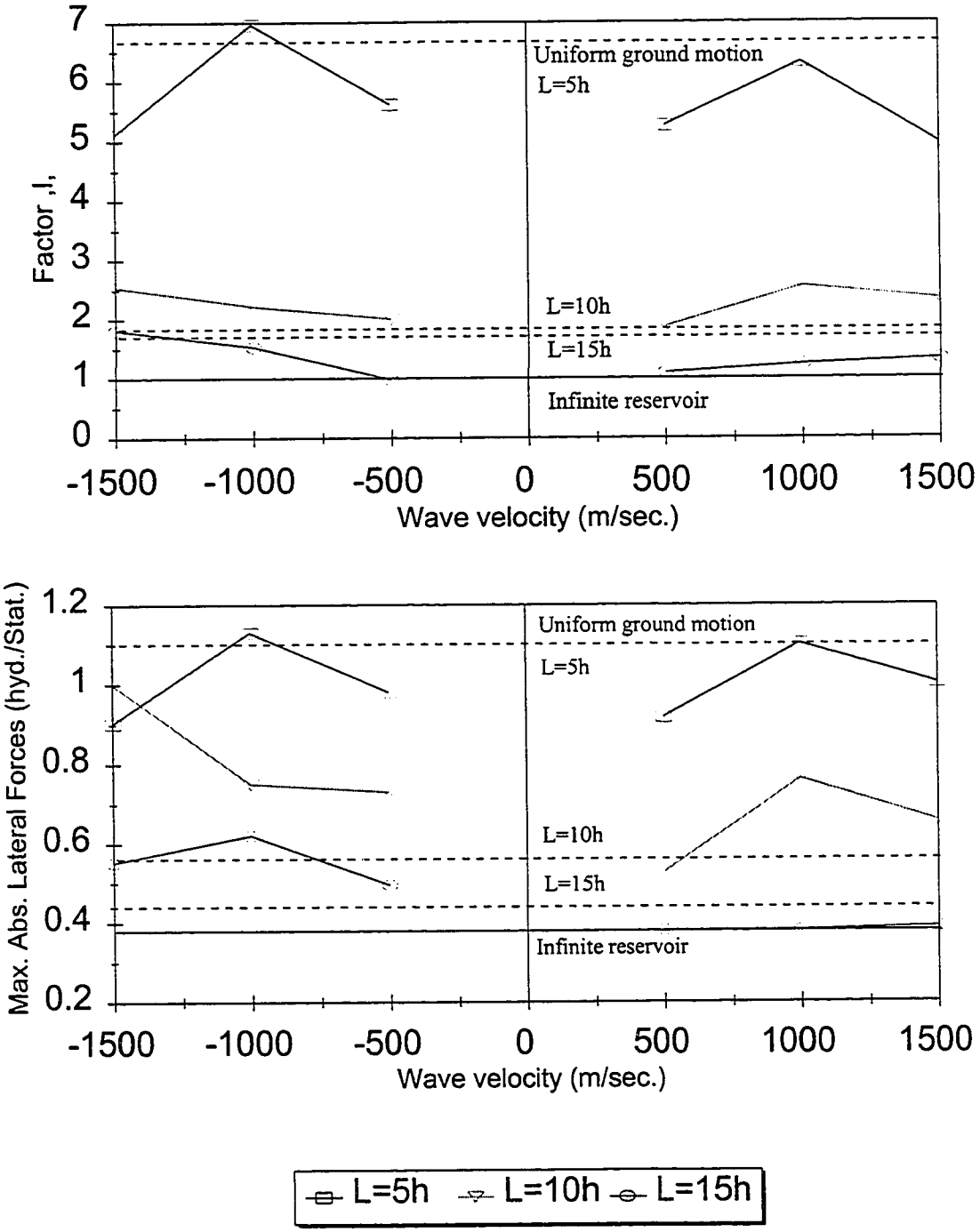

Figure 3.7 Response parameters of the lateral force on upstream face of the rigid dam (Horizontal ground motion)

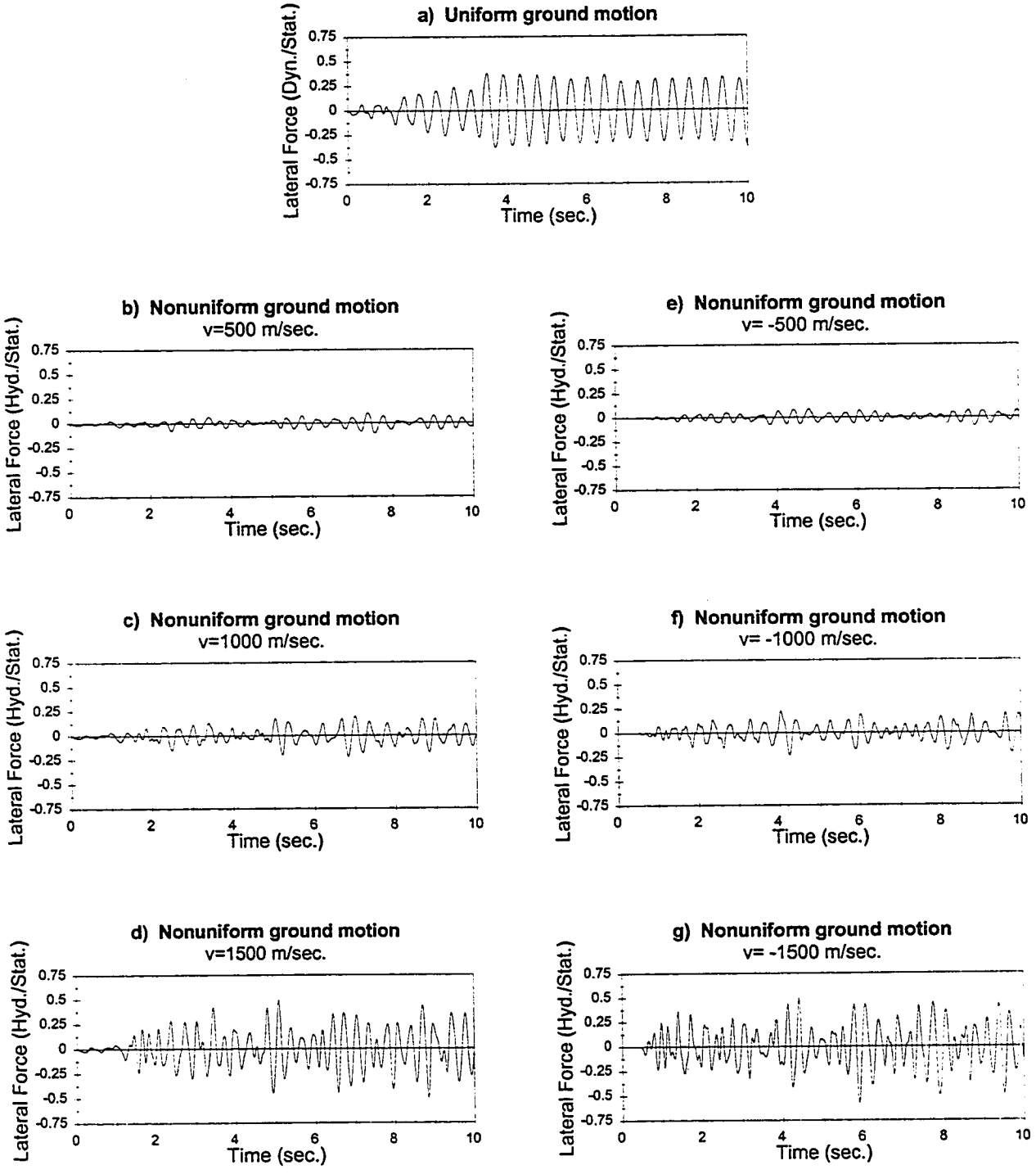

Figure 3.8 Lateral force time history on the upstream face of the rigid dam (Vertical ground motion, L/h=5)

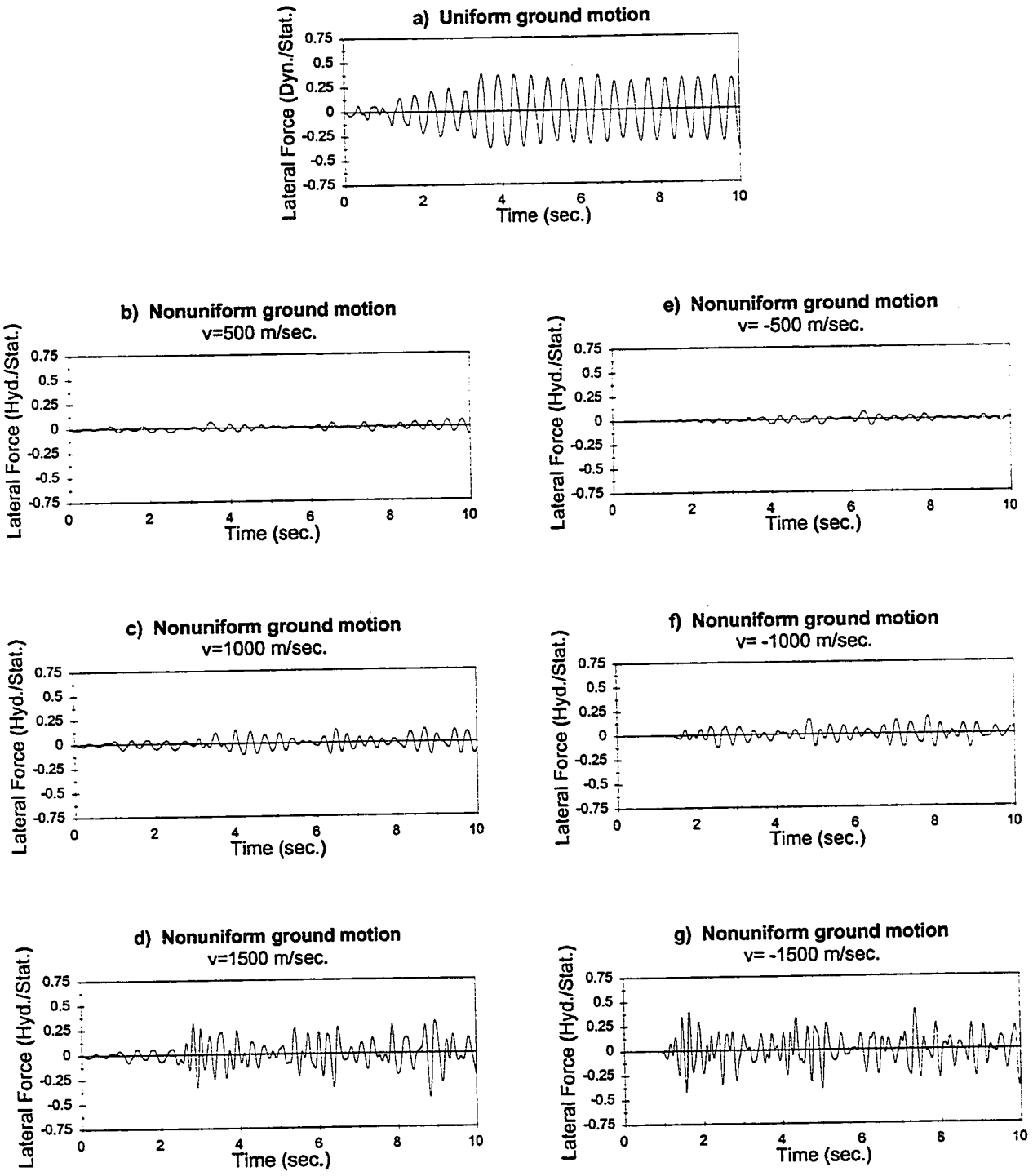

Figure 3.9 Lateral force time history on the upstream face of the rigid dam (Vertical ground motion, L/h=10)

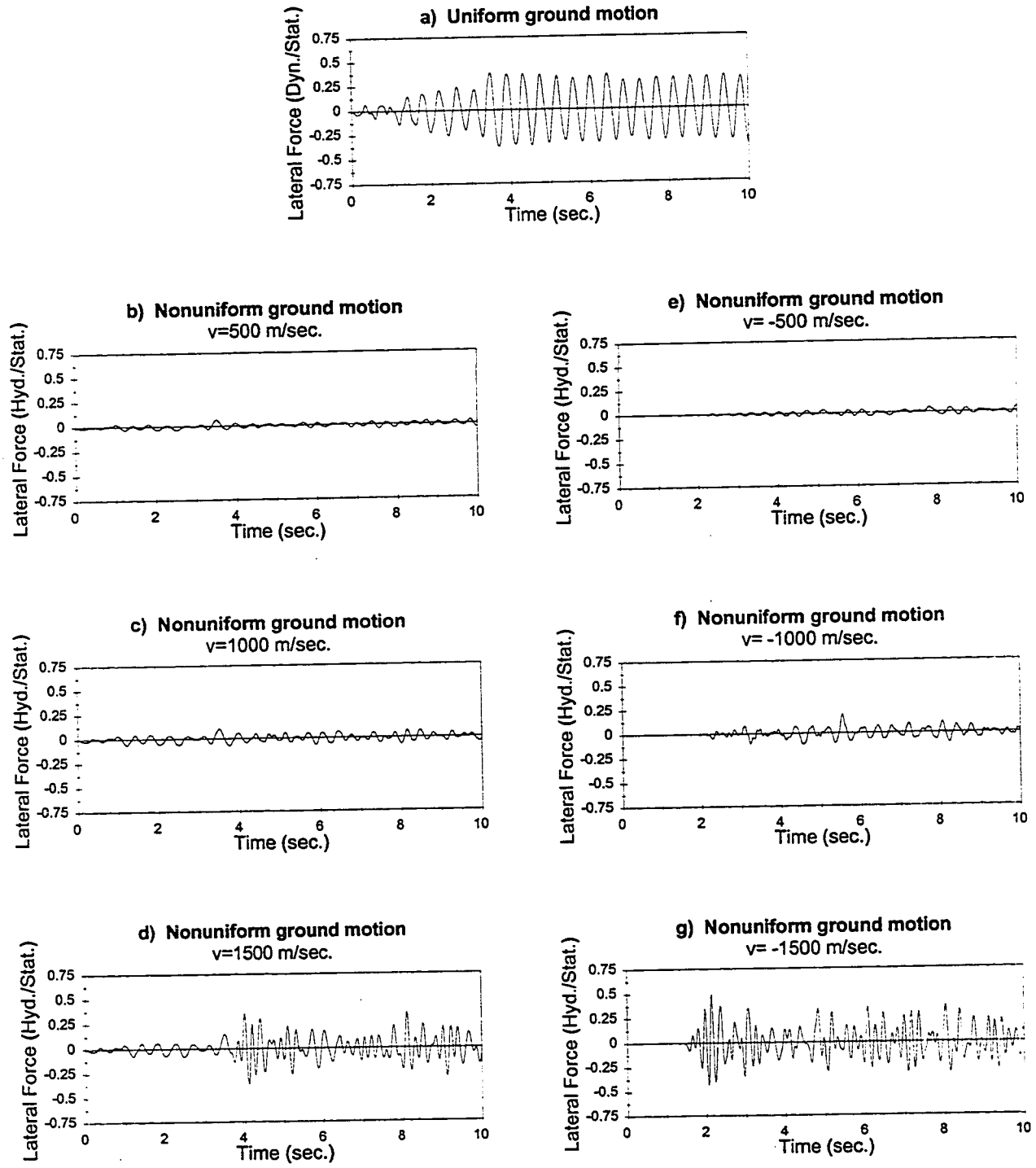

Figure 3.10 Lateral force time history on the upstream face the rigid dam
(Vertical ground motion, L/h=15)

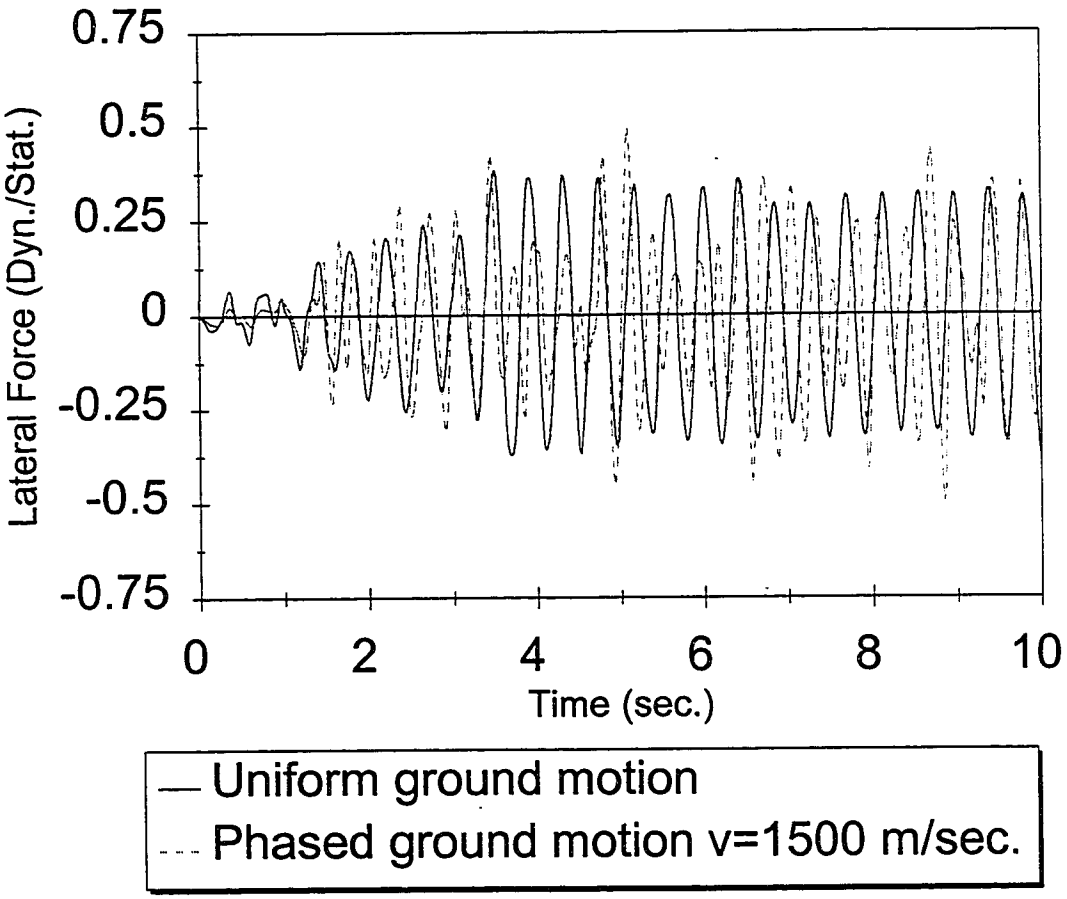

Figure 3.11 Comparison of lateral force time history on the upstream face the rigid dam (Vertical ground motion, L/h=5)

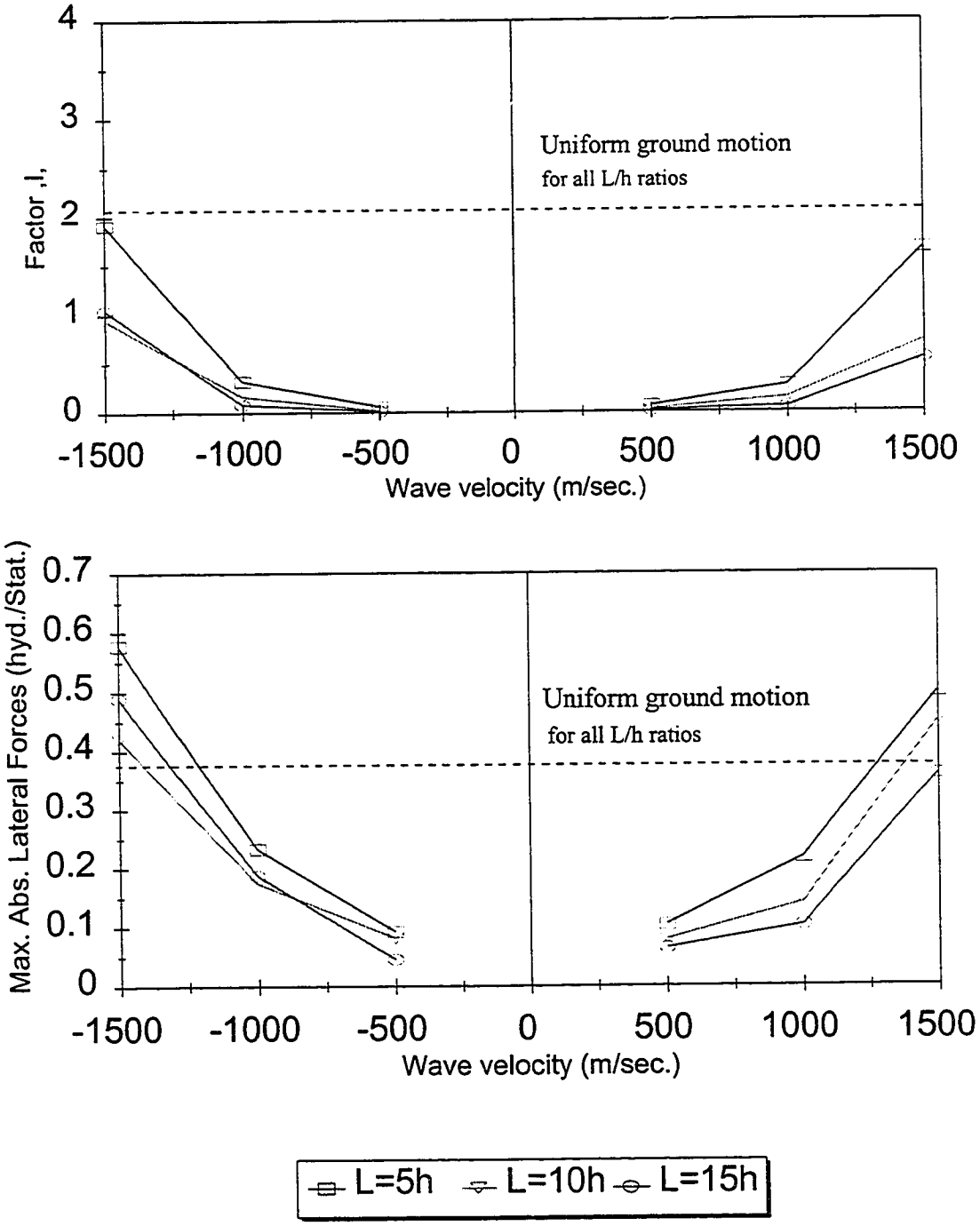

Figure 3.12 Response parameters of the lateral force on upstream face of the rigid dam (Vertical ground motion)

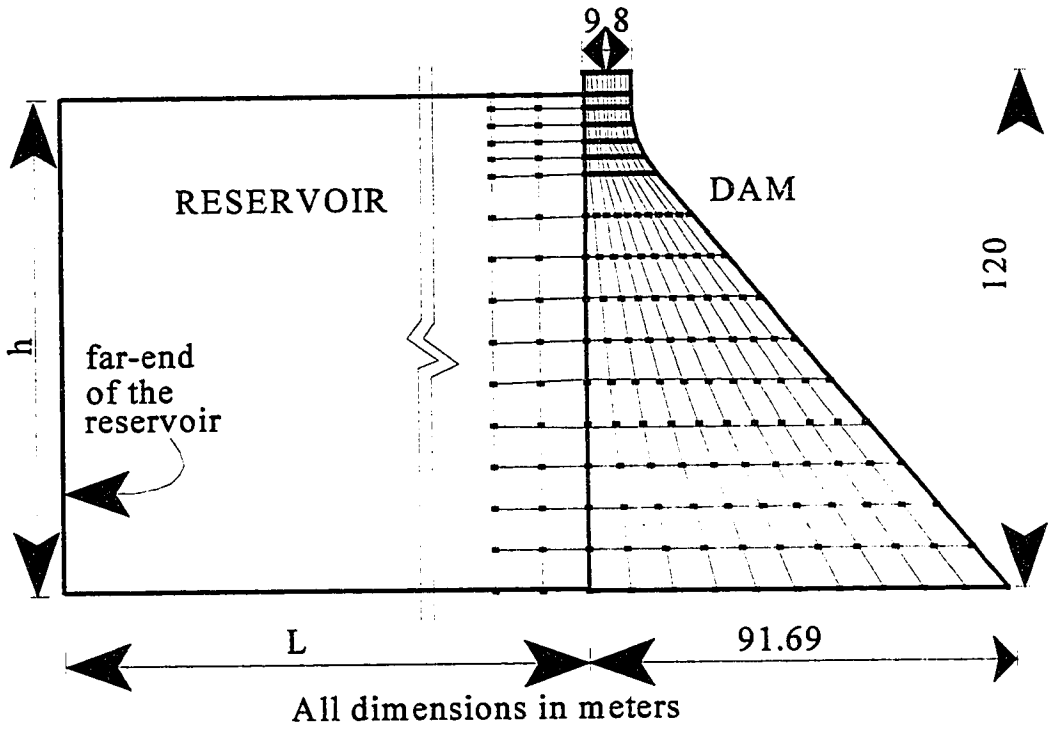

Figure 3.13 Finite element model of the dam-reservoir system

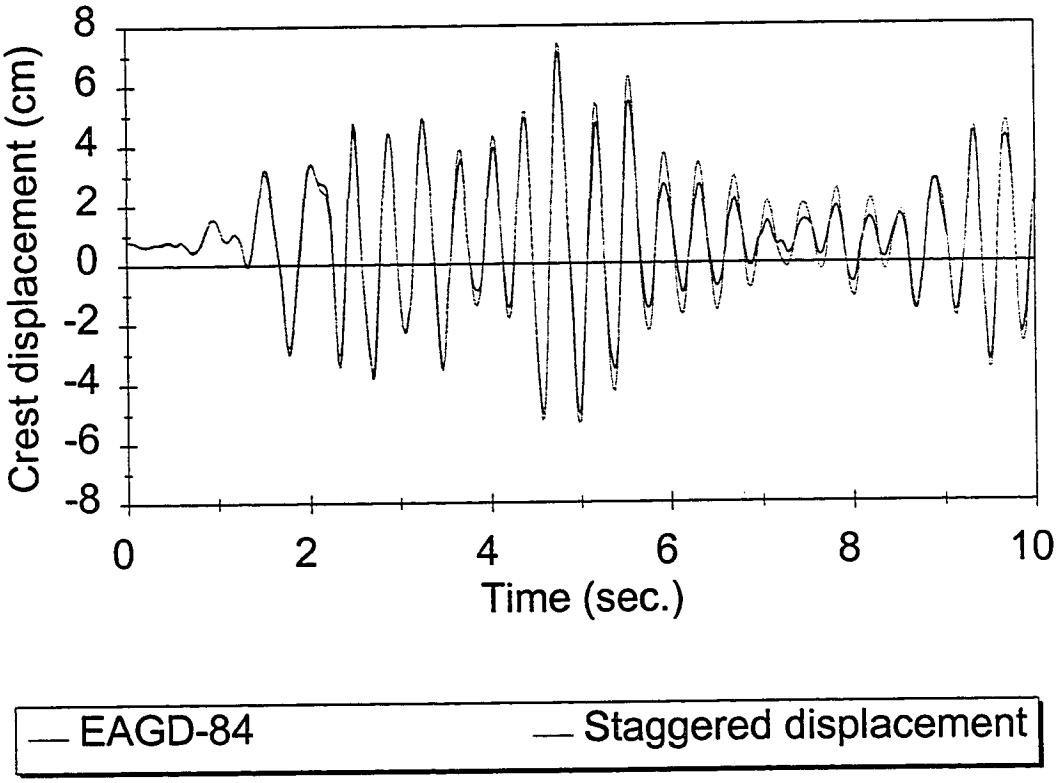

Figure 3.14 Comparison of the dam crest displacement

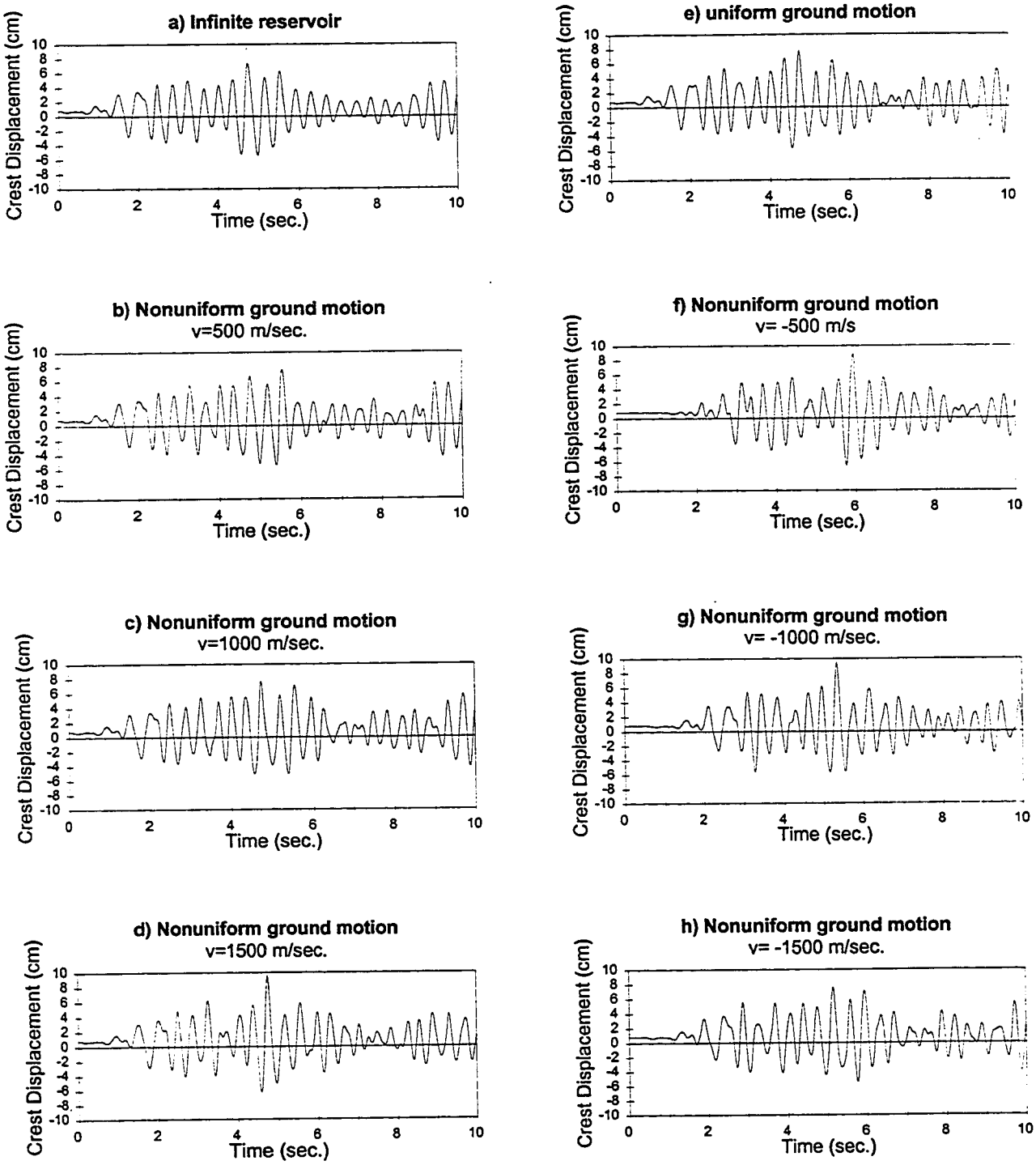

Figure 3.15 Dam crest displacement time history, (Horizontal ground motion, L/h=5)

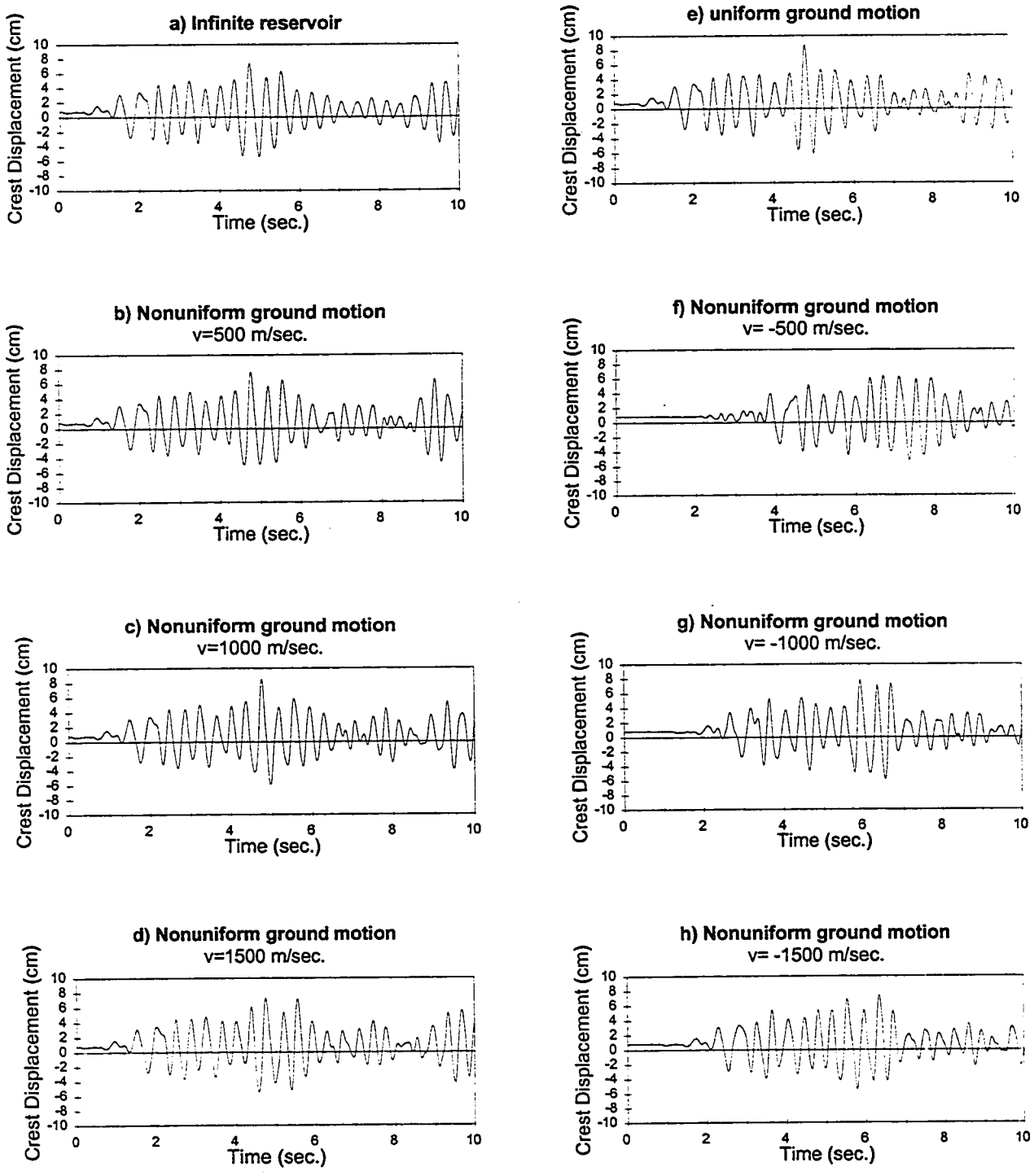

Figure 3.16 Dam crest displacement time history, (Horizontal ground motion, L/h=10)

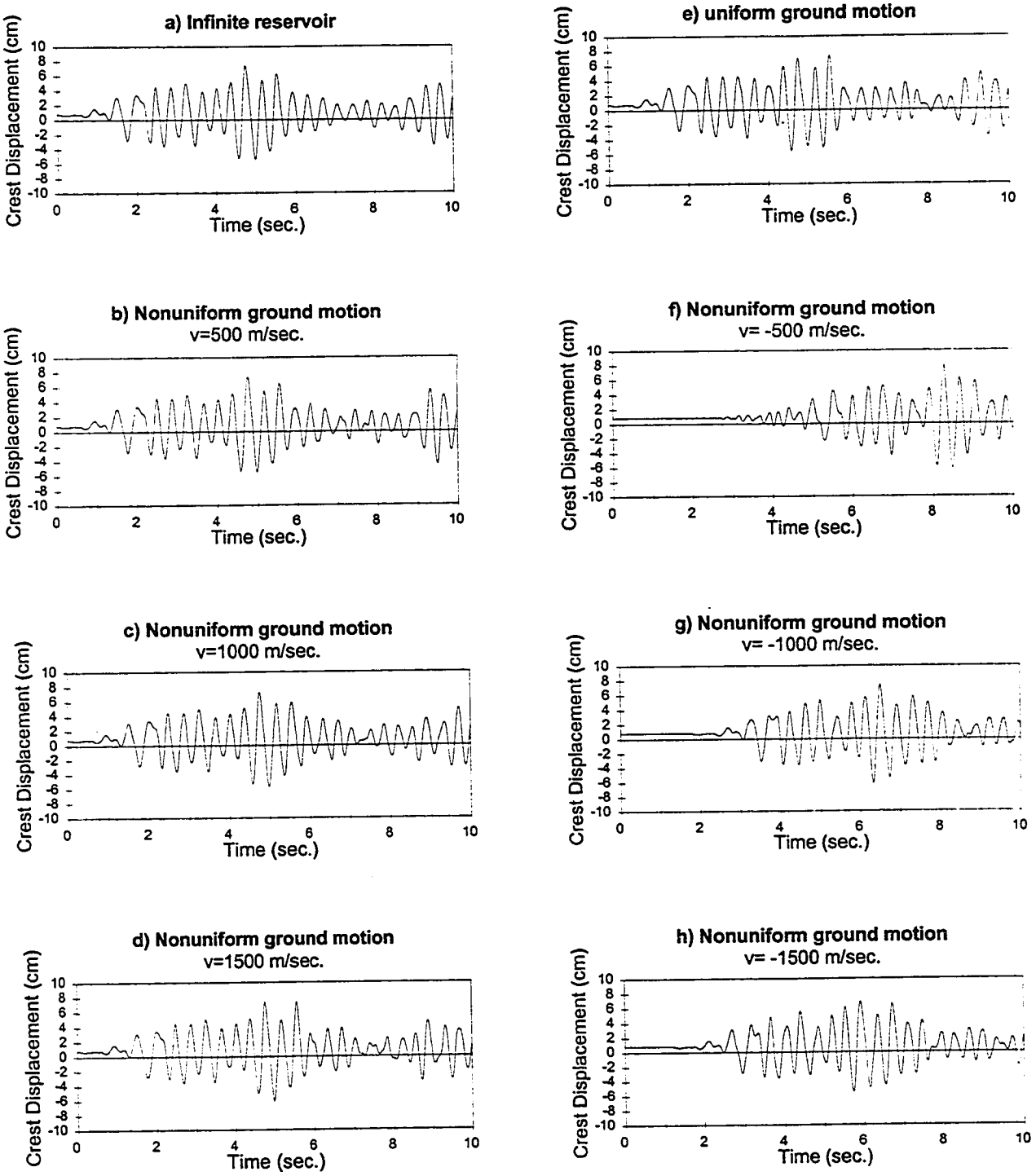

Figure 3.17 Dam crest displacement time history, (Horizontal ground motion, L/h=15)

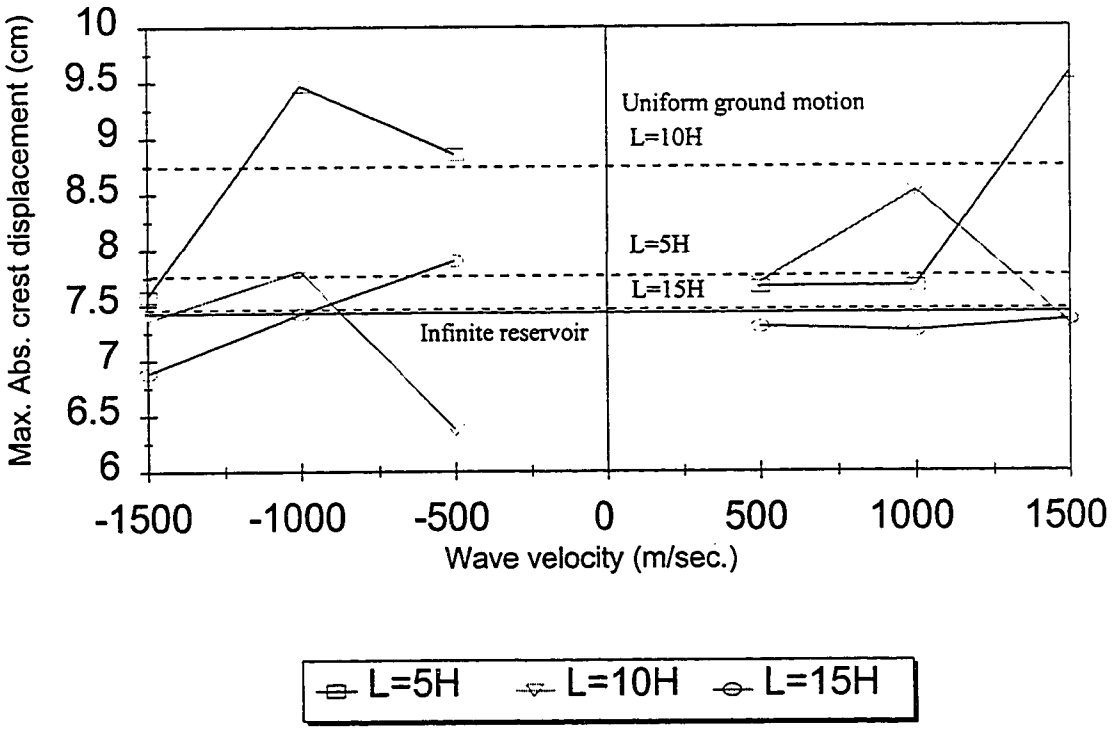

Figure 3.18 Maximum dam crest displacement response under the horizontal earthquake

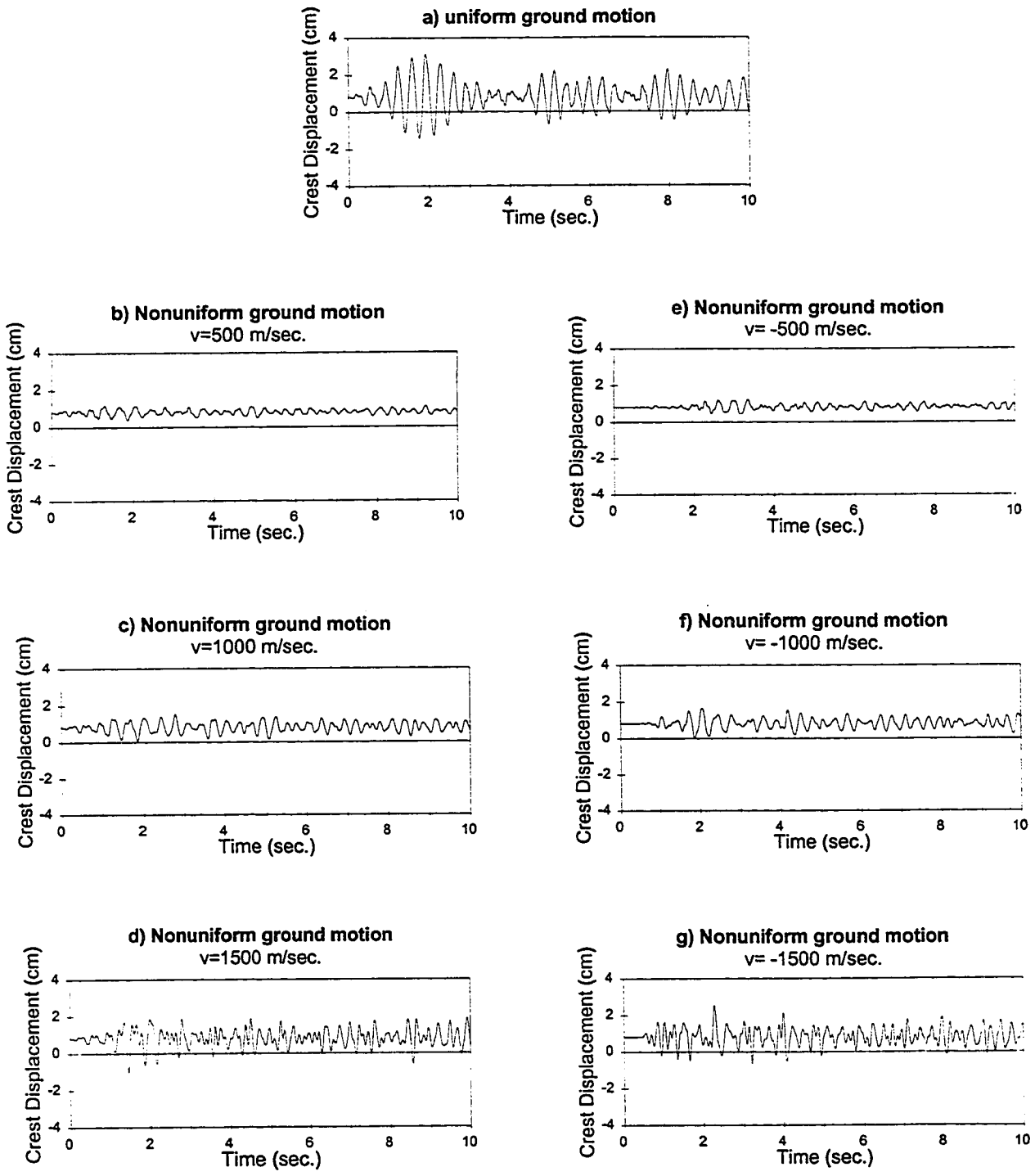

Figure 3.19 Dam crest displacement time history, (Vertical ground motion, L/h=5)

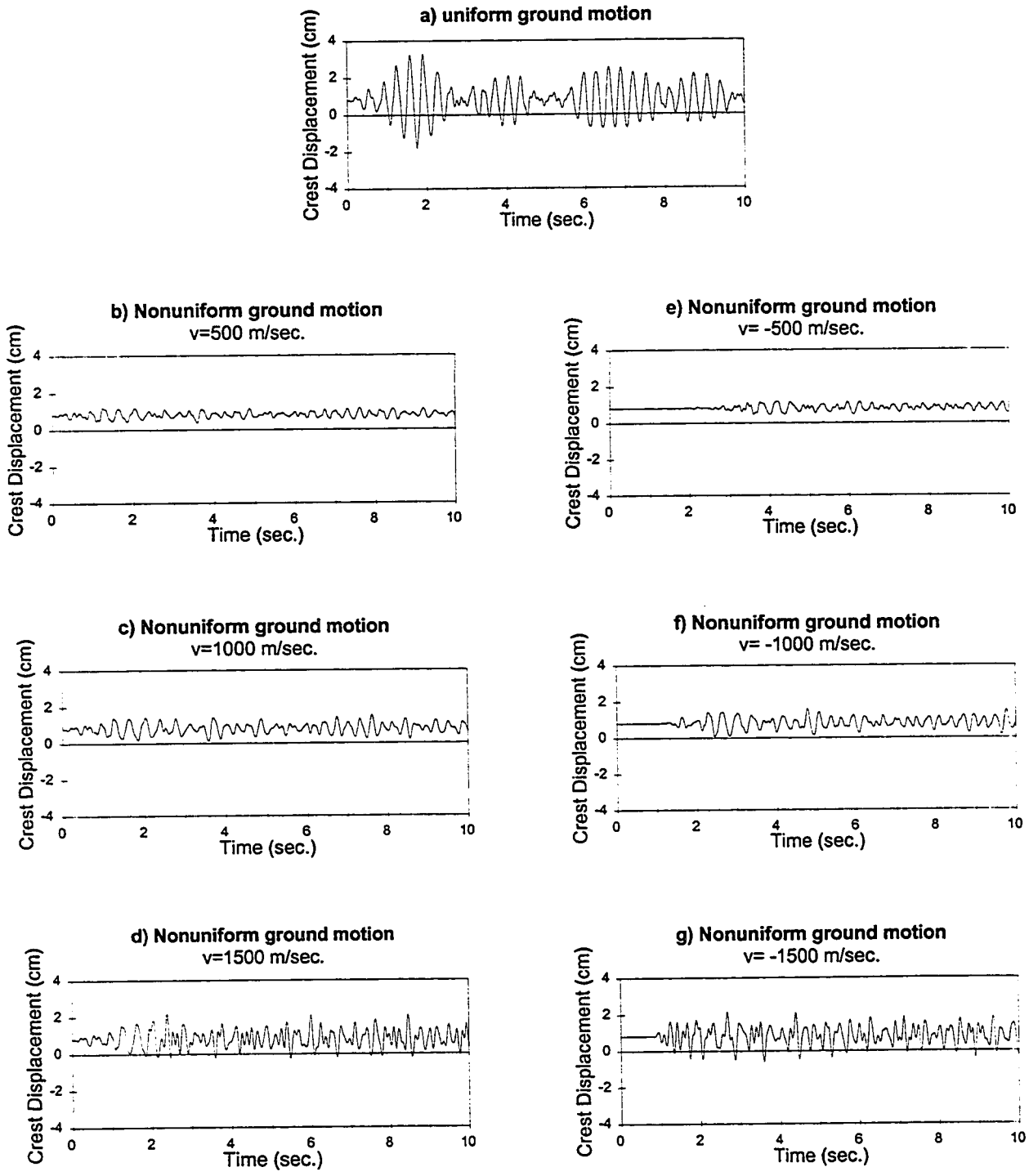

Figure 3.20 Dam crest displacement time history, (Vertical ground motion, L/h=10)

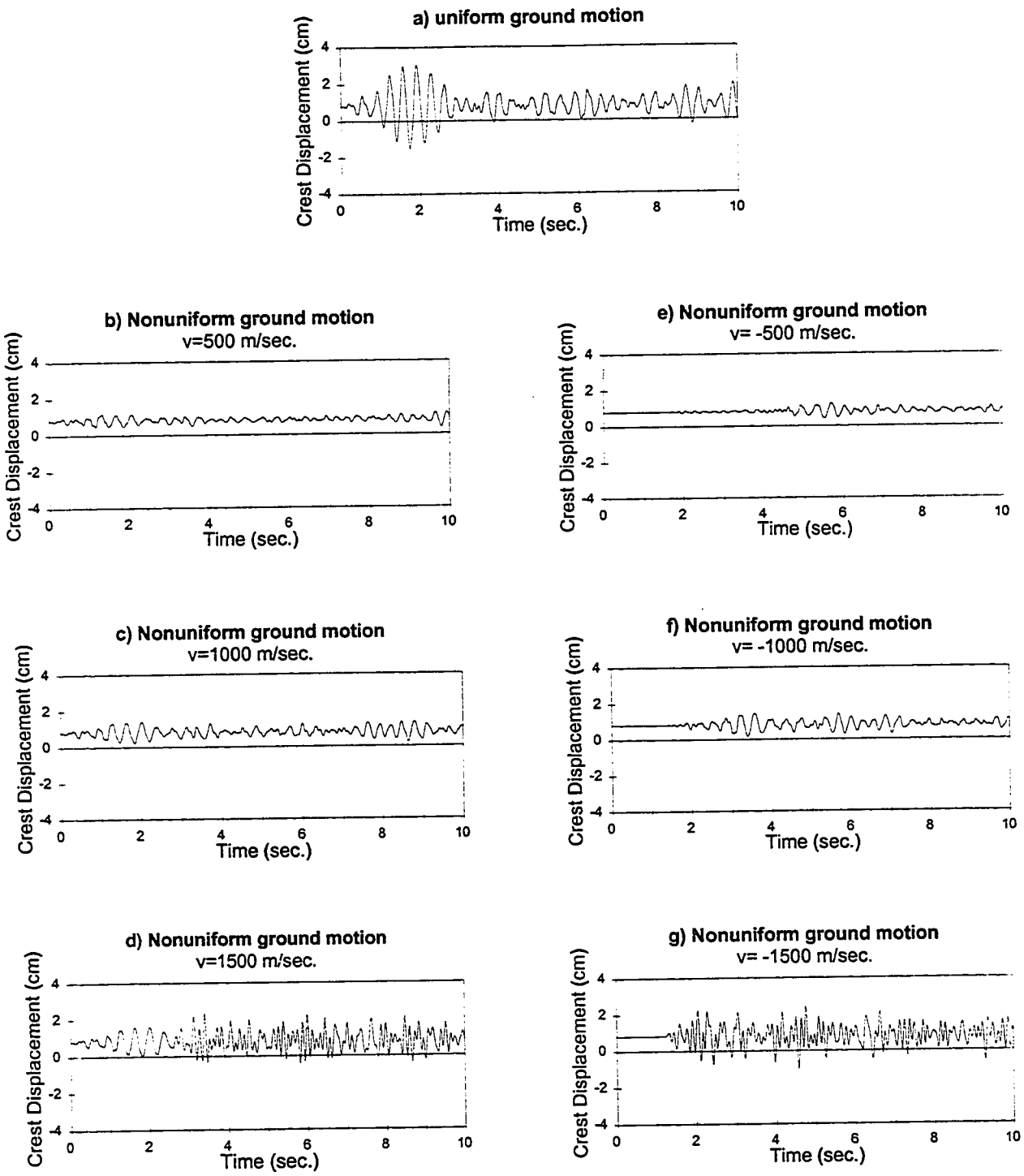

Figure 3.21 Dam crest displacement time history, (Vertical ground motion, L/h=15)

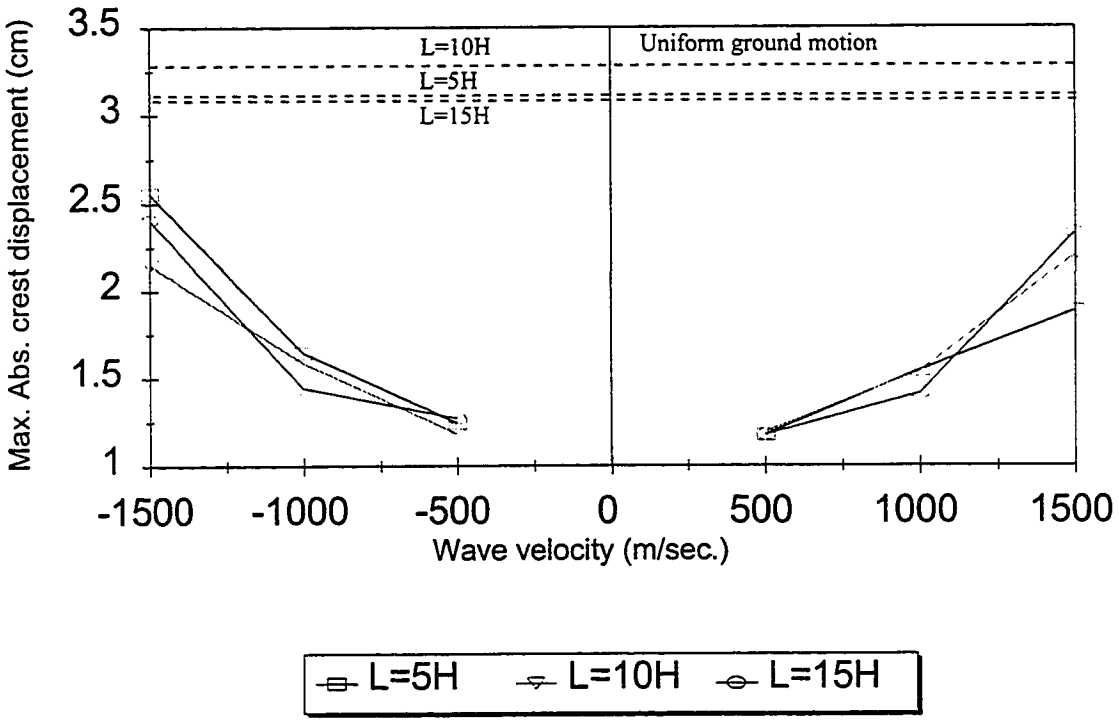

Figure 3.22 Maximum dam crest displacement response under the vertical earthquake

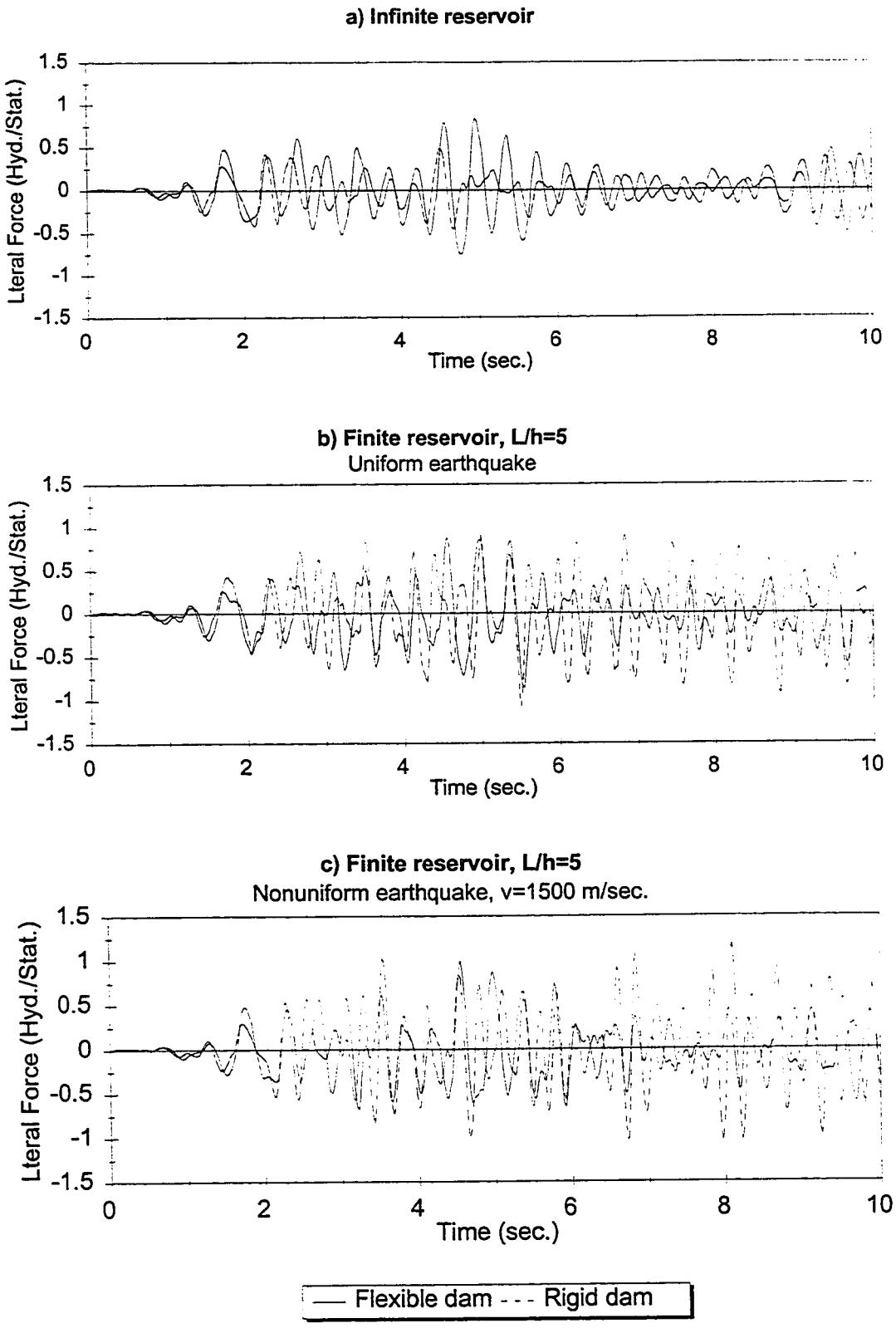

Figure 3.23 Hydrodynamic forces on flexible and rigid dams
(Horizontal ground motion, L/h=5)

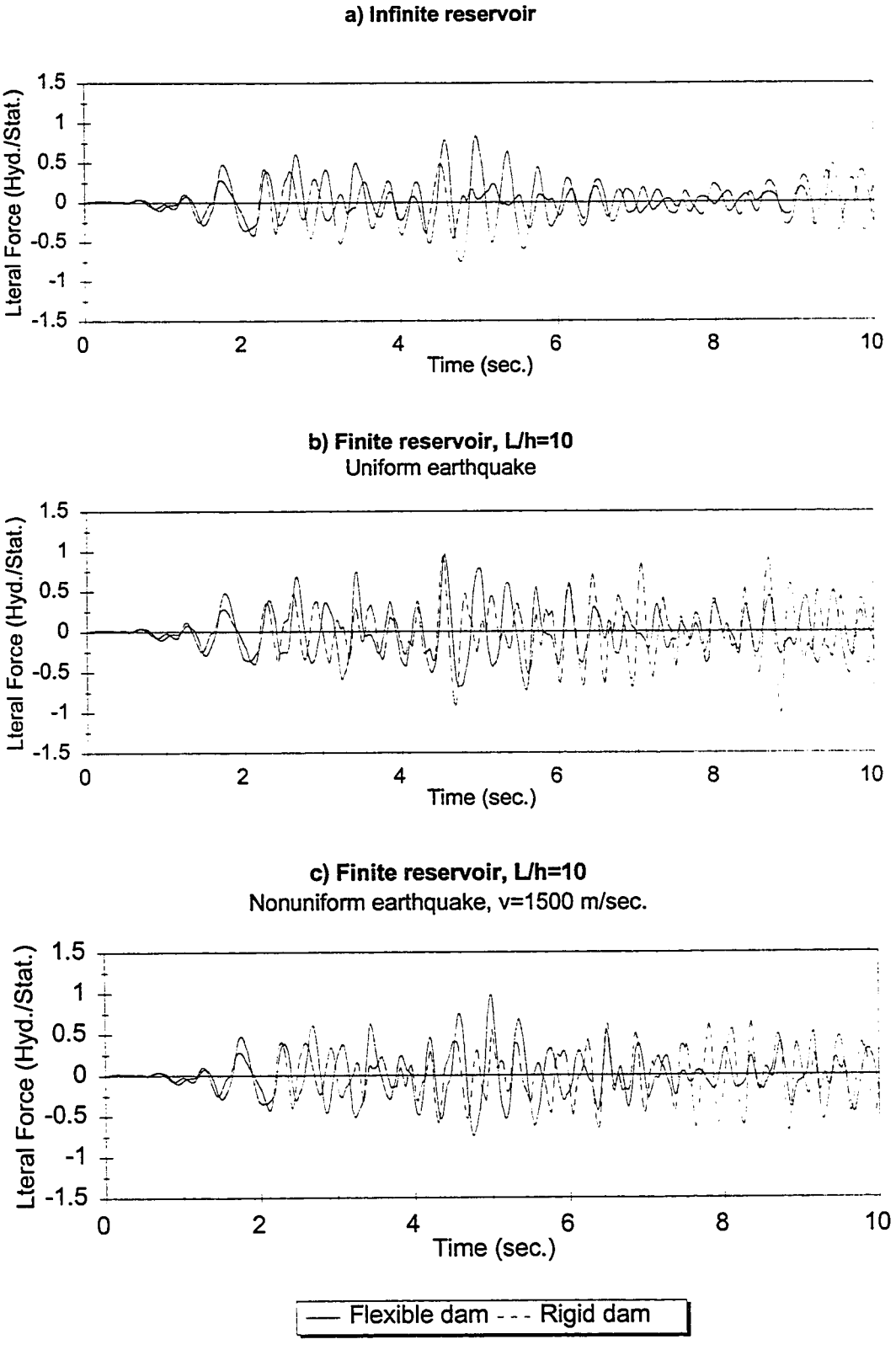

Figure 3.24 Hydrodynamic forces on flexible and rigid dams
(Horizontal ground motion, L/h=10)

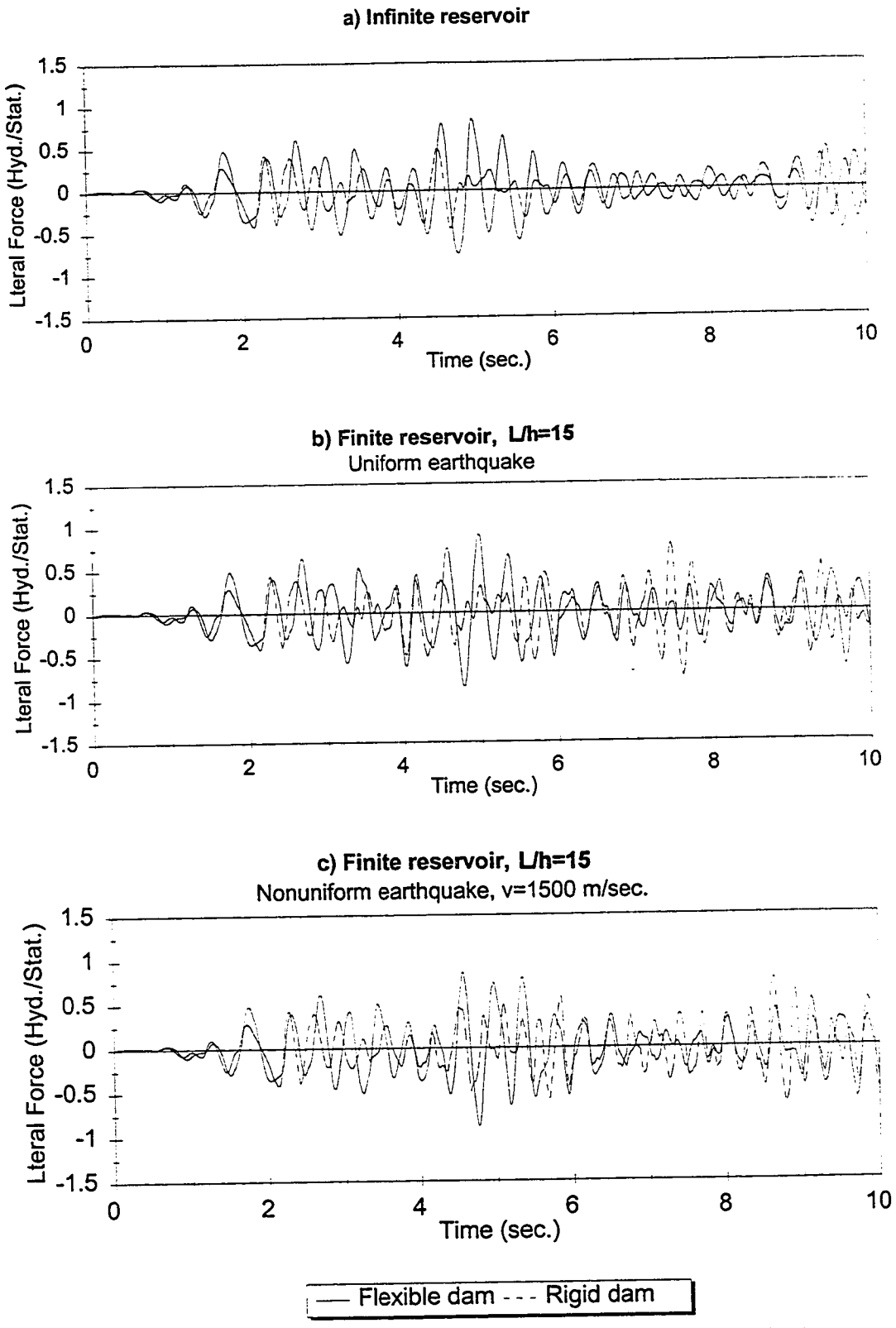

Figure 3.25 Hydrodynamic forces on flexible and rigid dams (Horizontal ground motion, L/h=15)

CHAPTER FOUR

NONLINEAR SEISMIC RESPONSE OF CONCRETE GRAVITY DAMS WITH DAM-RESERVOIR INTERACTION

4.1 INTRODUCTION

The seismic behaviour of concrete dams has been the subject of extensive research during the past decade because few dams suffered severe cracking during earthquakes. Rescher (1990) indicated that most concrete gravity dams will experience cracking even under operational loading conditions and moderate earthquake ground motions. Therefore, the assumption of linear behaviour may not be appropriate in the analysis of the seismic response of concrete gravity dams.

Concrete dams are distinguished from other structures because of their size and their interactions with the reservoir and foundation. The results obtained from the nonlinear analysis of concrete dams are strongly dependent on the approach to modelling of these interactions. It is a difficult task to develop a comprehensive analytical model to include both nonlinearity and interaction effects. The size effect can also influence the properties of the dam concrete. The fracture properties of normal concrete can be determined using laboratory tests. However, the dam concrete differs from the normal weight concrete because of

aggregate size and its poor strength. Little information is available on the fracture properties of the dam concrete. The fracture surface of the dam concrete specimens is characterized by mainly aggregate failure. Saouma et al. (1991) attempted to measure fracture toughness of a concrete specimen in the laboratory which was considered to be similar to dam concrete. They concluded that a definitive decision cannot be made concerning the results and their accuracy. Bruhwiler and Wittmann (1990) carried out a dynamic test to determine the material properties of the dam concrete under high rate of loading and an initially applied compression load. They found that the fracture energy of dam concrete is 2 to 3 times higher than that of ordinary concrete. The reason is related to the tensile strength characteristic of dam concrete. The tensile behaviour of concrete can be divided into two stages. In the first stage, the behaviour is linear until the tensile strength is reached. In the second stage, strain softening behaviour is observed. Fracture energy is sensitive to the tensile stress. In addition, increasing the preloading decreases the fracture energy.

To understand the nonlinear behaviour of concrete dams, modelling of the cracking and damage process is needed. Bazant and Oh (1983) proposed a fracture mechanics approach as a blunt smeard crack band. The proposed approach represented a significant advance in comparison to the linear fracture theory. The strain softening of the material was considered based on the fracture parameters, fracture energy, uniaxial tensile strength and crack band width. Fracture energy can be determined from the complete stress-strain curve. Formulas were derived to give the fracture parameters.

Two classes of solutions can be found in the nonlinear study of concrete gravity dams. Discrete crack approach is the first class of solutions which is based on the variable

mesh approach. Two methods of linear elastic fracture mechanics LEFM, and nonlinear fracture mechanics NLFM, can be used in this approach. The second class of solutions is the continuum model in which a fixed finite element mesh is used. Smeared crack model and damage mechanics are the two methods of solution in this class.

Bhattacharjee and Léger (1994) applied NLFM to predict the response of concrete gravity dams. The experimental work done on a model of a concrete gravity dam and a small beam specimen confirmed the applicability of the proposed NLFM approach. The coaxial rotation crack model gives a better response than the fixed crack model. Léger and Leclerc (1996) studied the nonlinear response of concrete gravity dams subjected to different earthquake ground motions. They found that the response is sensitive to time variation of the input motion. Most of the time, cracking response showed that the crack starts from the downstream side and moves toward the upstream side. This form of cracking does not promote dam instability. The cracks are either horizontal or they sloped downward. They found that the vertical ground motion acceleration component is not critical in seismic cracking response of dams.

The nonlinear response of a concrete gravity dam with an initial distribution of temperature gradient when subjected to the earthquake was studied by Léger and Bhattacharjee (1995). They used frequency-independent added mass matrix as a representative of dam-reservoir-foundation interaction. The reservoir and foundation were modelled as a series of dampers and springs such that the same response can be obtained for the linear response of the crest when compared with the case of actual interaction. Under earthquake excitation, when a rigid foundation is assumed with no reservoir bottom

absorption, no crack was observed at the top part of the dam. A crack was formed at the foundation level.

Bhattacharjee and Léger (1993); Léger and Bhattacharjee (1994) studied the energy response of concrete gravity dams. They used a stiffness proportional damping with α-method of integration. Newton-Raphson iteration technique was used to remove the unbalanced load. An energy balance error approach is used as a measure of damage. The seismic analysis of Koyna dam under both horizontal and vertical components of the earthquake was conducted. Without introducing the numerical damping, the analysis stopped after the first few seconds because of energy balance error due to spurious deformation of some elements. No discrepancies were found in the results of the analysis before the occurrence of instability, when compared with the case of α= -0.2 in which the analysis was successfully completed. Dissipated fracture energy is negligible in comparison to other sources of energy dissipation. The reservoir effect was represented by added mass technique.

The effect of hydrodynamic pressure inside the crack in the seismic analysis of concrete gravity dams was investigated by Tinawi and Guizani (1994). The pressure inside the crack does not change the response of the dam significantly. It was found that under high frequency content earthquakes, the hydrodynamic pressure inside the crack may increase when higher modes are significant. At the base of the dam, the hydrodynamic pressure may be 50% higher than the hydrostatic pressure.

The nonlinear response of the Pine Flat dam was studied using the discrete approach (Wepf et al. 1993). A fictitious crack approach was used to model the crack tip. Reservoir interaction was modelled using a boundary element. Linear response of the dam was

compared with EAGD-84 code analysis and good agreement was found. The nonlinear response of the dam including reservoir interaction was strongly affected in comparison with the added mass approach. The slope of the reservoir bottom strongly influenced the nonlinear response. The aggregate interlock effect was found to be important in the final cracking configuration of the dam.

The cracking response of a concrete gravity dam when subjected to earthquake loading can be different if nonuniform damping or uniform damping including the damping due to cracking is considered (Barrett et al., 1991). In the analysis, the dam was represented by a small number of elements. When the bottom few elements were cracked, a noticeable change in the response was observed.

Using different computer codes, Singhal (1991) found that the Westergaard's added mass approach yields higher values for crest displacement and stress than that obtained using other approaches. The reservoir bottom absorbtion and water compressibility did not change the response significantly.

Pekau et al. (1991, 1995) and Pekau and Batta (1991) presented a method to study the cracking of concrete gravity dams using the principle of Linear Elastic Fracture Mechanics (LEFM) and boundary element mode superposition analysis. The model was checked by a shake table test of cantilever beam made of gypsum. The impact of cracking surface was modeled as a load pulse.

Ayari and Saouma (1990) proposed a model for simulation of discrete crack closure. The model was applied in the dynamic analysis of the Koyna dam (India) under both horizontal and vertical components of the earthquake. The results were obtained for 5

seconds only of the earthquake in which the numerical damping was less than 10%.

Nonlinear seismic response of concrete gravity dams was studied by Skrikerud and Bachmann (1986). Fracture mechanics analysis using discrete crack approach was applied. The model was capable of initiation, opening, closing and reopening of discrete cracks. Special treatment was used to model aggregate interlock effect. The model was applied to a dam of rigid foundation with empty reservoir. The crack pattern was found to be very sensitive to the parameters chosen for the analysis. The first four seconds of an artificially generated time history was used for the purpose of analysis. The analysis stopped due to excessive damage. Nonlinear response of concrete gravity dams was also studied by Feltrin et al. (1990). A rigid foundation was assumed for Pine Flat dam and the reservoir interaction was included. The nonlinearity in concrete behaviour included the strain softening and aggregate interlock. Response of the linear model with and without the reservoir interaction was determined. Nonlinear response of the empty reservoir was studied by scaling the ground motion until cracking occurred. The cracks started at the top part from down stream face of the dam near the slope discontinuity and moved horizontally. A different response was observed under the effect of reservoir interaction. The first crack started at the foundation level and then it followed by a crack at the top part of the dam at the same location of the crack of empty reservoir case. The crest displacement was found to be higher than that of the empty reservoir. They concluded that the effect of dam-reservoir interaction must be included in the nonlinear analysis.

El-Aidi and Hall (1989 a,b) investigated the nonlinear response of concrete gravity dams. The water cavitation in addition to cracking of concrete was considered. Despite the

difficulties involved, the nonlinear model was applied for the case of preformed base crack, top crack and homogeneous dam without any cracks. In the case of homogeneous dam, the top crack initiated at t= 1.965 sec. Soon after initiation of the top crack, it went through the dam body and almost separated the top part from the rest of the dam. During the rest of the analysis, no other cracks were observed and only rocking and opening and closing of the crack were observed.

Fenves and Vargas-Loli (1988) proposed a method for dam-reservoir interaction which resulted in a symmetric matrix representation of the total equation of the system. The nonlinearity of the reservoir was introduced into the proposed method to investigate the reservoir interaction effect. They found that the effect of cavitation is not significant in the response of the structure.

Mlakar (1987) studied the nonlinear dynamic behaviour of concrete gravity dams using the ADINA code. It was found that the crack first started at the base. Then cracking initiated at the top part near slope discontinuity. The cracks near the slope discontinuity propagated instantaneously and passed through the cross section.

In this chapter the nonlinear fracture response of concrete gravity dams due to seismic loading is investigated. The dam-reservoir interaction is included in the time domain analysis using the method of staggered displacement. Smeard crack approach based on a nonlinear fracture mechanics crack propagation criterion is used to study the cracking and response of concrete gravity dams.

4.2 DISCRETIZATION OF THE COUPLED DAM-RESERVOIR EQUATIONS USING THE α-METHOD

The nonlinear seismic analysis of concrete gravity dams includes opening and closing of the cracks due to the cyclic nature of the earthquake. When the cracks are closed, cracked elements recover their strength and therefore the structure gains stiffness. As the cracks open, the stiffness of the structure reduces. The effect of opening and closing of cracks introduce high frequency shock waves into the structure. The numerical difficulties due to opening and closing of cracks can be overcome by using the α-method (Hilber et al., 1977; Hilber and Hughes, 1978).

The α-method of time integration algorithms introduces numerical damping to the system. It is an efficient method that is accurate in lower modes and dissipate energy in the higher modes when compared with other time integration techniques. Thus, using the α-method ensures that the response of higher modes is damped out.

Direct integration is used to determine the displacement and hydrodynamic pressure at the time increment i+1. The α-method is used for discretization of both equations of the coupled field problem (implicit-implicit method).

The governing field equations, equations (2.1) and (2.2), at time i+1 can be written as follows:

$$[M]\ \{\ddot{U}\}_{i+1} + [C]\ \{\dot{U}\}_{i+1} + (1+\alpha)\ [K]\ \{U\}_{i+1} = \{F_1\}_{i+1} + [Q]\ \{P\}_{i+1} + \alpha\ [K]\ \{U\}_i \tag{4.1}$$

$$[G]\ \{\ddot{P}\}_{i+1} + [C']\ \{\dot{P}\}_{i+1} + (1+\alpha)\ [K']\ \{P\}_{i+1} = \{F_2\}_{i+1} - \rho\ [Q]^T\ \{\ddot{U}\}_{i+1} + \alpha\ [K']\ \{P\}_i \tag{4.2}$$

where α is the integration parameter which is introduced in the coupled field equations. The coupled field equations (4.1) and (4.2) can be solved using the staggered displacement solution scheme. In this method, equations (4.1) can be approximated as:

$$[M]\ \{\ddot{U}\}^*_{i+1} = \{F_1\}_{i+1} + [Q]\ \{P\}^p_{i+1} - [C]\ \{\dot{U}\}^p_{i+1} - (1+\alpha)\ [K]\ \{U\}^p_{i+1} + \alpha\ [K]\ \{U\}_i \tag{4.3}$$

where $\{P\}^p_{i+1}$, $\{\dot{U}\}^p_{i+1}$ and $\{U\}^p_{i+1}$ are given by equations (2.25), (2.26) and (2.28). Combining equations (4.3) and (4.1) using equations (2.25), (2.26) and (2.28) gives:

$$[M]\ \{\ddot{U}\}_{i+1} = [M]\ \{\ddot{U}\}^*_{i+1} + \beta\Delta t^2\ [Q]\ \{\ddot{P}\}_{i+1} - \gamma\Delta t\ [C]\ \{\ddot{U}\}_{i+1} - (1+\alpha)\ \beta\Delta t^2\ [K]\ \{\ddot{U}\}_{i+1} \tag{4.4}$$

The lumped mass results in a diagonal mass matrix, this property is utilized in modifying equation (4.4) such that:

$$[M]\ \{\ddot{U}\}_{i+1} = [M]\ \{\ddot{U}\}^*_{i+1} + \beta\Delta t^2\ [Q]\ \{\ddot{P}\}_{i+1} \tag{4.5}$$

Substituting equation (4.5) into equation (4.2) then:

$$\left([G] + \rho\beta\Delta t^2 [Q]^T [M]^{-1} [Q] \right) \{\ddot{P}\}_{i+1} + [C'] \{\dot{P}\}_{i+1} + (1+\alpha) [K'] \{P\}_{i+1} = \{F_2\}_{i+1} - \rho [Q]^T \{\ddot{U}\}^*_{i+1} + \alpha [K'] \{P\}_i \quad (4.6)$$

In equation (4.6), the right hand side terms are known, thus, $\{P\}_{i+1}$ can be obtained. In order to correct the approximation made in equation (4.5), $\{P\}_{i+1}$ can be substituted in equation (4.1) to calculate $\{U\}_{i+1}$ and its derivatives. Therefore, the procedure of the staggered displacement method can be summarized by the following steps:

1. Knowing the displacement, velocity and pressure at time i, $\{\ddot{U}\}^*_{i+1}$ can be obtained from equation (4.3).

2. $\{\ddot{U}\}^*_{i+1}$ is introduced in equation (4.6) to calculate $\{P\}_{i+1}$.

3. $\{P\}_{i+1}$ is substituted into equation (4.1) to calculate $\{U\}_{i+1}$ and its derivatives.

In Chapter two, It was shown that the method of staggered displacement is unconditionally stable for the linear coupled equation of the dam-reservoir system with structural damping when α=0.0. For the nonlinear equations, the numerical solution is based on piece-wise linear solution. The solution stability depends on the length of the time steps and the introduced numerical damping.

The reservoir-dam interaction representation using the staggered solution technique is introduced to the nonlinear fracture analysis of concrete dams.

4.3 FRACTURE MODEL

The smeared crack model based on a nonlinear fracture mechanics crack propagation criterion is used to study the nonlinear behaviour of concrete gravity dams. The smeared crack model was used by Bhattacharjee and Léger (1994 and 1993). The main features of the model are: a) the strain softening of concrete due to micro cracking is included; b) the fracture band is rotated with the progress of damage; c) conservation of fracture energy is satisfied; and d) the opening and closing of cracks under cycling loading conditions are represented.

4.4 SEISMIC ENERGY BALANCE

In the design of structure subjected to earthquake loading, the energy equation can be used to study the energy absorbtion of different components. In a satisfactory design, the energy supply must be larger than the energy demand. In this regard, two approaches can be considered for the energy equation. Uang and Bertero (1990) used absolute and relative energy formulations for a single degree of freedom system. They found that absolute energy formulation is simple and more straightforward. Filiatrault et al. (1994) used energy balance to study the nonlinear behaviour of different structures under variable earthquake ground motion. Different time stepping algorithms were used to investigate the effect of numerical damping. Without the numerical damping, exact energy balance can be achieved. The two approaches to energy formulation were found to give different energy responses.

The energy equation of the dam structure governed by equation (2.1), can be written

as:

$$\frac{1}{2}\{\dot{U}_t\}^T[M]\{\dot{U}_t\} + \int\{\dot{U}\}^T[C]\{dU\} + \int\{r\}^T\{dU\} = \int\{f_1\}^T\{dU\} + \int\{\ddot{U}_t\}^T[M]\{dU_g\} + \int([Q]\{P\})^T\{dU\} \quad (4.7)$$

$$EK + ED + ER = EP + EQ + EH \quad (4.8)$$

In equations (4.7) and (4.8), {r} is the vector of the nonlinear restoring force. The absolute kinetic energy is EK, the viscous damping energy is ED, the nonlinear restoring work is ER, the work of preseismic applied force is EP, the absolute seismic input energy is EQ and the work done by the hydrodynamic pressure is EH. The relative displacement is {U} while $\{U_t\}$ is the total (absolute) displacement vector $\{U_t\}=\{U\}+\{U_g\}$. $\{U_g\}$ is the ground displacement vector. The restoring energy, ER contributes to the stored elastic energy in a system EE, and the energy dissipated due to fracture EF (EF= ER-EE), Thus:

$$EK + EE + ED + EF = EI \quad (4.9)$$

EK and EE contribute to the stored energy while ED and EF represent the dissipated energy. The input energy EI, is the sum of the seismic input energy due to the inertia force EQ, hydrodynamic force EH and work of preseismic applied load EP.

The energy balance error is computed as:

$$Error = \frac{(EP + EQ + EH) - (EK + ED + ER)}{(EQ + EH)} \times 100 \quad (4.10)$$

When the dam-reservoir interaction effects are represented by added masses, the hydrodynamic energy EH is excluded from the energy equation, EH=0. However, energy is added to the seismic input energy EQ and kinetic energy EK through the mass added to the structural system. In the analysis, the results of the fracture response are presented for the time before the five percent energy balance error is reached. The error in the energy balance represents an excessive amount of damage when numerical damping is introduced.

4.5 NUMERICAL RESULTS

The tallest monolith of the Pine Flat dam is chosen for the purpose of analysis. This particular dam was selected because it was the subject of numerous experimental and theoretical studies. It has a typical configuration of a concrete gravity dam. The dam is a concrete gravity structure with crest length of 560 m. It consists of thirty-seven 15.2 m wide monoliths and the tallest monolith of which is 122 m.

The modulus of elasticity, unit weight and Poisson's ratio of the concrete were taken as 27,580 MPa , 2400 kg/m^3 and 0.2, respectively. The tensile strength of the concrete is taken to be 2.758 MPa which is 10% of the compressive strength. Fracture energy of concrete is 150 N/m. A dynamic magnification factor of 1.2 is considered for the tensile strength and for the fracture energy. An elasto-brittle damping model in which cracked elements do not contribute to the damping matrix is considered for the analysis. The stiffness proportional damping equivalent to 5% damping in the first mode is used. The α-method of time integration is utilized (Hilber et al., 1977). The highest value of numerical damping (

α= -0.2) is used for effective dissipation of high frequency shock wave. The high value of numerical damping was found not to affect the lower modes of vibration (Hilber et al., 1977).

In order to determine the hydrodynamic pressure on the dam due to horizontal ground motion under the assumption of infinite reservoir, the reservoir is truncated at a reasonable distance. In the finite element formulation of the reservoir, Sharan boundary condition (Sharan, 1986) which truncates the reservoir, was applied at a distance L=10H from the dam. The velocity of pressure wave in water was taken as 1438.66 m/s. The elevation of the reservoir water is 116.88 m. For simplicity, the foundation is taken to be rigid and no absorbtion is considered at the reservoir bottom. The selected dam-reservoir system is shown in figure 4.1.

The first ten seconds of the horizontal S69E component of the July 21, 1952 Taft Lincoln earthquake, Kern County site record is shown in figure 4.2. The peak ground acceleration is 0.179g. The nonlinear analysis of the Pine Flat dam was carried out using the actual earthquake record when the dam-reservoir interaction was included. No damage was observed at the top part of the dam. Only a crack formed at the base of the dam and ran almost half the way through the dam. The analysis was then conducted with the earthquake record scaled to 1.5 times the peak ground acceleration (PGA) or 0.268g. A time step of 0.002 sec was selected for the analysis.

4.5.1 Linear Analysis

The results of the analysis using the staggered displacement method are compared with the dynamic analysis using EAGD-84 code (Fenves and Chopra, 1984) which assumes

infinite reservoir length. The EAGD-84 is a linear analysis computer code in the frequency domain which gives the steady state response of the system. The time domain solution using the staggered displacement method gives the steady state and transient responses of the system. In the case of a typical concrete gravity dam, the transient response is negligible. The dam crest displacements obtained from the two approaches are plotted in figure 4.3. The initial nonzero crest displacement at t= 0.0 represents the dam deformation due to the hydrostatic pressure component. Good agreement is achieved between the response obtained from staggered displacement method in the time domain and the EAGD-84 frequency domain solution. The small difference in the dam crest response is because the staggered solution method accounts for the effect of the slope of the upstream face of the dam while EAGD-84 assumes the dam face to be vertical. For a dam with large slope of the upstream face this effect may not be negligible.

4.5.2 Nonlinear Analysis

The nonlinear response of the Pine Flat dam was carried out with dam-reservoir interaction using the staggered method of solution. The results are compared with the nonlinear analysis when the dam-reservoir interaction effects are approximated using the added mass approach. The added mass method is the common approach in most of the nonlinear analyses of concrete dams. The fracture analysis of concrete dams is classified as nonlinear analysis with output that is sensitive to the input parameters such as cracking model, damping model and time step. It is useful to evaluate the fracture behaviour of concrete dams to a specific nonlinear fracture model. These effects are pronounced when the

dam-reservoir interaction is included in the analysis.

The time history of the dam crest is shown in figure 4.4 for the two cases of dam-reservoir interaction and added mass. The two approaches are close before any cracks are formed at the top part of the dam. The crest displacement responses obtained from the two approaches are different after initiation of the crack at the top part. The results of the analysis are shown before the five percent energy balance error criteria was invoked. The excessive error in energy balance indicates an excessive amount of damage which corresponds to large deflection of the structure. The results are not reliable for large deflection of the structure. The crest displacement responses obtained from the linear and nonlinear analyses are plotted in figure 4.5. In comparison with the linear analysis, it can be seen that base cracking does not change the response significantly. The difference between linear and nonlinear analyses is observed when top cracking is initiated at approximately 7 seconds. In the presented results, the first high peak of the ground acceleration at approximately 4 sec causes cracking. However, the solution remains stable until the second high peak at approximately 7 seconds when what is believed to be structural instability occurs.

The cracked configuration of the dam is shown in figures 4.6 and 4.7 at different times for the case of dam-reservoir interaction staggered displacement solution and the added mass approach. The figures show that including dam-reservoir interaction yields a different crack pattern than in the case of the added mass approach. The crack pattern predicted when the dam-reservoir interaction is included is similar to the observed damage to the Sefid-rud dam during the 1990 Manjil earthquake (Iran). The crack pattern in the Sefid-rud dam consisted of cracks at two levels in the upper parts of most of the monoliths (Ghaemian and

Ghobarah, 1997). Results of the numerical analysis carried out by Wepf et al (1993) shows a crack pattern which is very close to the crack pattern obtained in this study. The dam-reservoir interaction was included in their analysis using boundary element techniques.

When the dam-reservoir interaction is included in the analysis, cracking of the top part starts later than in the case of added mass. Once started, the cracking in the case of dam-reservoir interaction moves faster than in the added mass case. In a fraction of a second after crack initiation, the maximum damage is reached. The reason for late cracking at the top part of the dam in the case of interaction may be due to the damping.

The energy response of the Pine Flat dam is shown in figures 4.8 and 4.9 for the case of dam-reservoir interaction and the added mass, respectively. When the top crack occurs, the seismic energy EQ has a peak for both cases of the analysis. This peak in the case of added mass approach is at 4.4 seconds and for the case of staggered method is at 6.87 seconds. At the time of peak ground acceleration t= 3.7 seconds, peak of the kinetic energy response is higher in the case of added mass approach than the case of dam-reservoir interaction method. This is due to the dam-interaction effect which shifts the peak of the kinetic energy response away from the peak of the earthquake record. In both cases of added mass approach and staggered solution method, the fracture energy dissipation is negligible when compared with the other sources of energy. The variation of the energy balance error is higher when dam-reservoir is included than the added mass approach. The high energy balance error is due to the numerical damping inherent in the numerical method. However, before failure, the maximum error remains less than 5 percent. It is noted that the added mass approach accounts for the hydrodynamic force input in the form of the inertia force input.

Thus, before cracking, the seismic energy input in the case of added mass method and the dam-reservoir interaction approach are comparable.

Spurious deformation modes will occur particularly if there is a lateral spread of the cracking profile. Introducing of numerical damping provides a convergent numerical solution when the energy balance error is below a certain level. The increase of the energy balance error is an indication of diffused crack pattern over a band of elements, as shown in figure 4.6f at time of approximate 7 sec. The energy balance error is approximately 30% while in the cases shown in other figures, the energy balance error is below 5%

4.6 CONCLUSIONS

The nonlinear seismic fracture response of concrete gravity dams is conducted when the effect of the dam-reservoir interaction is taken into account. The dam-reservoir interaction is included in the time domain analysis using the staggered solution method. Smeared crack analysis model based on a nonlinear fracture mechanics crack propagation criterion is used to study the cracking and response of the dam. Results of the analysis are compared to the case when the dam-reservoir interaction was represented by added masses. It is found that the nonlinear analysis of concrete gravity dams that includes dam-reservoir interaction gives a crack pattern that is close to the observed damage of the Sefid-rud dam during the 1990 Manjil earthquake. The predicted crack pattern is different from that of the case when the dam-reservoir interaction is approximated using the added mass approach. It is concluded that proper modelling of the dam-reservoir interaction is important in the nonlinear response analysis of concrete gravity dams.

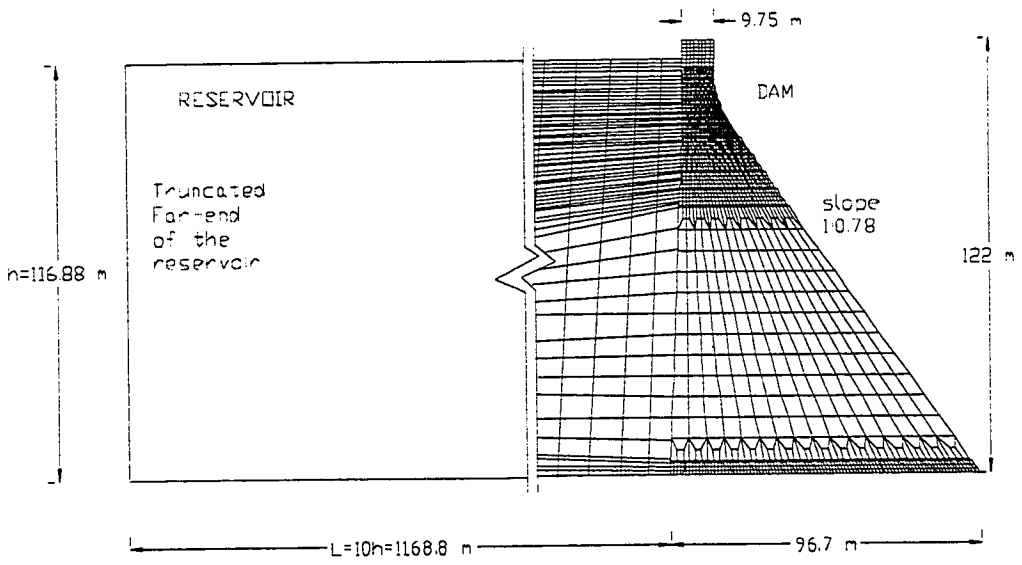

Figure 4.1. Finite element model of the dam-reservoir system

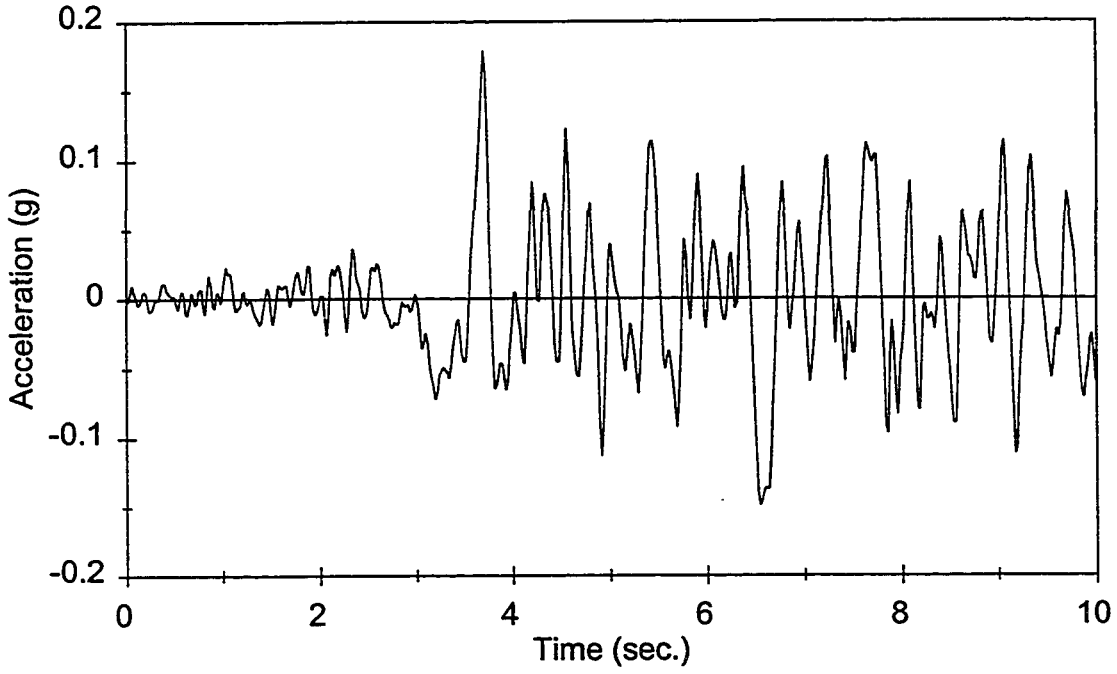

Figure 4.2. First ten seconds of the horizontal S69E component of the July 21, 1952 Taft Lincoln earthquake, Kern County site record,

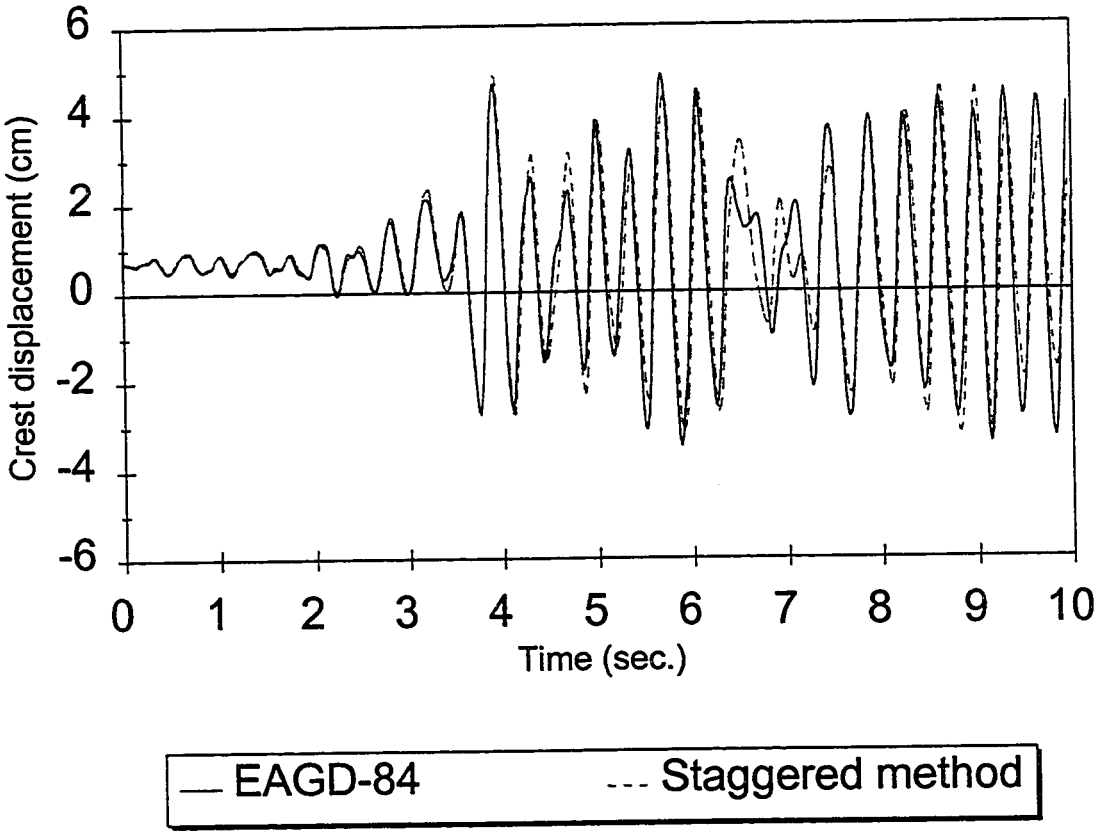

Figure 4.3. Dam crest displacement- linear analysis

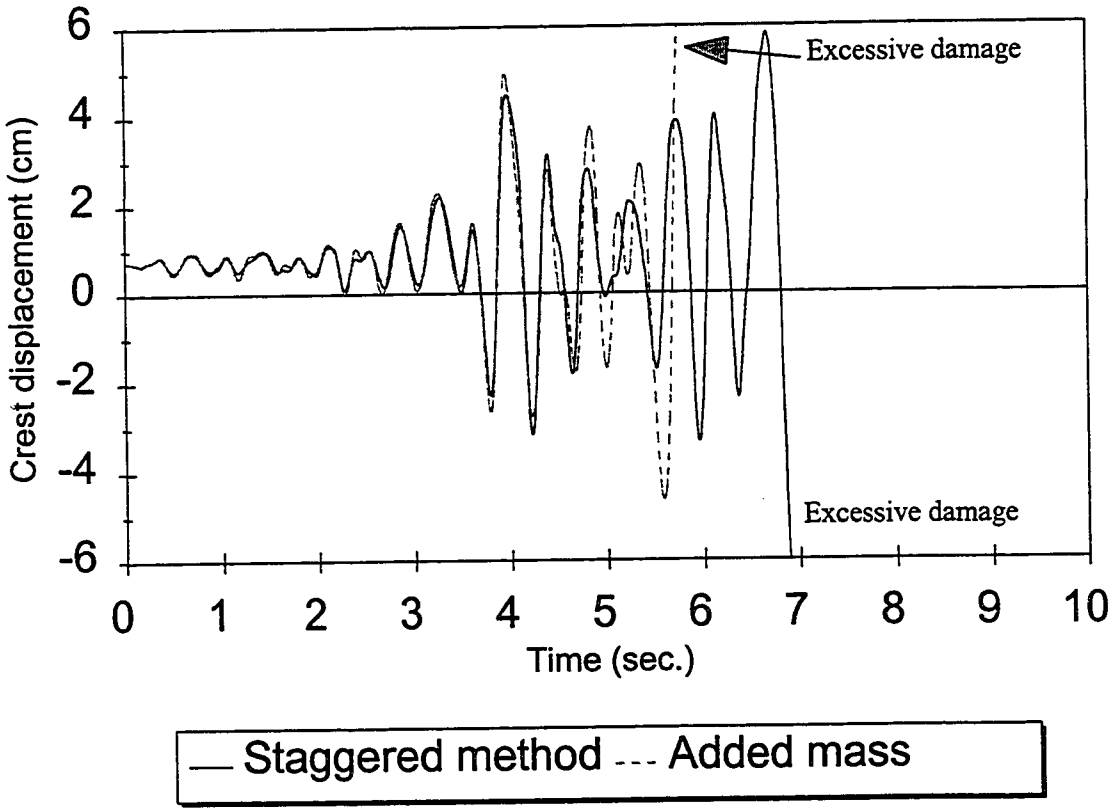

Figure 4.4. Dam crest displacement- nonlinear analysis

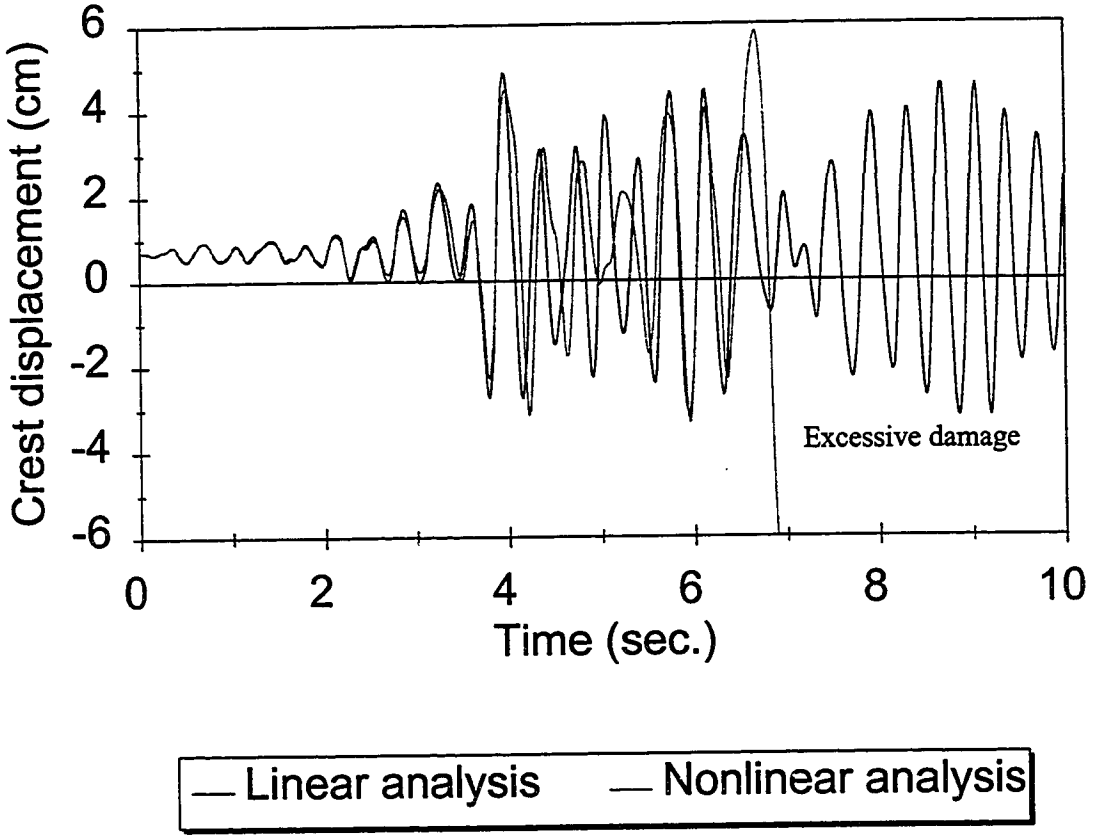

Figure 4.5. Dam crest displacement response

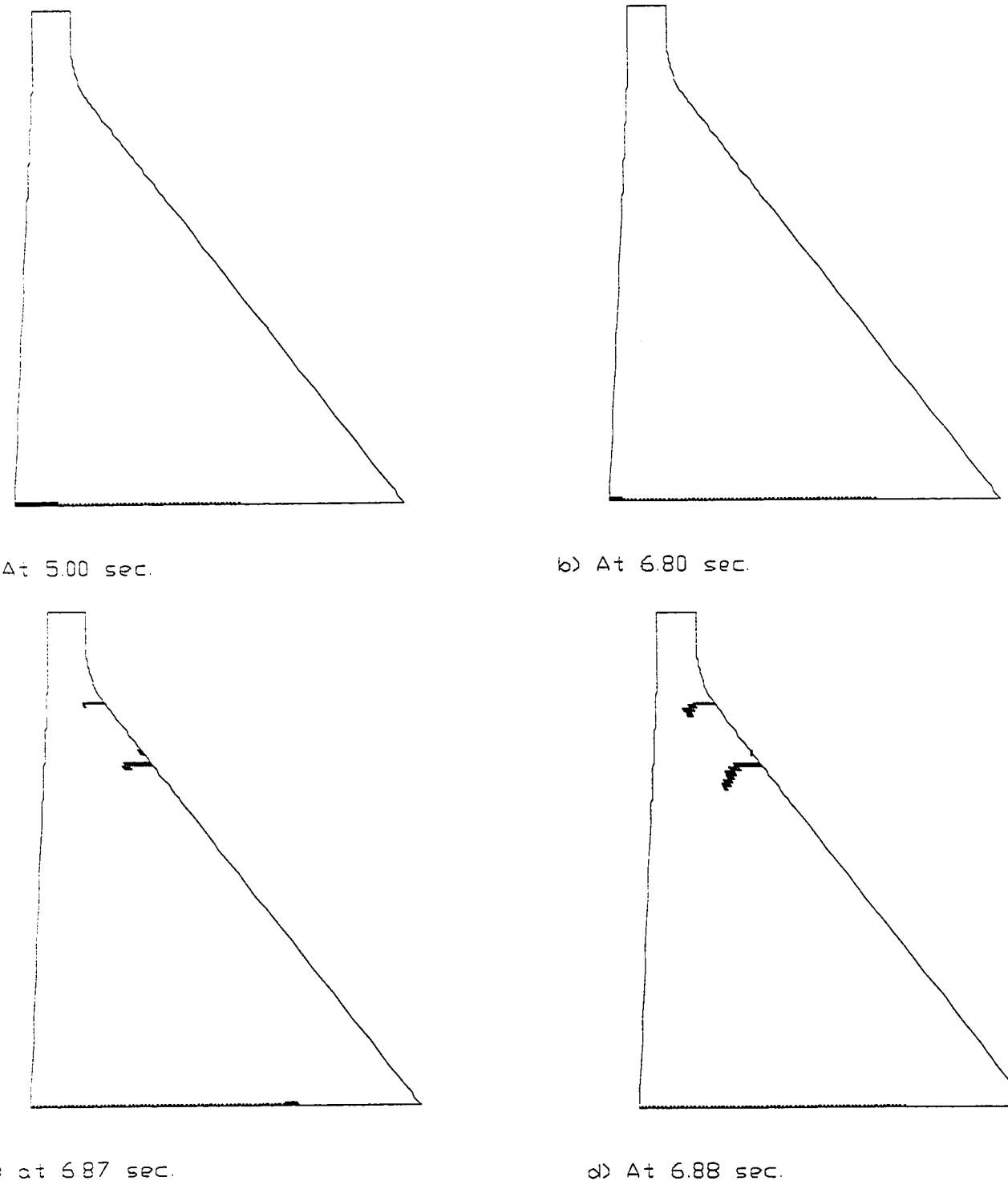

Figure 4.6. Crack profiles of the Pine Flat dam including dam-reservoir interaction

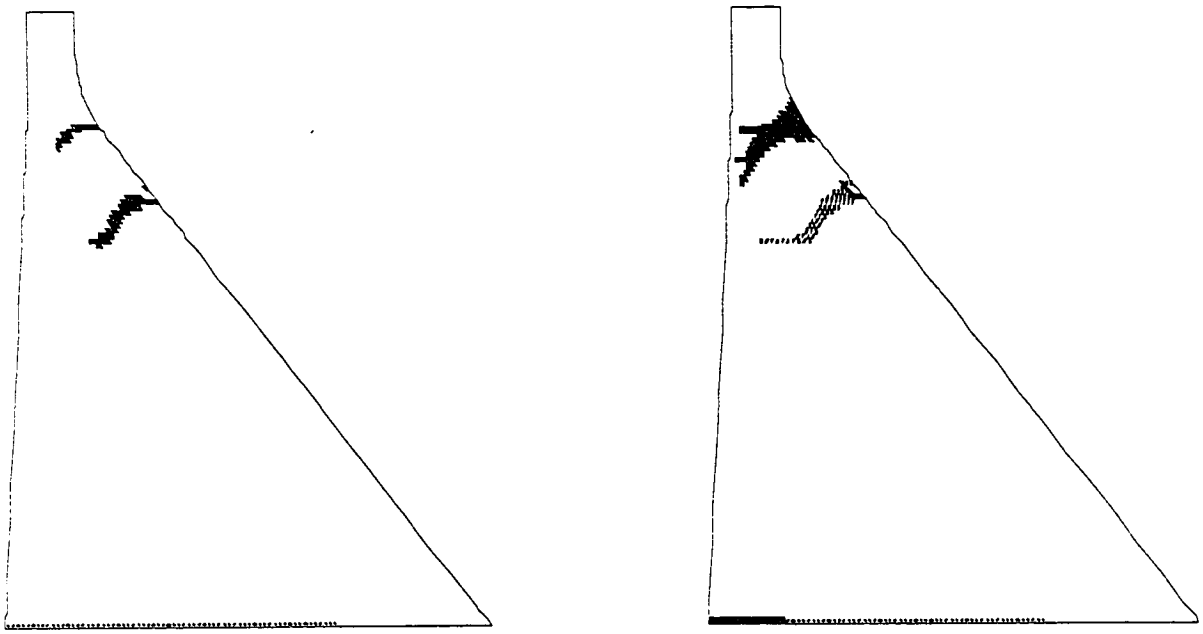

e) At 6.89 sec.

f) At 7.00 sec.

Figure 4.6. (Cont.) Crack profiles of the Pine Flat dam including dam-reservoir interaction

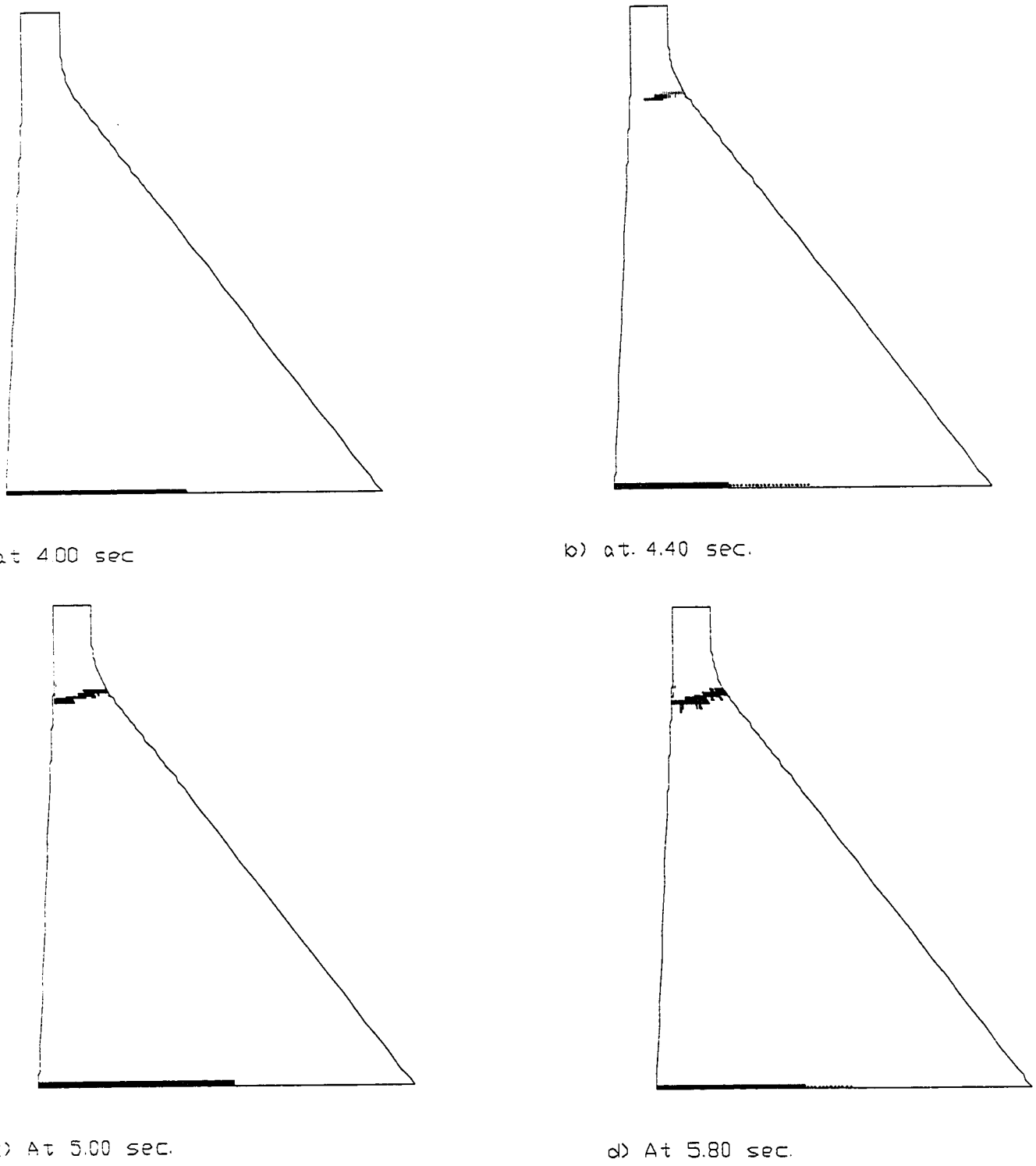

Figure 4.7. Crack profiles of the Pine Flat dam using added mass

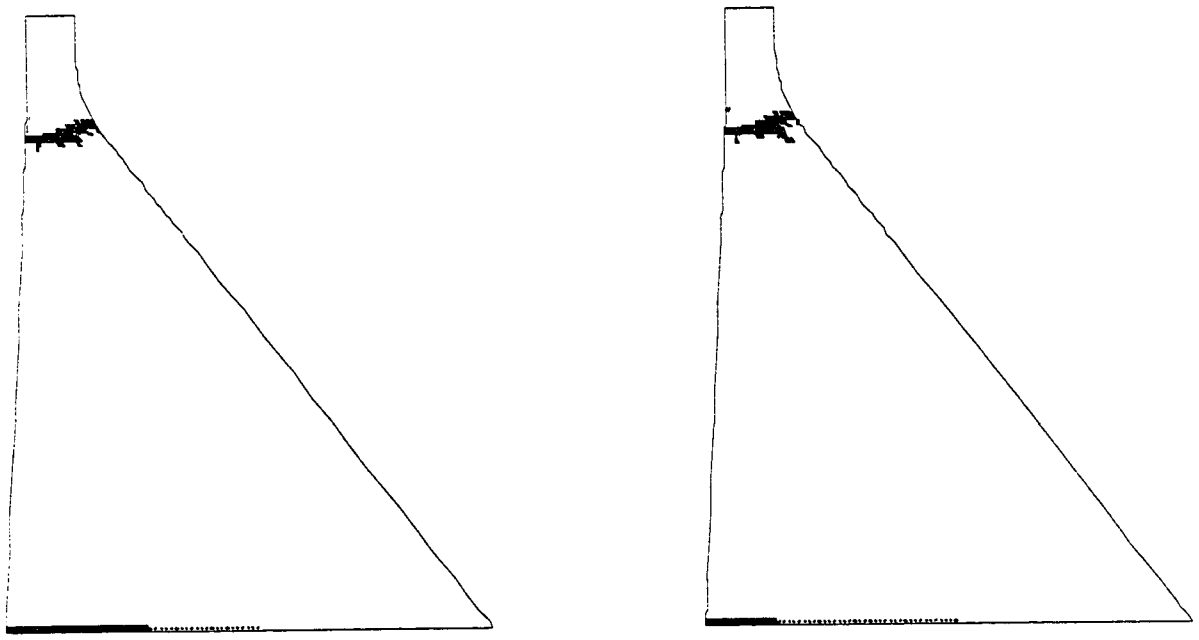

Figure 4.7. (Cont.) Crack profiles of the Pine Flat dam using added mass

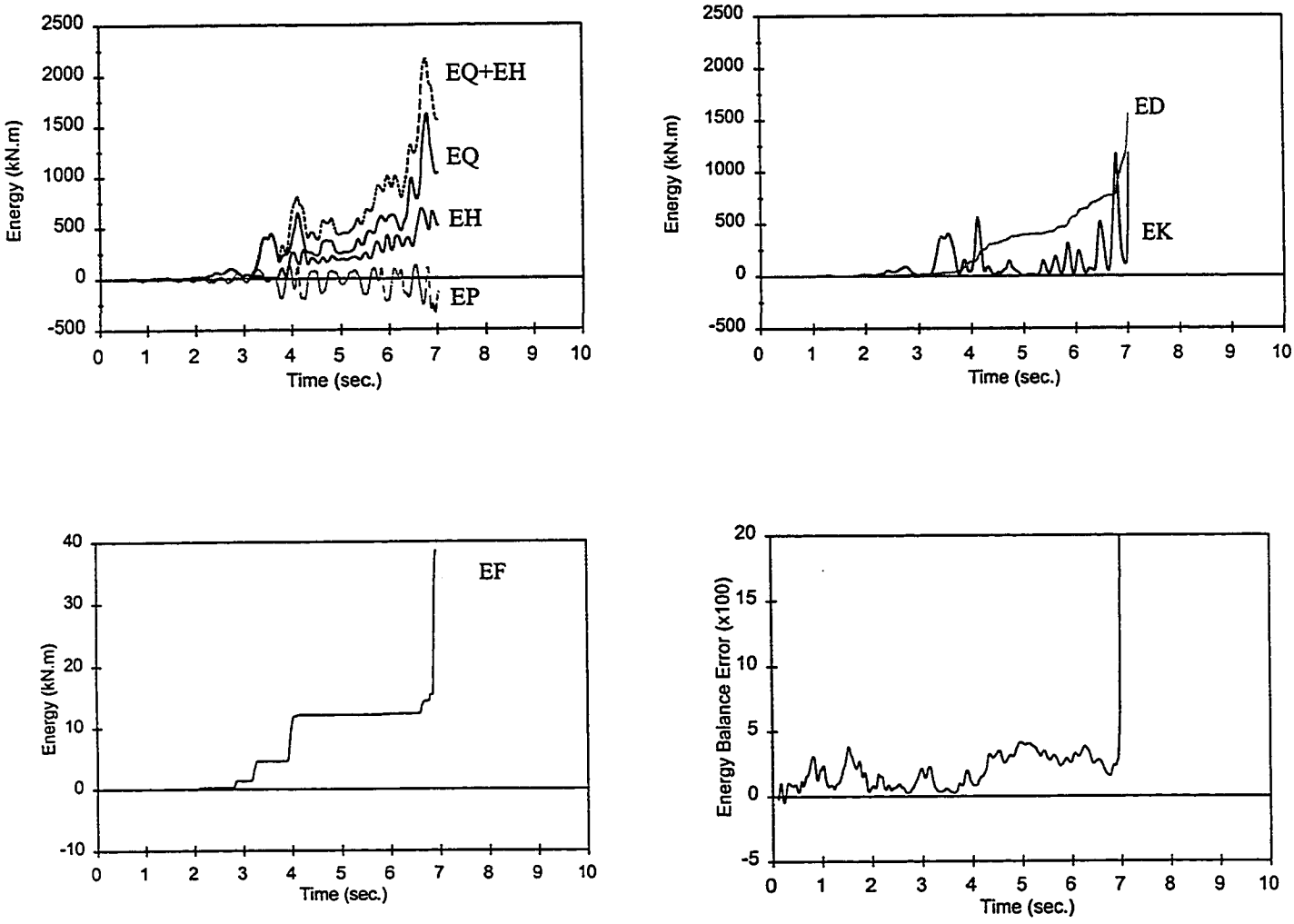

Figure 4.8. Energy response and energy balance error in the dam-reservoir interaction

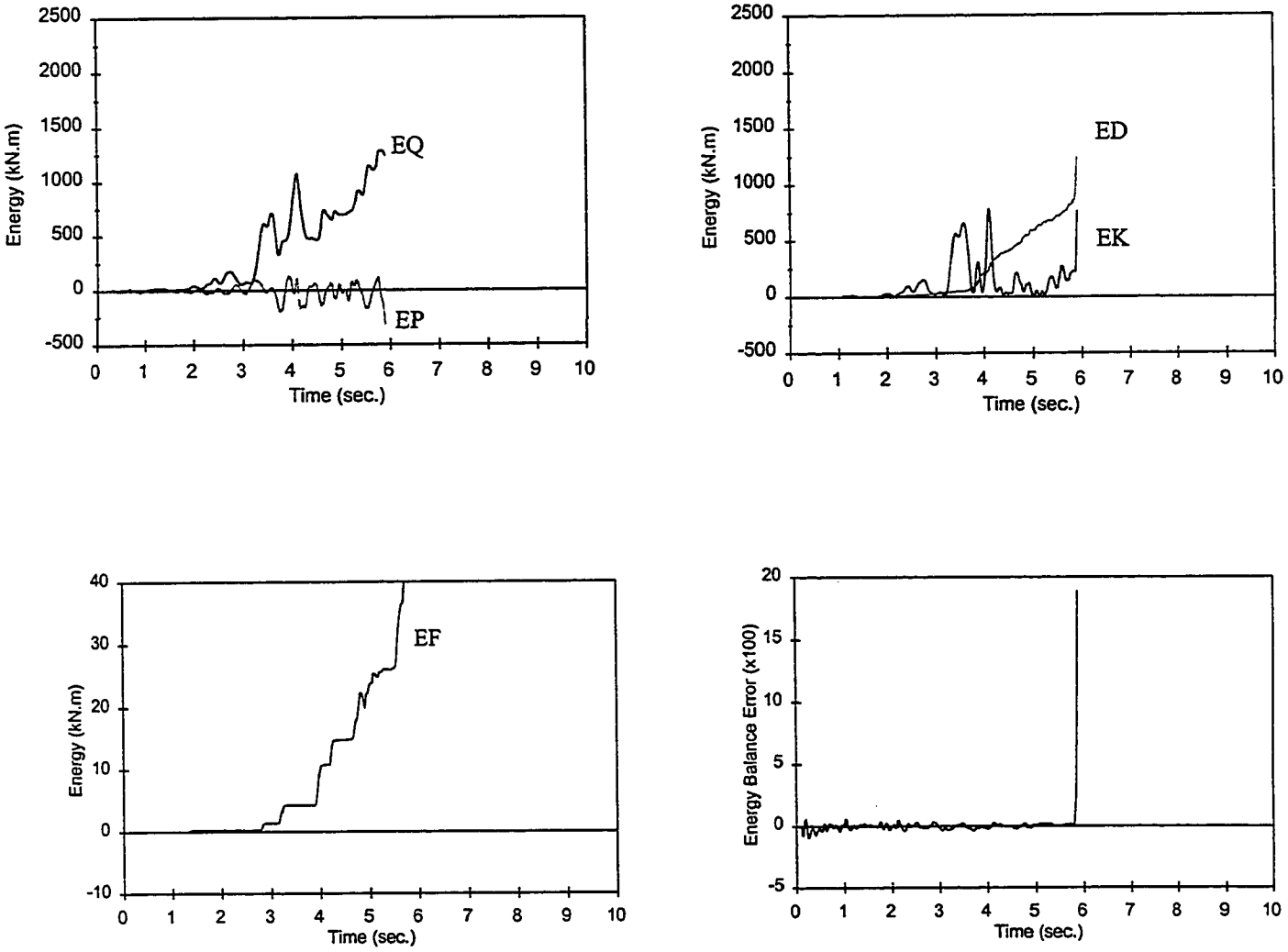

Figure 4.9. Energy response and energy balance error in the added mass approach

CHAPTER FIVE

EXPERIMENTAL STUDY OF SMALL SCALE DAM MODELS

5.1 INTRODUCTION

The dynamic response of dams is a complex problem because of dam-reservoir-foundation interaction effects. Most of the research conducted in the area of dam engineering is theoretical in nature. Although substantial progress has been achieved in mathematical modelling, none of the various models has been verified and several assumptions in the analysis remain to be substantiated. Field tests are expensive and difficult to run. They can not provide insight information on dynamic behaviour of the dams (Paultre and Proulx, 1995; Rea et al., 1975). Dam model testing has the potential of being used for analysis verification purposes. In small scale model testing of concrete dams, it is important that both material criteria and load criteria are met. Due to the complex nature of the problem, the large size of the structure and difficulties in physical modelling, little experimental work has so far been pursued.

Oberti and Lauletta (1960) studied structural stability of dams by means of physical models. The main purpose of the test was to observe the resonance amplitude of the models when the frequency of vibration coincides with the frequency of free vibration of the test

specimen. The model was attached to a steel platform and the whole assembly was suspended from a steel frame by means of a spring. The model was subjected to both horizontal and vertical vibrations. The concrete of the model used litharge for aggregate and plaster of paris as binder.

A significant number of the early experimental research programs were concerned with the development of materials for the dam model. Raphael (1963) investigated the properties of plaster-celite mixtures for use in dam models. He found that plaster-celite has the same Poisson's ratio as that of concrete while its strength can be controlled to be lower. Plaster is the material providing strength and the celite is the medium for retaining the required quantity of water in contact with the plaster. It was found that the strength and elasticity of plaster mixtures are profoundly affected by the water content. Yoshida and Baba (1965) performed dynamic tests on models of arch dams. A scale of 1:50 was used to model the Futatsuno arch dam in Japan which is 76 m high and of 210 m crest lengths. The model was built of plaster, diatomite, lead powder and water. The model collapsed due to resonance on the shake table with an empty reservoir. They also studied the dynamic behaviour of Ikehara arch dam in Japan which is 111 m high and of 460 m crest lengths. The dam model was built of plaster and was tested with full and empty reservoirs. Random vibration and actual earthquake loading were applied using a shake table. Oberti and Lauletta (1967) tested more models of the dam with different heights and crest lengths. Most of the tests were done on arch dams with height varying from 56 m up to 187 m with scale factors of 75 to 180. For each dam, three models were constructed. The models were made of litharge and gypsum mix whose density was about 39.2 N/m^3 and the elastic modulus were 29.4 to 98 kPa. The

input earthquake intensity was increased beyond the elastic range up to failure of the model.

To investigate the magnitude of acceleration at which the failure of the Toktogul dam in Russia occured, Lyatkher et al. (1977) conducted a test on a model of scale 1:100. The test was carried out in a centrifugal force field. The model was made of plaster with rubber crumbs, bentonite and lead powder. A container with the model of foundation and dam filled with water, was placed on a vibrating platform. Bakhtin and Dumenko (1979) used the mass ratio of the material components as P:Li:R:Pb:M:W=1:1:2.5:30:1:4 in which W is the mixing water, P is plaster binder with fillers as limestone powder Li; and R is rubber crumb. Lead powder Pb, was used as the weighing substance. Mineral oil AK-10 ,M, was used for neutralizing the binding properties of the Lead powder and to reduce the modulus of elasticity and tensile strength of the model material. The reservoir water was modelled using calcium chloride solution with unit weight of 1.4 ton/m^3 poured into a stationary tank attached to the model by a thin rubber diaphragm. The seismic load was applied using a shake table. They found that the most critical zone in concrete gravity dams during a seismic event is the upper quarter of the dam at which failure of the model occurred. Niwa and Clough (1980) investigated the use of plaster, celite, sand and lead powder to construct the models. They tested models of an arch dam and a concrete gravity dam monolith using shake table. Difficulties were encountered with model cracking due to shrinkage during the drying process. Gutidze (1985) conducted an experimental program to determine the seismic stress state in a dam. A model was built using cement-sand base with the addition of rubber crumbs and bentonite clay. Different scale models of an arch dam were built for elastic and inelastic response studies. For the first 8 modes of vibration, the maximum elastic

displacement and natural frequency were measured. Norman (1986) applied an impact load on the foundation using a steel mass to provide input motion to the foundation block of a dam model. This method was used to apply a dynamic failure load to the model. Donlon (1989); and Donlon and Hall (1991) tested a small scale model of a dam monolith using shake table. Difficulties were encountered due to shrinkage cracking of the model in the process of drying. To repair the cracks, polymer-based material was used in the lower part of the dam.

Mir and Taylor (1995) conducted an experimental investigation of the nonlinear seismic response of a low-height concrete gravity dam. They could overcome the shrinkage problem by special effort in mould treatment, curing and by minimizing friction between the mould and model material. They modelled a small 30 m high dam. The model material properties almost attained all of the target values. They used Westergaard's added mass approach for simulating the hydrodynamic pressure. Scaled masses were evaluated at 64 equidistant levels along the height of the model and were separated by plastic sheets containing air bubbles. The hydrostatic reservoir forces were simulated by a very rigid rectangular steel tank attached to the upstream face of the dam. They found that the hydrodynamic pressure using Westergaard's added mass was not reasonably representative, especially near the top of the model. They concluded that low-height dams are usually damaged at the base. Excluding the reservoir (hydrostatic and hydrodynamic) loads, cracks form at both heel and toe of the dam. When the effects of the reservoir were included, the crack occurs only at the heel and is restricted to a very small length. The hydrostatic pressure was found to cause sufficient compressive stress at the toe of the dam to prevent the initiation

of the toe crack. They also found that sliding and overturning of a gravity dam monolith under earthquake loading is not a serious concern. Mir and Taylor (1996) investigated base sliding of a concrete model of a rigid gravity dam using a shake table. They concluded that for dams of normal geometry the likelihood of overturning about its toe is low, if the uplift pressure is not significant.

In the field of fracture mechanics and crack propagation in concrete gravity dams, several attempts were made to test small scale dam models using static loads (Bolzon et al., 1994; and Pellegrini et al., 1994) and in a centrifuge (Plizzari et al., 1994; and Renzi et al., 1994). However, in all these tests, no modelling of the hydrodynamic forces during earthquakes was attempted.

The difficulties in physical modelling of concrete dams are mostly in material modelling and the availability of suitable equipment for testing. Some of the materials used in modelling are hazardous and prone to shrinkage cracking in the process of drying. The objective of this experimental program is to develop a new testing approach using small scale modelling to investigate the linear dynamic response of concrete gravity dams. The attention is focused on the stress distribution at the top part of the dam near the slope change of the downstream face where major cracking has been observed to occur. The dam model is constructed of plain concrete. The static and dynamic loads are applied using actuators. The inertia effects are included in the applied loads and the dynamic loads are applied pseudo statically. The measured response of the model is compared with the predicted analytical response.

5.2 DIMENSIONAL ANALYSIS AND SIMILITUDE REQUIREMENTS

It is difficult to maintain both kinematic and dynamic similarities between model and prototype of a concrete gravity dam (Shames 1982). Although, the introduction of the idea of "distorted model" allowed the relaxation of some requirements for similarity, satisfying the basic requirement is difficult and can hardly be achieved. To simplify the dimensional analysis, the dam and reservoir interaction with the foundation is neglected. For the case of a dam-reservoir system, three basic requirements that relate model and prototype parameters are obtained as follows:

$$\frac{S_r T_r^2}{\rho_r L_r^2} = 1 \tag{5.1}$$

$$\frac{A_r T_r^2}{L_r} = 1 \tag{5.2}$$

$$\varepsilon_r = 1 \tag{5.3}$$

where T, L, S, A, ϵ and ρ are the time, length, stress (or pressure), acceleration, strain and mass density, respectively. Index r, represents the ratio of these parameters in the prototype and model.

Equating the gravitational force (g) in model and prototype results in the following two formulas (Donlon 1989):

$$T_r = \sqrt{L_r} \tag{5.4}$$

$$S_r = \rho_r L_r \tag{5.5}$$

Due to the limited range of mass density of available fluids, S_r may be large for small scale models. This shows a possibility that the model material can be significantly weak but of approximately the same mass density as the prototype. If water is selected as reservoir fluid in the model, the restriction is imposed on the material properties of the dam model, modulus of elasticity, tensile and compression strength, by a factor of $1/L_r$ of that of the prototype. In addition to the difficulties associated with modelling the interaction between dam and reservoir, the problem of modelling is complicated by two factors: a) if the model is to be brought to failure, high range of shaking frequencies is required and, b) the properties of dam material and reservoir fluid provide a limitation for ρ and therefore for S_r.

Satisfying the mass density in the model is quite difficult. For proper modelling, the mass density in the model should be greater than that of the prototype by a factor of L_r/S_r. L_r is a large number for the case of small scale modelling of the dam and S_r can not be large enough to compensate for L_r. Therefore, a large ratio of weight density is needed. For example, a dam model of 1:100 dimensional scale should have a weight density of 100 times larger than that of the prototype, if the same material strength properties are used for both the model and the prototype.

5.3 EFFECT OF GRAVITY ON SMALL SCALE MODELLING

In geometrically similar and undistorted model, the Buckingham π-theorem (Shames, 1982) requires three independent scaling factors for the variables of the system. In small scale modelling, the first independent scale ratio is the length ratio. If the mechanical properties of the model material is selected to be the same as that of the prototype, one independent parameter remains to be chosen. Selecting the acceleration ratio to be the same in the model and the prototype, the mass density of the model material should be increased by a factor of a length ratio. Another approach would be to set the mass density ratio to unity. This requires the acceleration in the model to be increased (Dancygier 1995).

In the proposed testing approach, the materials of the prototype and the model are selected to have the same mechanical properties. Parameters such as Poisson's ratio and the strain at the yield are also taken to be the same for prototype and model. For the same mass densities in the model and the prototype, the acceleration of the model should be increased in order to properly represent the inertia force effects. Some researchers used a centrifuge to apply acceleration to the model that is increased by the scale factor of the model. In the present experimental program, the effect of the inertia force was calculated and added to the applied cyclic load, thus avoiding the difficulties associated with dynamic load scaling.

If the weight density is scaled in the model, adequate vertical force due to weight will exist to prevent early cracking of the model. When weight density is not scaled, the applied horizontal loads will cause high tensile stresses at the heel which may result in early cracking of the model dam. In the proposed testing approach, the effect of weight on the stresses is calculated and added to the test measurements.

The early cracking of the model at the base may be a problem associated with modelling that needs to be addressed. Cracking of the dam prototype at the base was demonstrated analytically, however, it does not imply instability. Thus, the area of interest is at the top part of the dam where major cracking may lead to loss of function of the structures as well as dam safety concern.

To check the distortion of the stress at the base of the dam model, the stress at the base is written as (Dancygier 1995):

$$\sigma = \sigma_g + \sigma_{ng} \tag{5.6}$$

where σ_g is the stress due to gravity load and σ_{ng} is the stress due to the non-gravity external loading. The distortion due to gravity modelling can be computed as follows:

$$D^t = \frac{\sigma^{true} - \sigma^s}{\sigma^{true}} = \frac{1}{1 + \frac{1}{n-1}\frac{\sigma^m}{\sigma^m{}_g}} \tag{5.7}$$

where n is the linear dimension scale factor, σ^{true} is the true value of the stress at the base and σ^s is the scaled value of the stress at the dam base using the test results. σ^m and $\sigma^m{}_g$ are the total stress and stress due to gravity in the model, respectively. The scale factor used in the test to extrapolate the stress for the prototype is unity (i.e., σ_r=1).

The ratio of total stress to stress due to gravity can be written as:

$$\frac{\sigma^m}{\sigma^m_g} = \frac{-\frac{P^m}{A^m} + \frac{M^m C^m}{I^m}}{-\frac{P^m}{A^m}} = 1 - \frac{6\,M^m}{h^m P^m} \qquad (5.8)$$

where h^m is the base length of the model and P^m is the weight of the model and A^m is the area of the model at the base. Equation (5.8) gives a factor for correcting the distortion in the measured stress at the model base due to the effect of gravity.

5.4 EXPERIMENTAL APPROACH

The complexity in the scale model testing of dams arises from material modelling and modelling of the dam-reservoir-foundation interaction. In most of the experimental work, a rigid foundation and incompressible water are assumed in the process of modelling. To avoid the difficulties associated with material modelling in dynamic load testing, the proposed approach is based on quasi-static (cyclic) loading. In order to replace the dynamic and inertia loads by quasi-static loads, it is necessary to determine the loads acting on the dam due to a given earthquake ground motion. The simplified method of analysis of concrete gravity dams (Fenves and Chopra, 1985, 1986, 1987) is used to calculate the hydrodynamic pressure and inertia force. The dynamic loads are replaced by equivalent concentrated static forces acting on the upstream face of the model. These equivalent cyclic static forces representing

the hydrodynamic and inertia forces on the dam are added to the hydrostatic pressure.

The simplified method of analysis is a procedure to calculate the maximum response of the dam using the response spectrum approach. For a dam-reservoir system, the distribution of the maximum hydrodynamic pressure and the inertial force distribution are determined considering the effect of dam-reservoir interaction. The height of the reservoir, the properties of the dam concrete, the damping of the structure, the wave reflection coefficient of the reservoir bottom materials and the acceleration response spectrum of the ground motion are the parameters used to evaluate the equivalent lateral force distribution.

Once the distribution of the sum of dynamic and hydrostatic loads is established, the location of the concentrated forces can be determined based on the number of concentrated loads used in the test. A mechanism is designed to apply both loads at common concentrated points on the upstream face of the model. The number of concentrated points is limited by the space available on the upstream face of the model.

In order to decide on the number of concentrated loads needed to accurately represent the hydrostatic and dynamic loads on the dam, a finite element analysis was performed. In the analysis, the number of concentrated loads that are assumed to represent the applied loads was varied. A balance needs to be struck between load modelling accuracy and practical experimental limitations. The results of the analysis were found to be sufficiently accurate when the distributed loads are represented by a minimum of four concentrated loads.

The problem of modelling is simplified if the same material as the concrete of the prototype is used in the model. Using the same properties of concrete in the model and prototype requires that the effect of increased density of the model material be compensated

for. In the test set-up no supplementary self weight is provided to compensate for scale reduction. However, the effect of the weight was accounted for analytically. For a start, this testing program and the associated analyses are limited to the linear behaviour of the dam-reservoir system.

5.5 MODELLED DAM

A configuration similar to that of the existing Pine Flat concrete gravity dam is selected for the purpose of modelling and testing. The concrete gravity dam is of a typical configuration and consists of thirty seven 15.2 m wide monoliths and crest length of 560 m. The tallest monolith is 122 m high. The configuration of the tallest monolith which is used for the purpose of modelling, is shown in figure 5.1 (Donlon and Hall 1991).

The model dimensional scale is selected as 1:100. Wooden forms are constructed to the scaled dimensions of the dam with special attention to the accurate modelling of the curves near the top part of the model. Figure 5.2 shows the wooden forms of the scaled Pine Flat dam model. The forms were lightly oiled to enable easy stripping of the forms without damage to the model. Portland cement concrete with the maximum specified aggregate size of 20 mm is used. On the day of pouring, the slump of the delivered concrete mix was measured at 60 mm. The concrete model was covered with burlap and cured twice daily. Forms were removed after 48 hours and the concrete was moistened twice a day for 7 days. The model was left for more than 28 days before testing. Thirteen test cylinders were poured. The compressive strength, f'_c and tensile strength of the concrete are given in table 5.1. The

tensile strength was determined using the split cylinder test f_{sp}. The modulous of elasticity of concrete was determined from the cylinder tests to be 35,000 MPa.

Table 5.1 Results of cylinder testing (MPa)

Cylinder number	7 days	28 days		Day of test	
	Compression	Compression	Tension	Compression	Tension
1	20.20	27.20	2.52	36.7	3.79
2	19.70	23.90	2.23	38.4	3.80
3	18.60	26.70	2.40	-	-
Average	19.50	25.90	2.38	37.5	3.79

5.6 TEST SET-UP AND INSTRUMENTATION

The load application system was designed to transfer the loads from two actuators to four locations on the upstream face of the model. The horizontal ground acceleration recorded at Kern County during the 21 July 1952 Taft earthquake was selected for calculating the hydrodynamic pressure and inertia force distribution. The distribution of the dynamic load was obtained from the simplified analysis method (Fenves and Chopra, 1985; 1986 and 1987). The dam was divided into 10 blocks of equal height. Rigid foundation with full reservoir and no reservoir bottom absorbtion was assumed. The damping effects due to the dam-reservoir interaction were considered in the analysis. The hydrodynamic pressure distribution at the upstream face of the dam and the inertia forces at the centre of the mass

of each block were calculated. It was found that the effect of higher modes is small in comparison with the total response of the dam. The total dynamic load was divided into four concentrated loads acting at the upstream face of the dam. The hydrostatic load was also divided into four concentrated loads having common points of application with the dynamic loads. The dynamic and hydrostatic loads were then scaled to represent the loads that will be applied to the model dam. The distribution of the dynamic and static loads on the model are shown in figure 5.3.

In order to check if the selected four concentrated loads can accurately represent the distributed loads on the upstream face of the prototype dam, the deflection of the dam is compared for the two cases of loading. The dam deflection calculated using the finite element analysis is shown in figure 5.4. The deflection of the dam when subjected to the actual distributed loads and the four concentrated loads are found to be close.

Two actuators are used to apply the hydrostatic and dynamic loads. The hydrostatic load is kept constant while the hydrodynamic load is varied cyclically to represent the cyclic nature of the dynamic load. The characteristics and capacities of the two actuators are listed in table 5.2.

Table 5.2 Characteristics of the actuators

Actuators	Model MTS	Force capacity kips (kN)	Stroke in (mm)	Piston area in^2 (mm^2)
Static load	204.71	±55 (245)	6 (150)	18.53 (11955)
Dynamic load	202.01	±250 (1112)	8 (200)	89.36 (55720)

The loading mechanism for applying four concentrated quasi-static loads on the dam is shown in figures 5.5 and 5.6. The transfer of the four concentrated loads to the specimen was made by using 4 U-shaped channels which are glued to the model. Figure 5.7 shows the attachment of the U-shaped channel to the upstream face of the model. The high strength structural epoxy "Sikadur" injection gel is used for bonding of the U-shaped channel and specimen. Its non-abrasive texture permits application with pumps or automated pressure injection equipment. The two component, solvent-free epoxy material conforms to ASTM C-881 Type I, II, IV and V Grade 3, Class B and C for epoxy resine adhesive. Table 5.3 shows the mechanical properties of the Sikadur injection gel.

Table 5.3 Mechanical properties of Sikadur injection gel

Compressive strength		Bond strength		Modulus of elasticity	
23°C	MPa	Hardened concrete to steel	MPa		GPa
1 day	48	2 day (dry cure)	23	28 day	3.7
28 day	62	14 day (moist cure)	18		

Figures 5.8 and 5.9 show details of the test set-up for the experimental program. The dam model is anchored to a thick steel platform supported on a large size I-beam. The actuators are installed at different elevations on two different heavy steel reaction frames. Two load cells are used to measure the applied load from each actuator. The static actuator is connected to a control unit to maintain the applied static load at a constant level. Continuous adjustment to the static load was needed as the model was deflecting due to the

applied cyclic loading. A MTS 436.11 control unit provides automatic control of the hydraulic pressure. Figure 5.10 shows a schematic of the MTS control unit connections.

Twenty strain gages are placed at ten locations on the model to capture the horizontal and vertical strains. The strain gages used are of N11-FA-30-120-11 type from Showa Measuring Instrument Co. with gage length of 30 mm. The deflection of the upstream face is measured using Linear Potentiometer Differential Transducers (LPDT). A second LPDT installed at the base near the upstream face of the dam model to monitor the strain and crack opening at the base. Both LPDTs can measure displacements up to 5 cm. Four load cells measured the applied concentrated loads at the upstream face of the model face. Figures 5.11 and 5.12 show the location of the strain gages, LPDT's and load cells. All the instruments were connected to the computer controlled data acquisition system for automatic data recording at 5 second intervals.

5.7 SUMMARY

A new approach for small scale model testing of concrete gravity dams is proposed. The testing procedure uses a distorted model which is a hybrid of analysis and experimental techniques. A mechanism is designed to apply both dynamic and hydrostatic loads to the upstream face of the dam model. The procedure involves the calculation of the dynamic forces on the dam for a given ground motion and the simulation of these forces using a number of quasi-static concentrated loads applied at the upstream face of the model. Approximating the reservoir forces on the dam by four concentrated loads appears to provide

a reasonably accurate experimental representation of the dam-reservoir interaction effect.

The proposed experimental technique can be used in the comparative testing of models of dams with different structural characteristics such as original and rehabilitated dams where analytical modelling may be difficult. In the test set-up, it is not necessary to model the entire dam. Instead, modelling and testing may be applied to the top part of the dam only thus focusing on the areas of high stresses and potential cracking.

The results of the testing program and comparison with analytical predictions are described in Chapter 6.

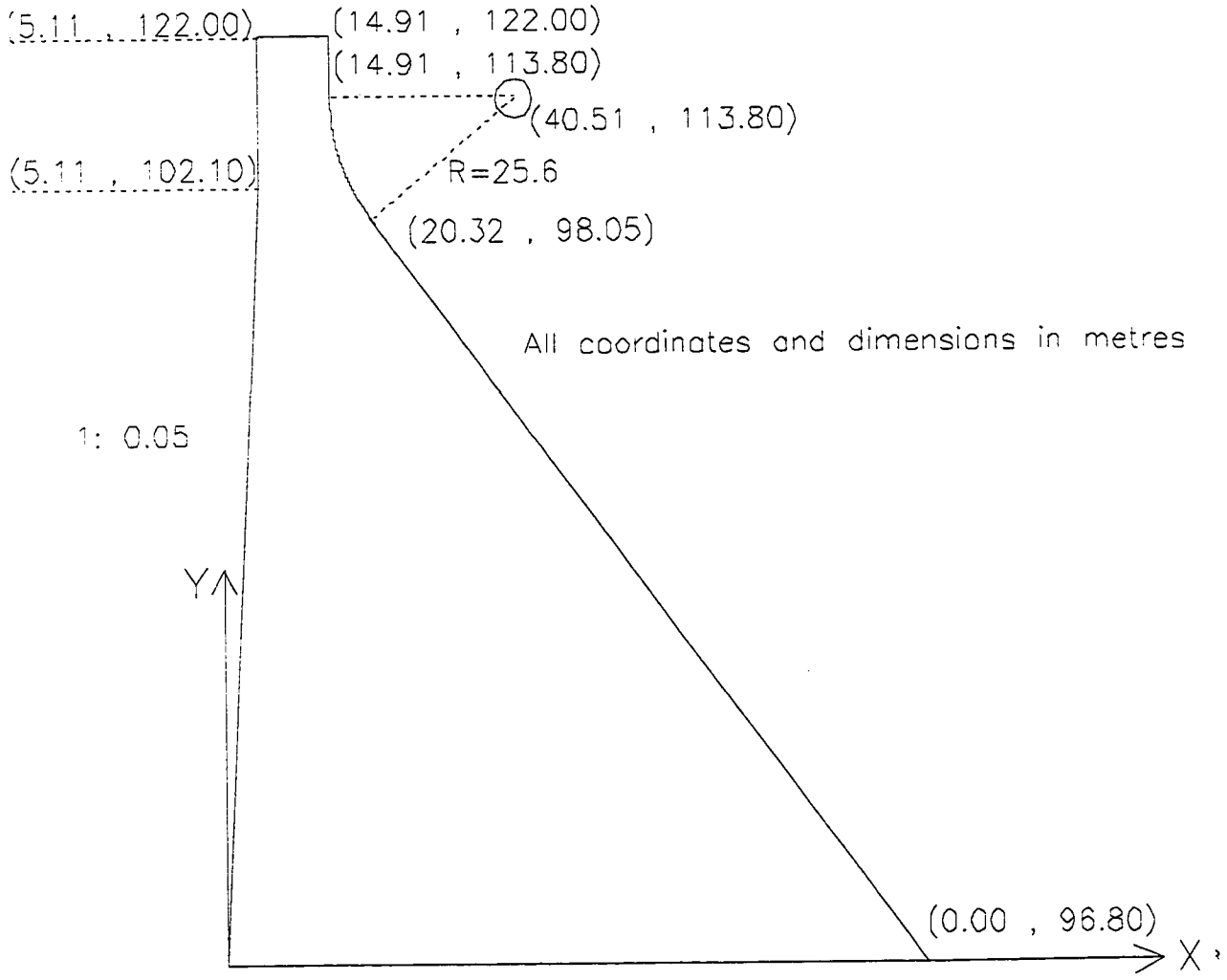

Figure 5.1 Configuration of Pine Flat concrete gravity dam (Donlon and Hall, 1991)

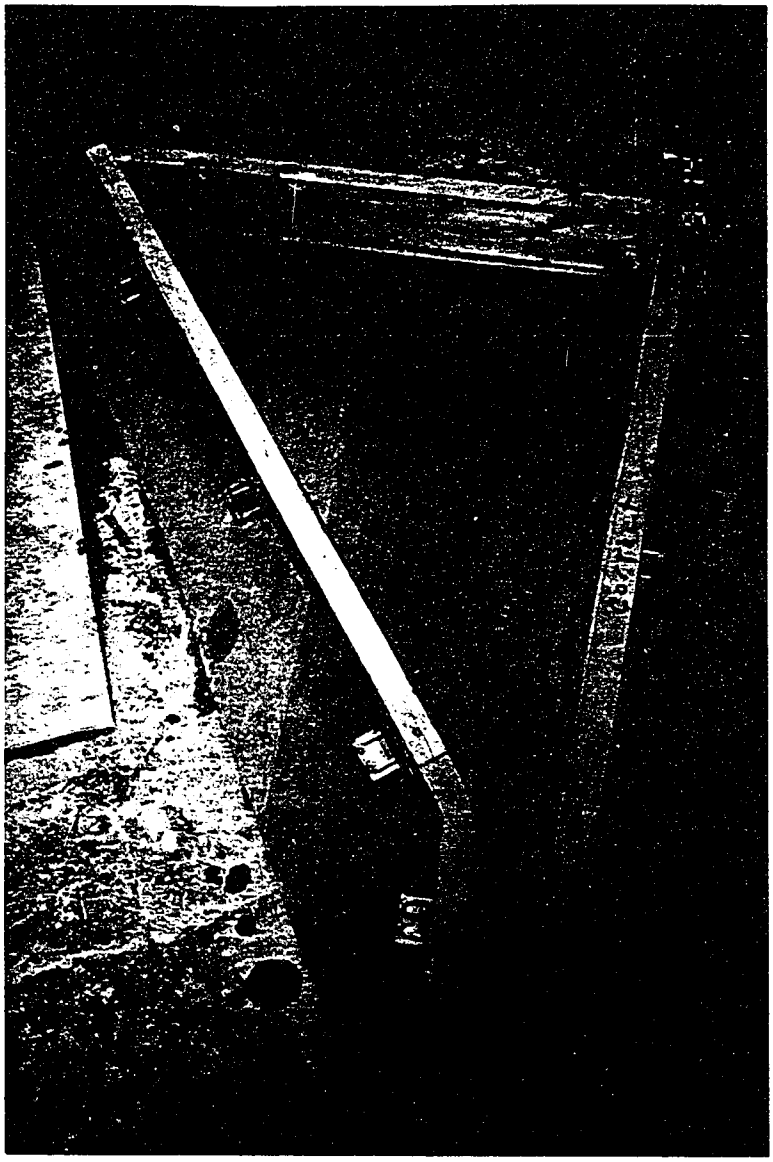

Figure 5.2 Specimen wooden form

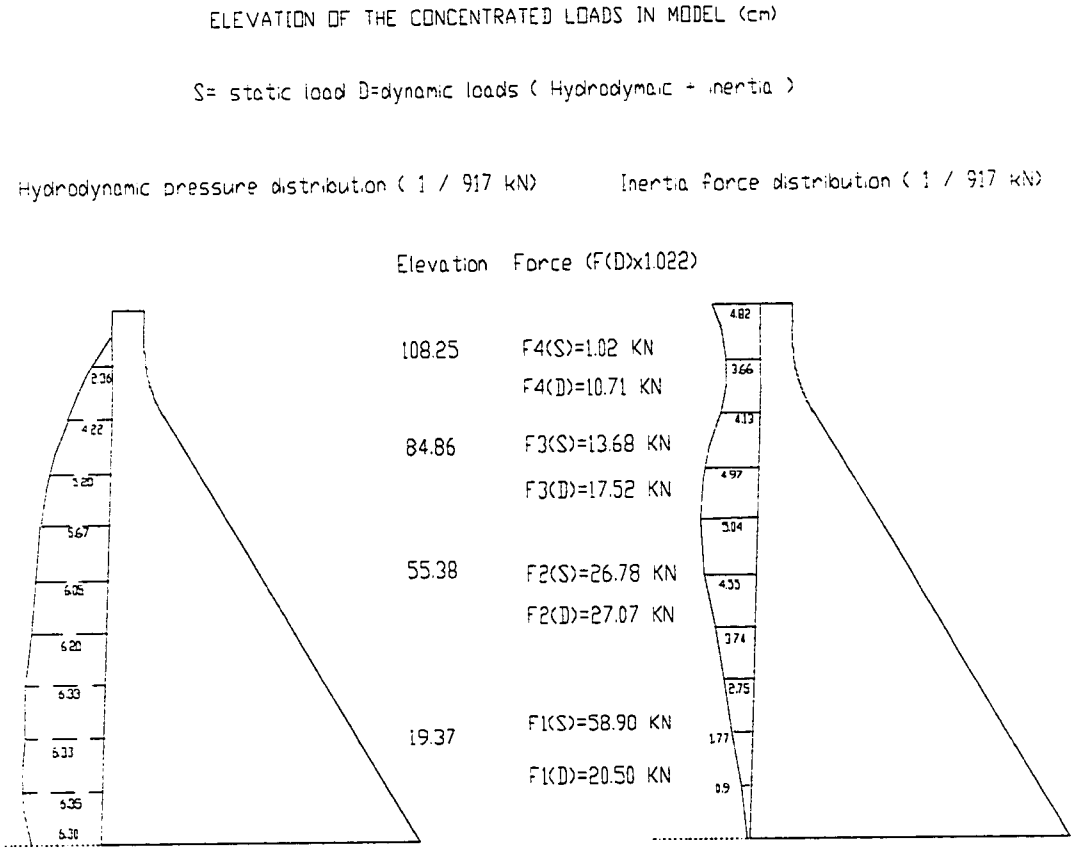

Figure 5.3 Maximum dynamic load distribution due to Taft earthquake record

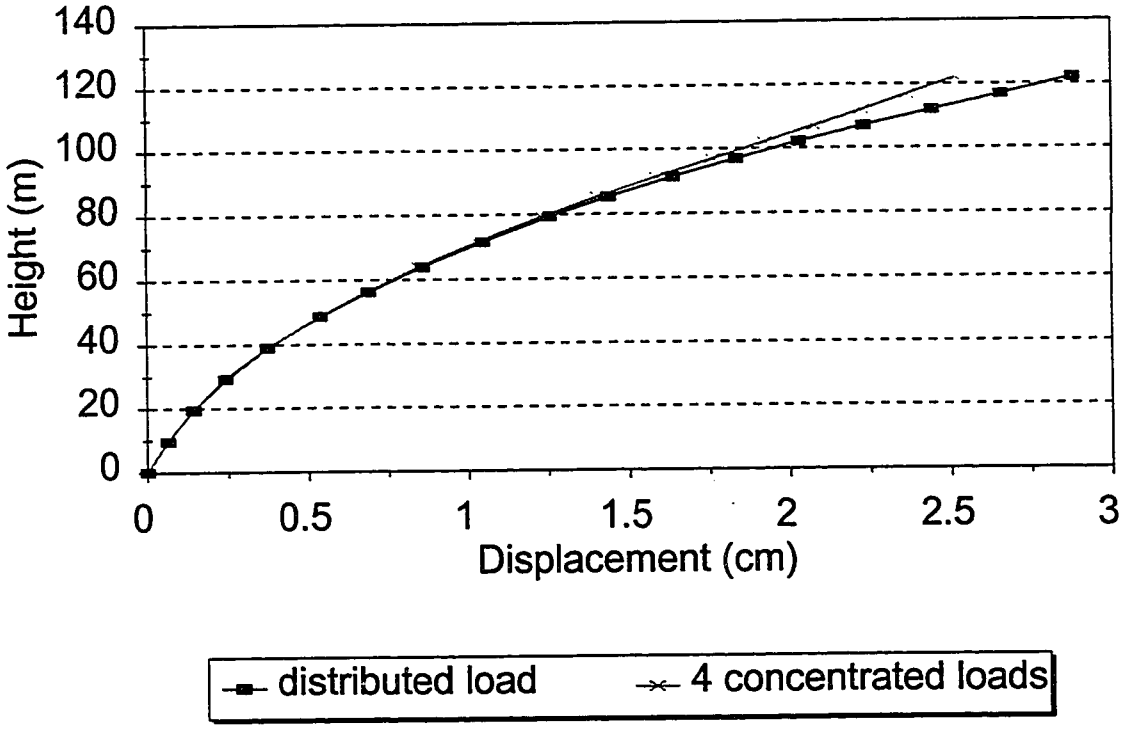

Figure 5.4 Deflection of the dam due to distributed and concentrated loads
(case of hydrostatic and maximum dynamic load due to the taft earthquake record)

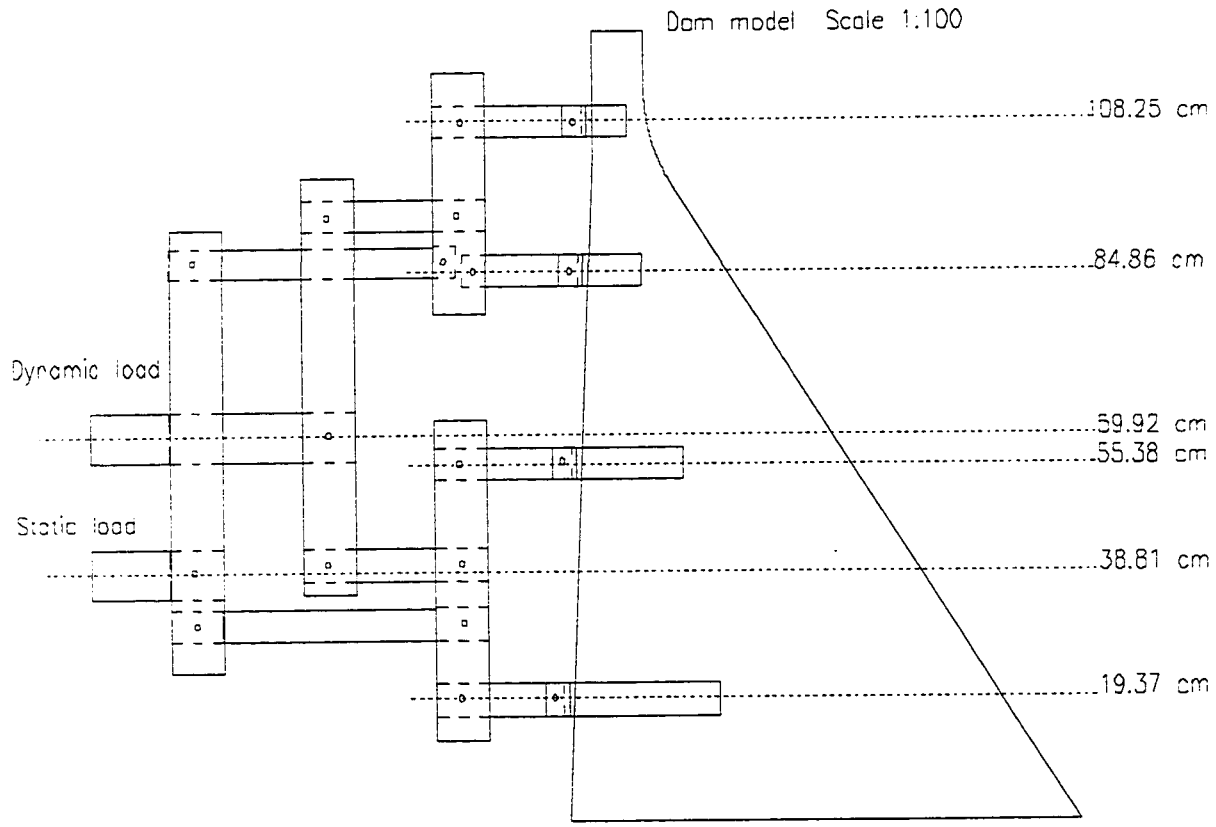

Figure 5.5 Loading mechanism for static and dynamic loads

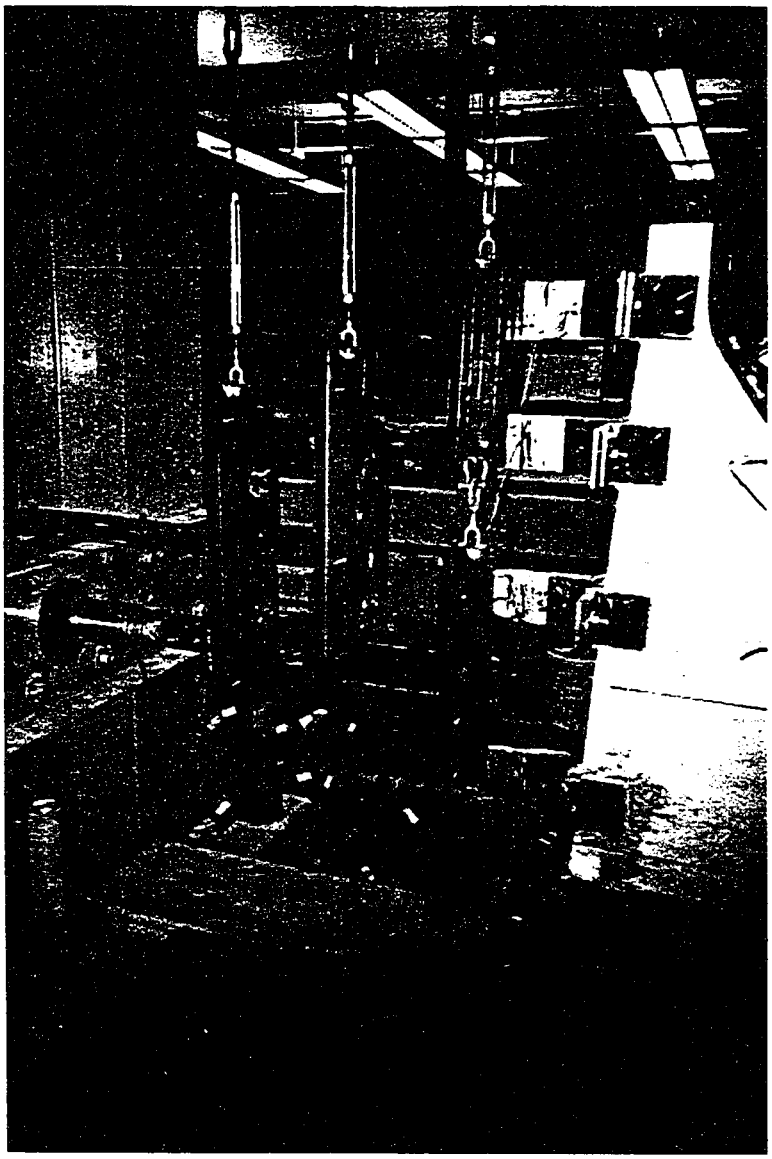

Figure 5.6 Loading mechanism

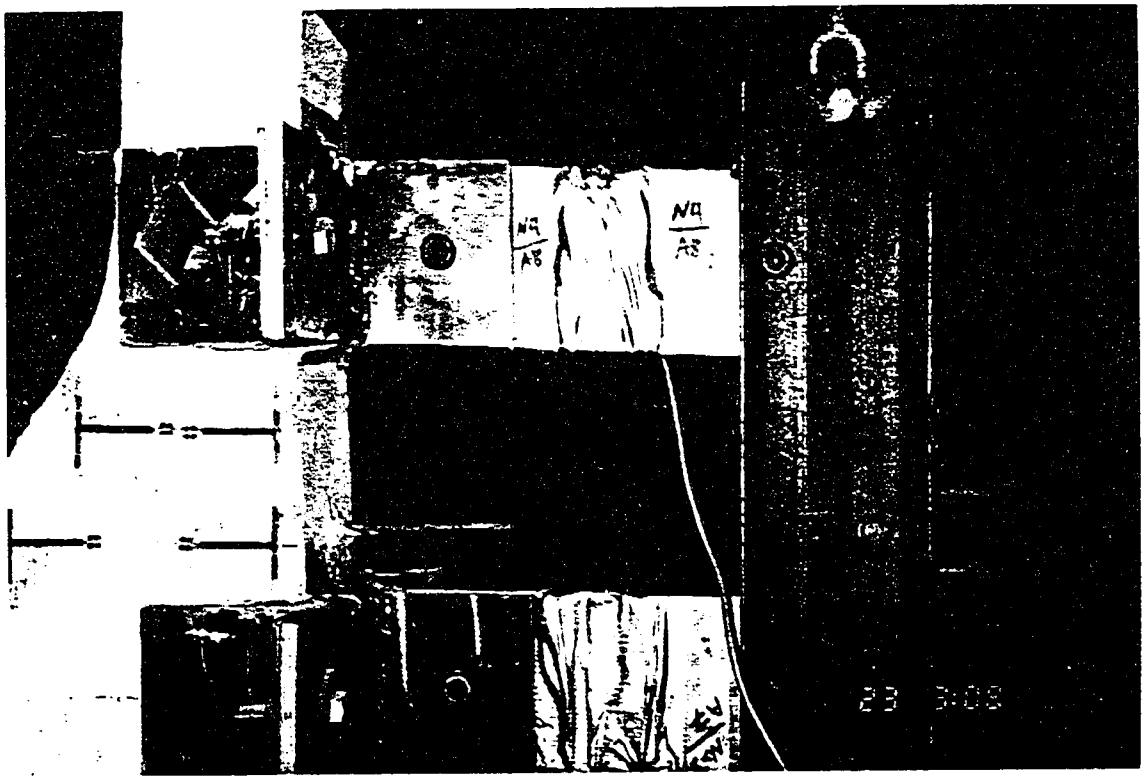

Figure 5.7 Attachment of U-shaped channel to the specimen

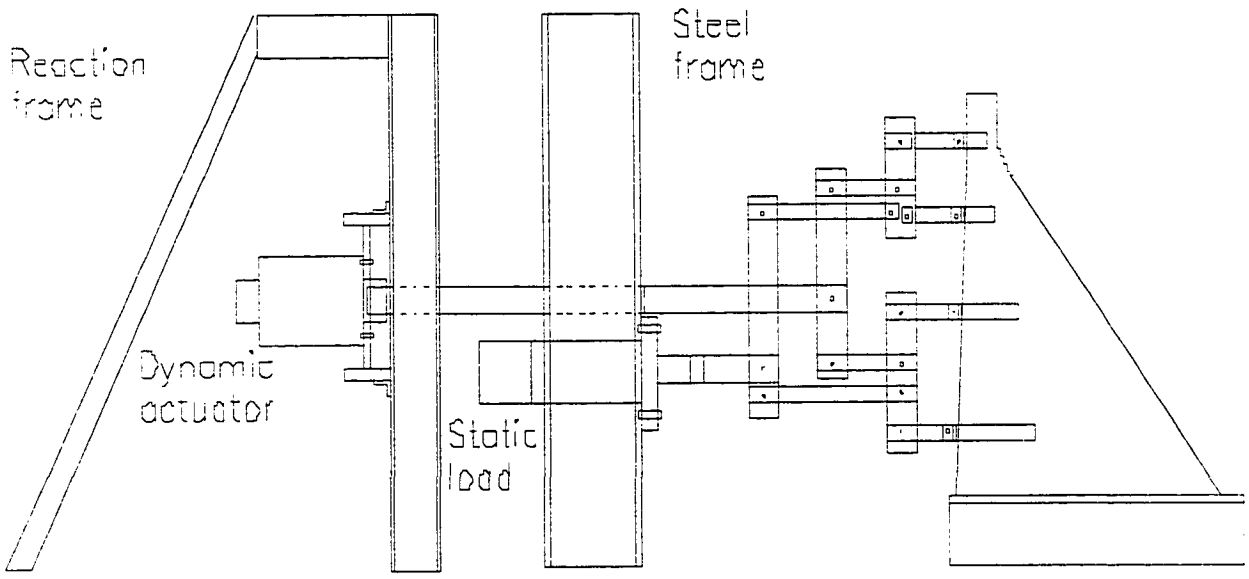

Elevation view

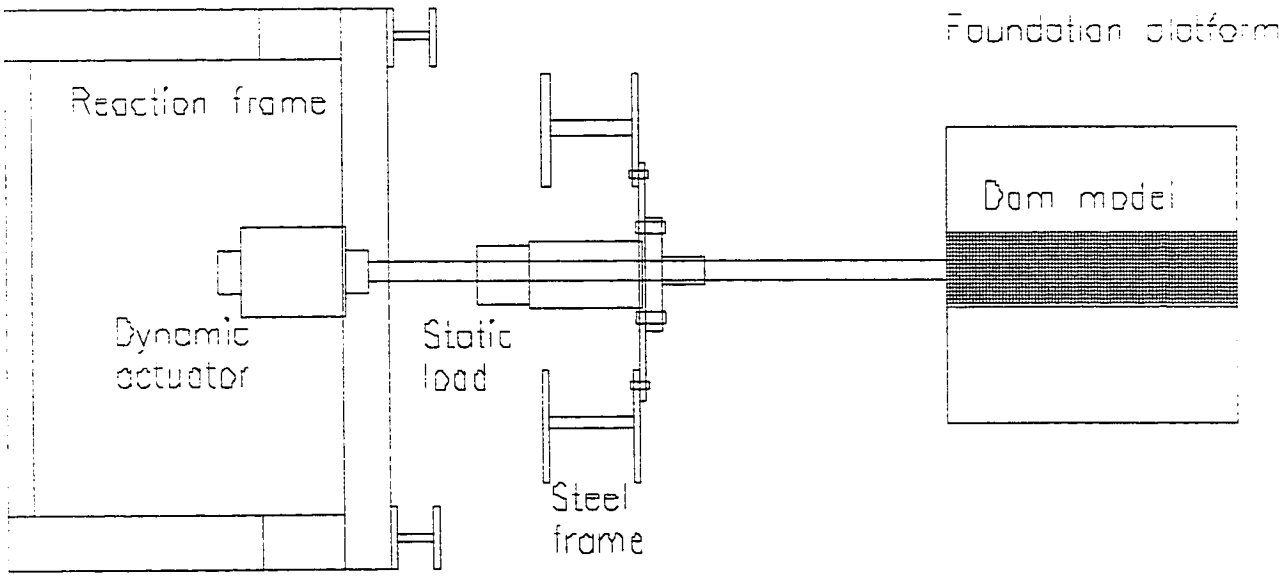

Plan view

Figure 5.8 Test set-up

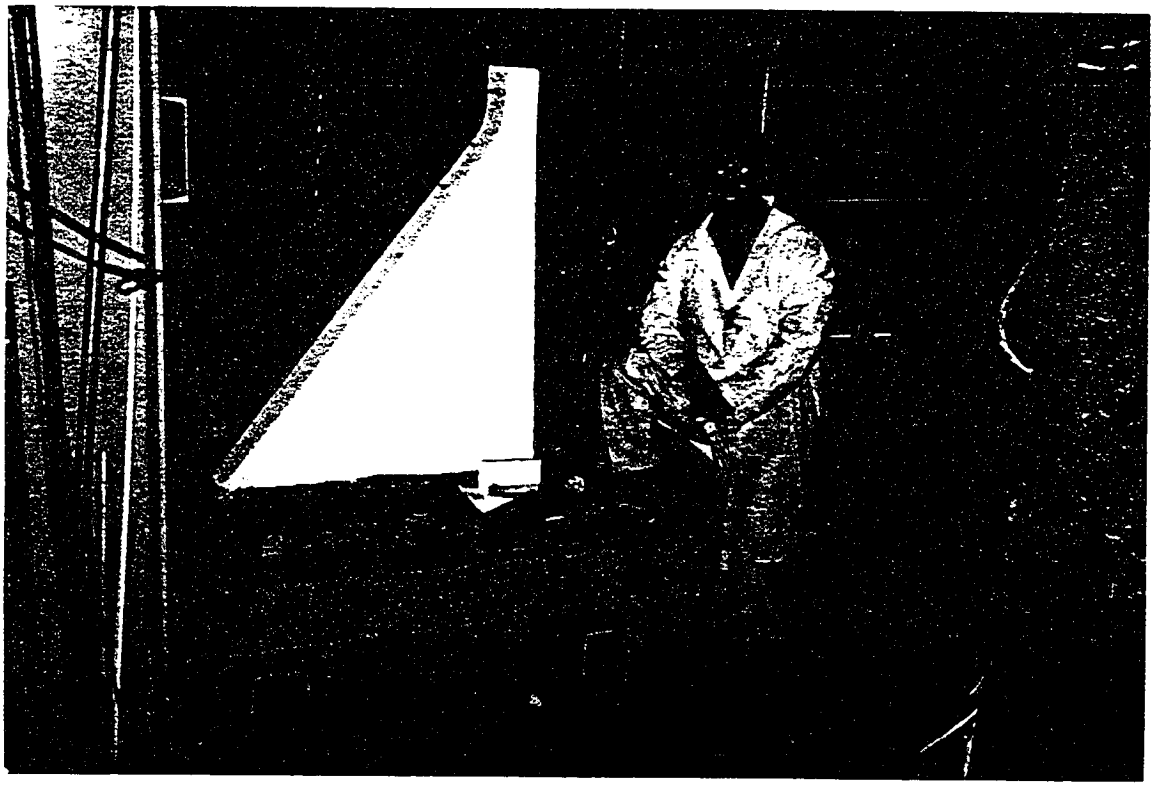

Figure 5.9 Dam model on foundation platform

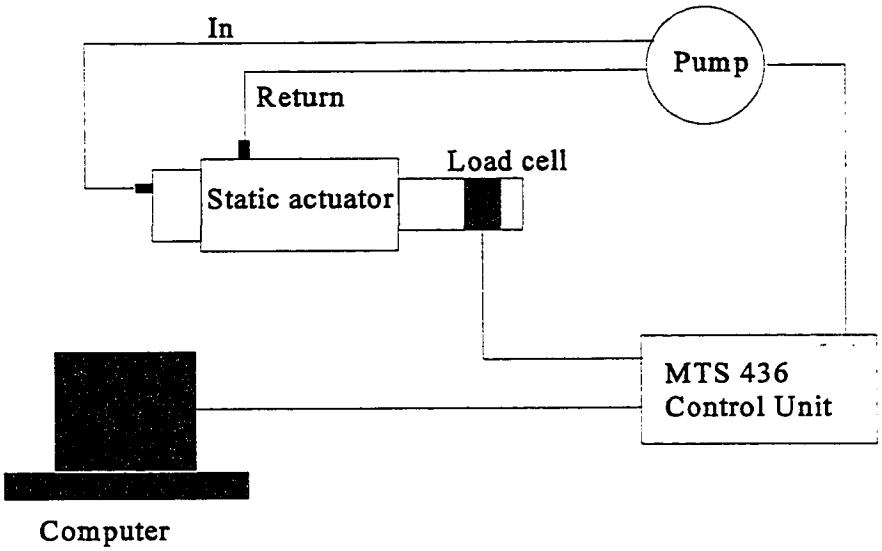

Figure 5.10 Schematic view of MTS control unit connections

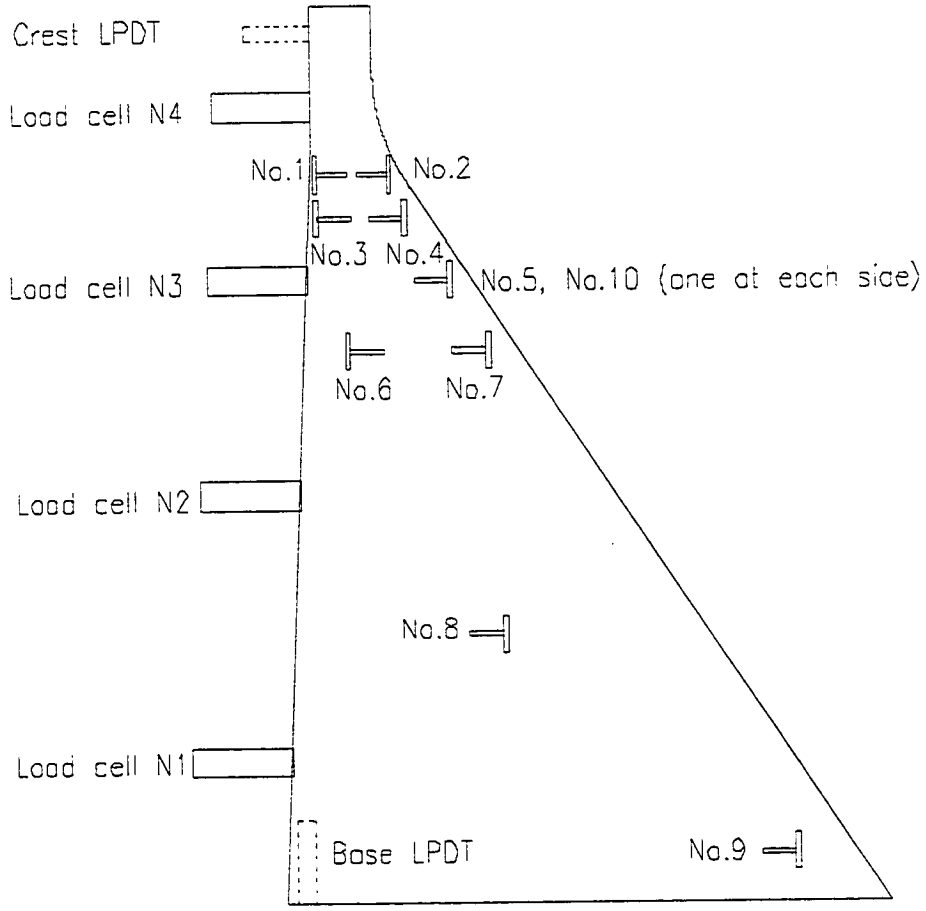

Figure 5.11 Location of the strain gages, displacement transducers and load cells on the dam model

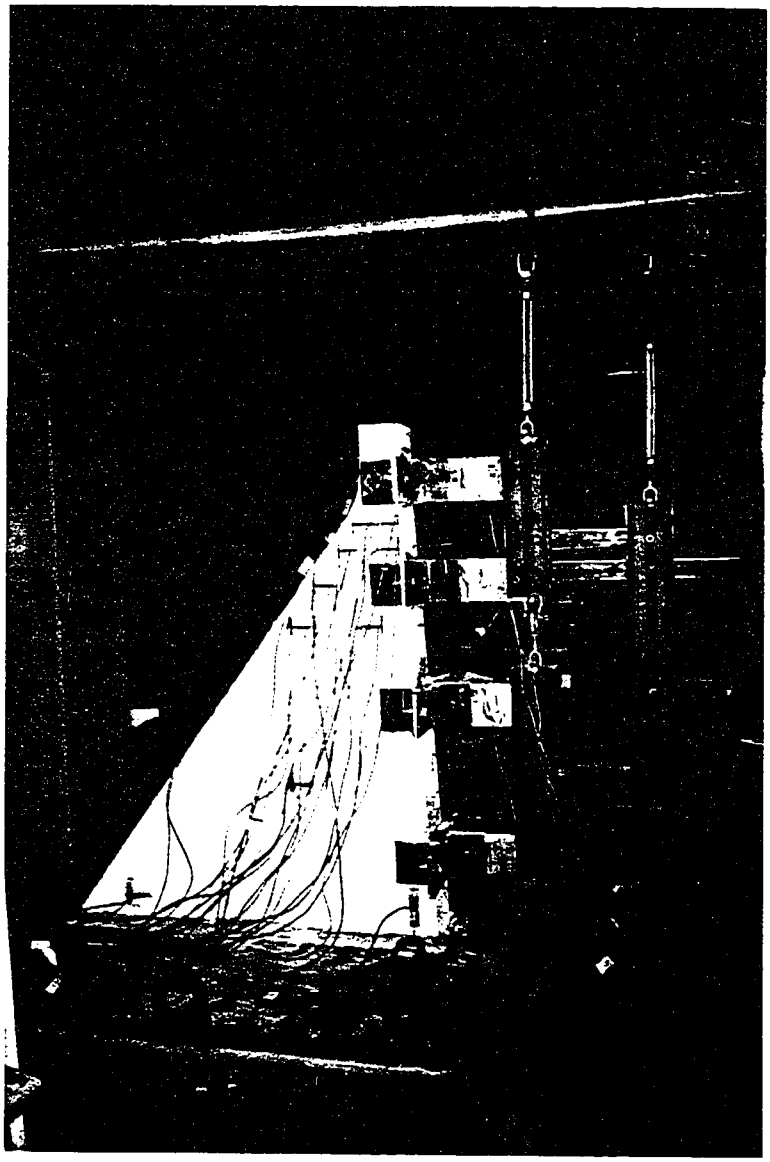

Figure 5.12 Specimen instrumentation

CHAPTER SIX

BEHAVIOUR OF THE DAM MODEL

6.1 INTRODUCTION

The criterion of safe performance for a dam during an extreme event is that the dam shall continue to safely retain the reservoir water. The complete assessment of dam safety requires a comprehensive knowledge of design and a judgement based on experience and analysis. To achieve an engineering judgement the, Canadian Dam Safety Guidelines (1996) requires that "stability and stress shall be evaluated in concrete dams". It also requires a *physical model study* to assist in evaluating the behaviour and performance of dams.

The Canadian Dam Safety Guidelines (1996) requires that "Concrete dams shall be designed to resist and prevent

- sliding at the dam-foundation interface, *within the dam* and at any plane in the foundation
- overturning of the structure
- *overstressing of the concrete dam or foundation*
- excessive seepage through the foundation and through joints in the concrete dam".

The guidelines offer no strict rules for performing the analysis in the process of safety assessment. The guidelines safety requirement can be achieved by applying a nonlinear fracture analysis or by model testing.

In this chapter, the results of the experimental measurements of the dam model performance are presented. Experimental results are compared with theoretical predictions.

6.2 TESTING PROGRAM

In order to check the test set-up and to ensure that all equipment and instrumentations are functioning properly, the first test was conducted using hydrostatic load only. The load was gradually increased to approximately 60 kN. Results of the first test are shown in figures 6.1, 6.2 and 6.3. The measured load distribution using the load cells at the concentrated load locations is plotted in figure 6.1. The proper representation of the hydrostatic loading is demonstrated. The load-base strain relationship is plotted in figure 6.2. The base tensile strain is measured in a vertical direction by the LPDT located near the heel of the model dam at the base. Cracking was first observed at the base at an applied load of 45 kN. The specimen attained a maximum load of 60 kN before rapid loss of strength due to the crack propagation.

The strain measurements at the 10 strain gage locations (figure 6.3) indicated that at locations no. 1, 6 and 8, the concrete experienced tensile strains while all the other locations showed compressive strains in the both x- and y-directions. The maximum tensile strain occurs at the base of the dam at the upstream face (heel). This confirms that in the case of

hydrostatic loading, a crack is initiated at the base of the upstream side of the dam. After cracking occurs, strains at other locations remain almost constant. This indicates that most of the energy input due to increasing the hydrostatic load is dissipated by increased crack width at the heel where the crack was initiated.

In the second test, both dynamic and static loads are applied. The static load is kept constant at 30 kN while the dynamic load is increased cyclically up to 40 kN. The loading routine and the measured load distribution on the upstream face of the dam are shown in figure 6.4. The variation of base strain, crest displacement and the strain measurements at all the strain gage locations are shown in figures 6.5, 6.6 and 6.7. The variation of the applied load resultant with the strain at the base is shown in figure 6.5. Cracking is initiated at the base of the concrete dam model on the upstream side at static plus dynamic loads of approximately 45 kN. The failure load capacity of the dam model is reached at 65 kN. The measured crack mouth opening displacement with the applied load is plotted in figure 6.5. The plot is in a different format from the traditional crack mouth opening displacement graphs due to the cyclic nature of the applied load.

The variation of the load with the crest displacement is plotted in figure 6.6. As expected, the dam model behaviour is elastic until the initiation of the crack, when the response becomes nonlinear. The variations of the strains at various locations with the applied load are plotted in figure 6.7. The maximum tensile strain is approximately 0.025×10^{-3} at locations no. 1 and 3. This shows that when the hydrodynamic load is applied to the dam, the maximum tensile stress is shifting toward the upper part of the dam near the slope discontinuity. When the hydrostatic and dynamic loads are acting in opposite directions, the

dynamic loads have higher values at the top part as compared with the hydrostatic load. This is the main reason for cracking and damage at the top part of concrete gravity dams when the dynamic loads are taken into account.

A third test was conducted to evaluate the behaviour of a dam anchored to the foundation and to evaluate the effect of the ratio of the static / dynamic load on the test set-up and on the performance of the model. The dam base was anchored to the foundation using 4 anchor bolts. The anchors were glued to a hole drilled at the bottom of the dam and bolted to the foundation. The static load was kept constant at 70 kN. The dynamic load was cycled from 10 kN up to 100 kN, increasing by 10 kN per cycle. The results of the test are shown in figures 6.8, 6.9 and 6.10. The dam model behaviour shown in figure 6.8 is more ductile when compared with the previous case. The cracking strain was reached at static plus a dynamic load of 45 kN. Comparing figures 6.5 and 6.8, indicates that in the second test after crack initiation, the stiffness and strength deteriorated rapidly such that cracking load and failure load are very close. This shows brittle behaviour of the model in the second test. In the third test, the static plus dynamic load was increased to almost three times the cracking load. This performance indicates the effectiveness of the anchoring method proposed for the third test.

The crest displacement variation with the applied load is plotted in figure 6.9. The maximum crest displacement is 17.5 mm which is almost 3 times higher than the crest displacement in the second test. The variation of the crest displacement in figure 6.9 is bounded in a narrow range which is similar to figure 6.6 from the second test. This represents the almost elastic then brittle behaviour of the model.

Figure 6.10 shows strain variation at the different location in the third test which are fairly similar to the strains measured in the second test (figure 6.7). Since the loading capacity was increased substantially in comparison with the second test, all the ten locations experienced higher strains in comparison with the previous tests. Location no.1 reached tensile strain of approximately 0.07×10^{-3}.

6.3 ANALYSIS

Analysis of the dam model and prototype was performed in order to evaluate the proposed experimental approach. The evaluation is based on the results of static and dynamic analyses of the dam-reservoir system.

6.3.1 Effect of Gravity on the Dam Model

Considering the maximum modelling load which is obtained from the first and second tests, the moment at the base $M^m_{ng} = \sum_{i=1}^{4} F_i h_i$ is calculated to be 23.93 and 32.03 kN.m. respectively. The distortion at the failure stage can be found for the first two tests using the equations (5.7) and (5.8). The third test was excluded because anchoring at the base causes additional distortion of the results. The parameters of the equations for the model are: n=100, h^m=0.968 m, P^m = 13.58 kN, M^m_{ng}=23.93 kN.m (first test) and M^m_{ng} =32.03 kN.m (second test). From equation (5.7), the stress correction factor due to the gravity load distortion is, D^t = 111% and 116% for the first and second tests, respectively.

With the scaling of the weight density in the model, there is enough vertical force

(p^m) to prevent early cracking of the model at the base. Higher values of the external load result in higher distortion. This is because the bending moment in the model at the base M^m_{ng}, increases and consequently the value of the distortion factor D^t is increased.

6.3.2 Static Response of the Model and Prototype

To evaluate the performance of the test set-up, a comparison is made between the test measurements and analytical predictions. Linear finite element analyses of the dam model and prototype are carried out for the third test specimen. In the finite element analysis of the model, the reservoir effect and the inertia force due to weight of the structure are represented by four concentrated loads acting at the upstream face. In order to obtain the maximum state of stress and strain, two cases of maximum loading are analyzed. The hydrostatic load is taken constant at 70 kN while the dynamic load is taken as ±100 kN.

The finite element analysis is conducted for three different cases using four concentrated loads: a) Model dam, b) Prototype, c) Model dam with the appropriate mass density factor. Results of the analyses are compared with experimental measurements. It is found that the strains in the prototype and dam model agree closely when the mass density factor is taken into account. Figures 6.11 and 6.12 show the predicted and measured strains. In these figures, location number zero refers to the dam base at which there was no strain gage. Strain gage at location number 9 and the strain gage in the horizontal direction at location number 7, were damaged during the test. Figures 6.11 and 6.12 show that the predicted and measured strains are in good agreement at location numbers 2, 4, 5 and 7 which are far from the local effect of the concentrated loads. This confirms that the

performance of the test set-up and measurements of the strain gages are a reasonable representation of the loading and strains the maximum stress zones in an actual dam.

The predicted maximum tensile stress contours using the finite element analysis are shown in figure 6.13. The principal tensile stress contours in the prototype (figure 6.13 b) and model with the appropriate correction for the mass density (figure 6.13 c), are found to be similar. It is important to note that the mass density can be compensated for in the distorted model by the analytical correction factor. It is also concluded that in spite of violating the mass density scale in the specimen the stress distribution at the top part of the dam model remains very similar to that of the prototype. At the top part of the dam the effect of mass density is low.

6.3.3 Dynamic Response of the Dam-Reservoir System

The finite element analysis of the prototype dam is conducted including the dam-reservoir interaction when the dam is subjected to earthquake ground motion. An infinite reservoir with rigid dam foundation and no reservoir bottom absorption is considered in the dynamic analysis. The horizontal S69E component of the Kern County site record during the July 21, 1952 Taft Lincoln earthquake scaled to PGA of 0.242 g, is used in the analysis. In the dynamic analysis, the hydrostatic load was decreased to the corresponding value in the third test. The dynamic load applied in the third test corresponded to PGA scaled to 0.242 g. Figure 6.14 shows that the stress distribution in the prototype dam using finite element analysis including dam-reservoir interaction, when the PGA of the horizontal component of the Taft earthquake record is scaled to 0.242 g, is in good agreement with the test

measurement for the model using four concentrated loads (figure 6.13c). The agreement is close especially at the critical zone on the downstream face of the dam near the slope discontinuity. At the upstream face of the model, the stress contours are distributed as shown in figure 6.13 due to the concentrated nature of the applied load.

6.4 CONCLUSIONS

The proposed new approach for small scale modelling of concrete gravity dams is evaluated. The efficiency of the testing approach was investigated by comparing the measurement with theoretical predictions.

It is concluded that approximating the reservoir forces on the dam by four concentrated loads provides a reasonably accurate experimental representation of the dam-reservoir interaction effect. Measured strains during the testing of the model with the same material properties as the prototype, are found to be in good agreement with strains calculated using the finite element approach. The stress distribution at the top part of the dam model and the prototype of the same material properties are found to be in close agreement.

The proposed experimental technique has the potential for being used to validate some of the assumptions adopted in the formulation of the dynamic analysis solutions for the response of dam-reservoir systems. The approach has the recognized limitations of relying on analytical methods for the calculation of the equivalent quasi-static load to simulate hydrodynamic and inertia forces and to analytically include the gravity effects in the stress and strain distributions in the dam.

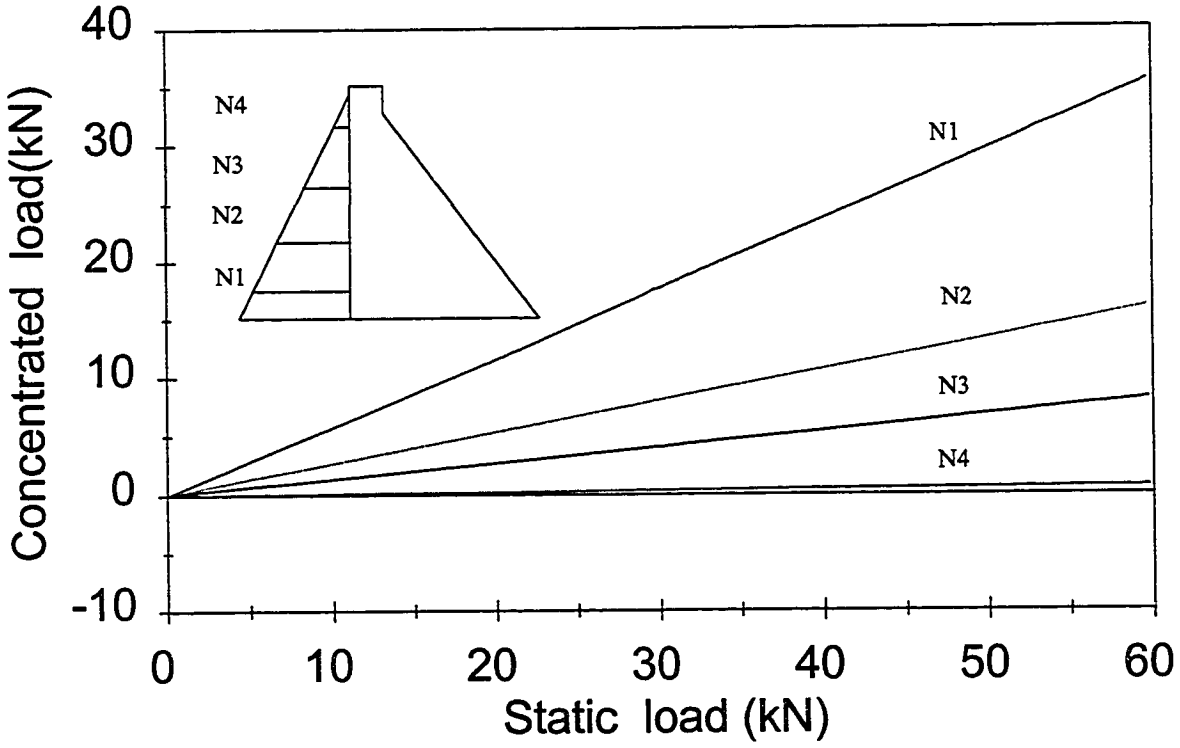

Figure 6.1 Distribution of applied static load in the first test

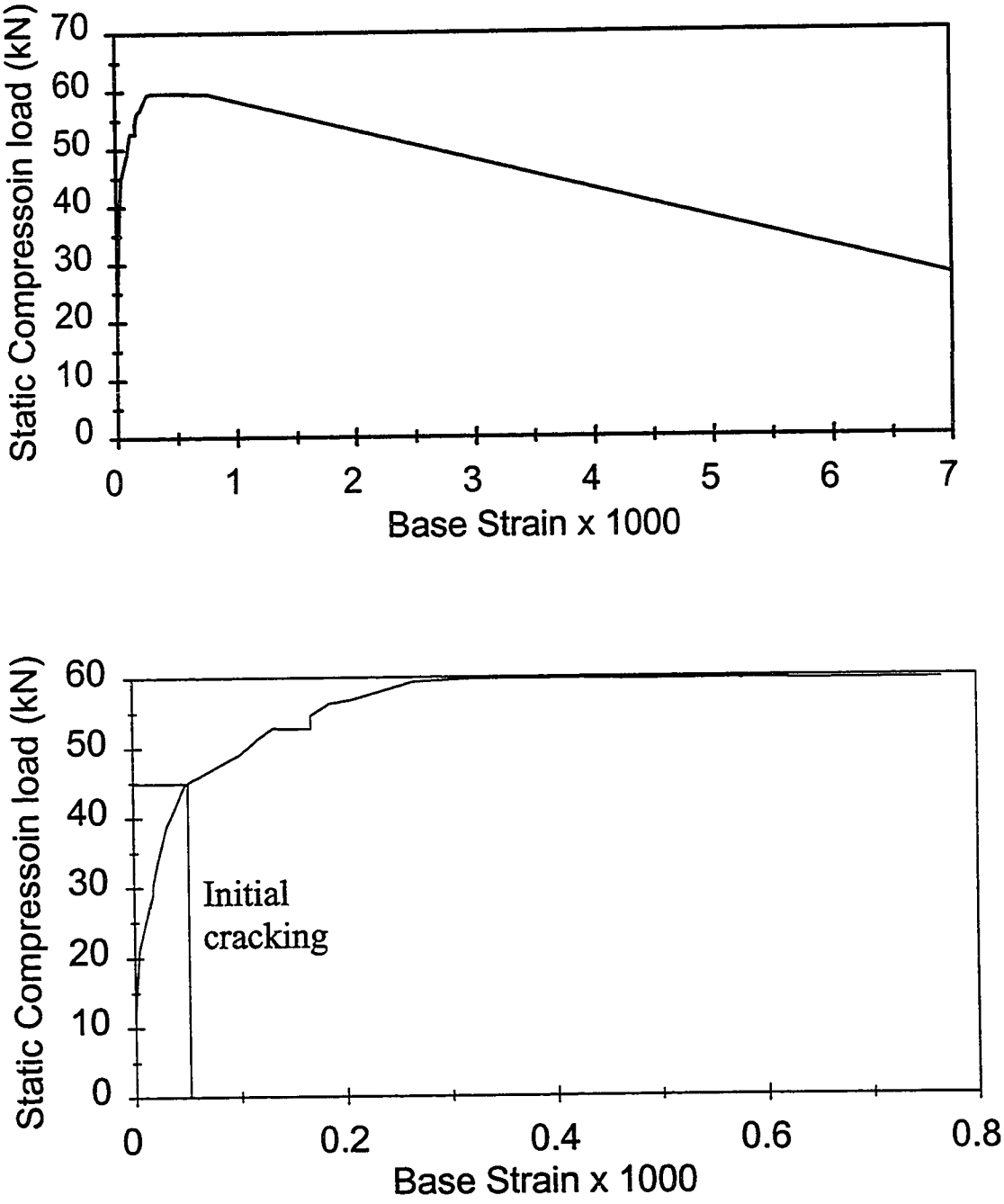

Figure 6.2 Variation of base strain in the first test

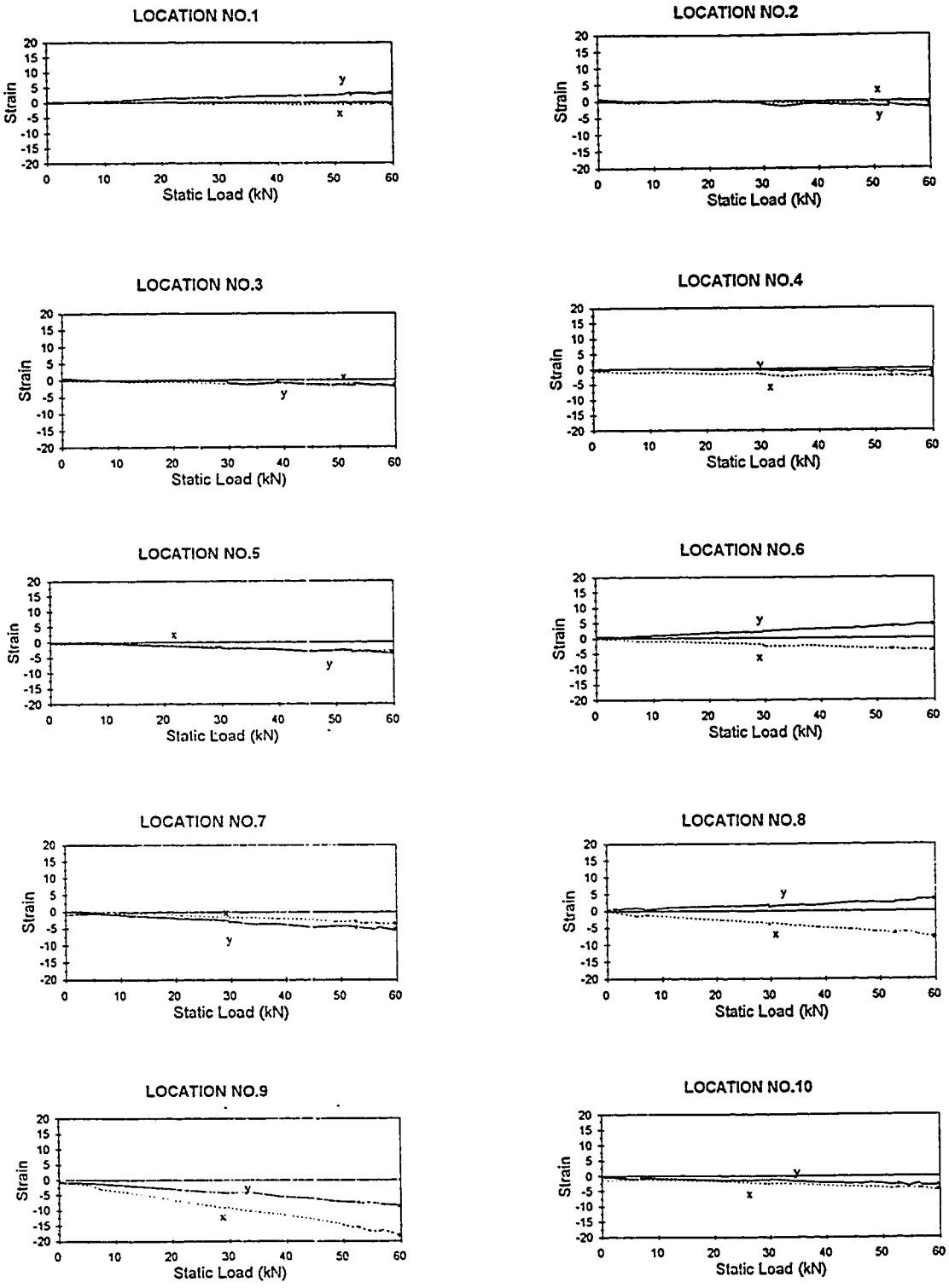

Figure 6.3 Strain variation at different locations in the first test (strain × 10^6)

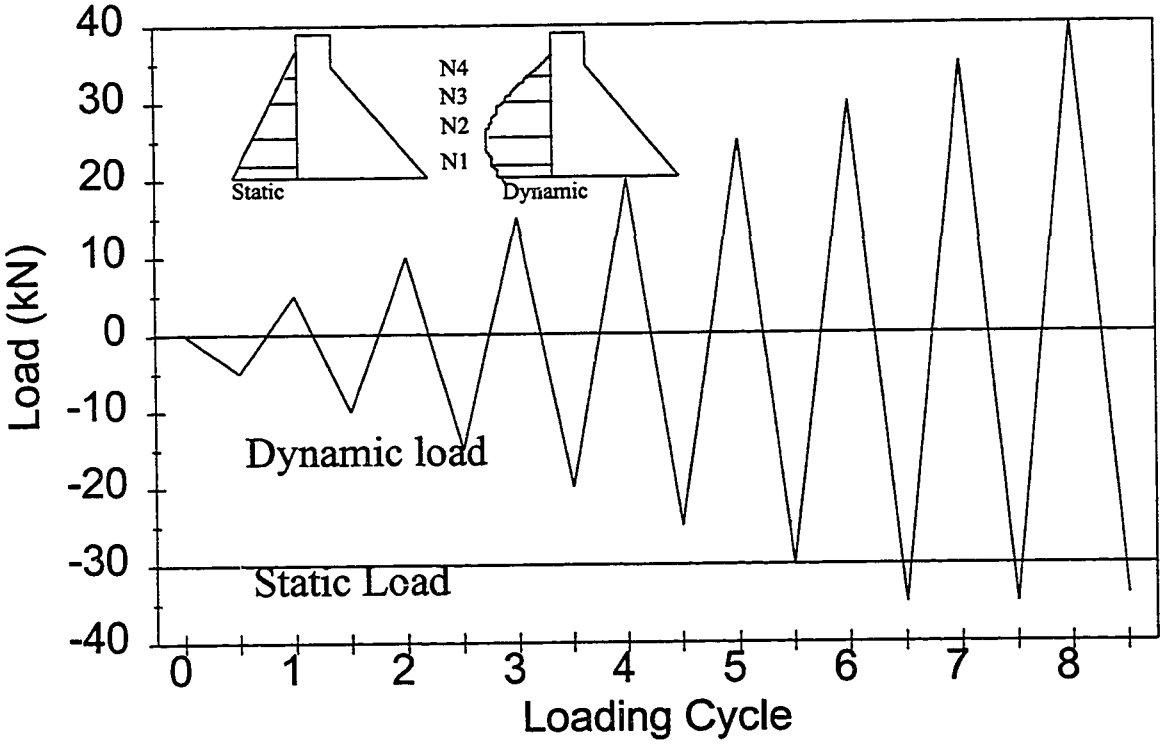

Figure 6.4 Applied static and dynamic loads in the second test

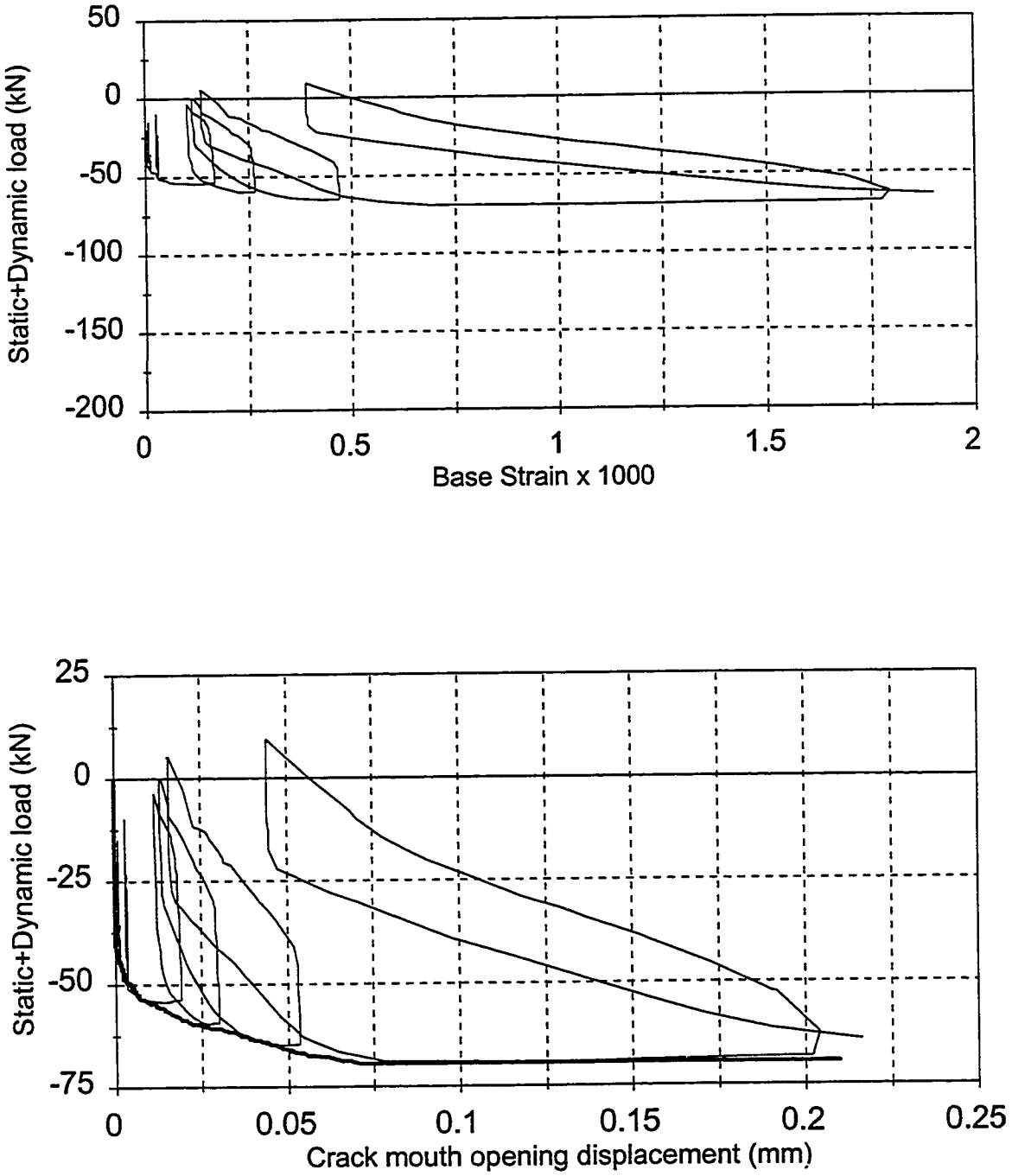

Figure 6.5 Variation of base strain and displacement in the second test

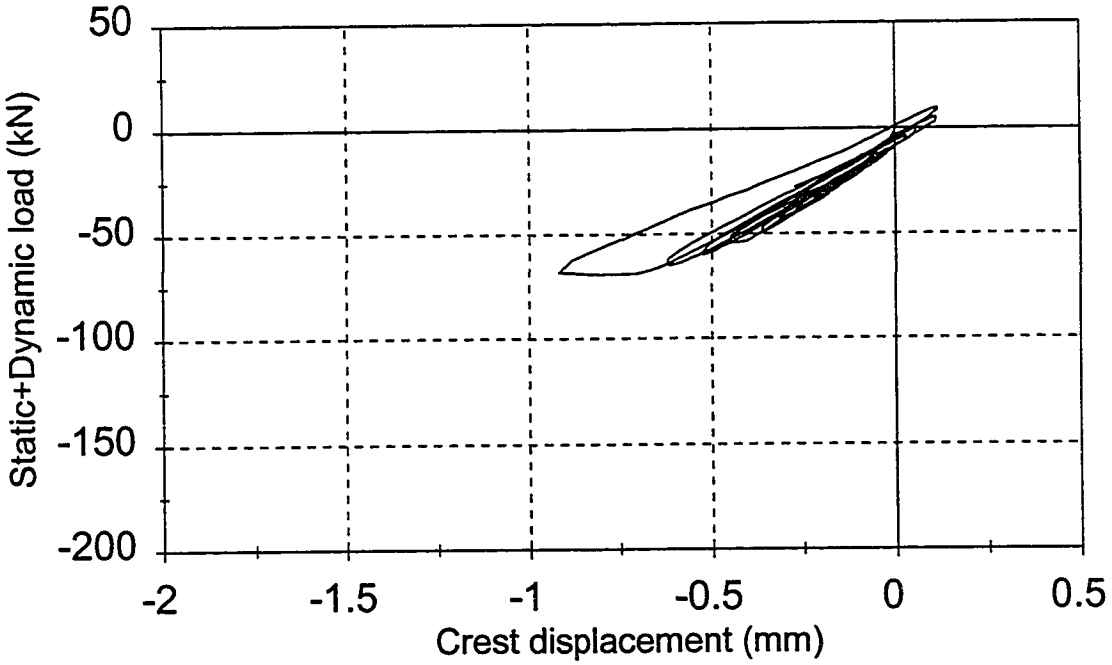

Figure 6.6 Crest displacement in the second test

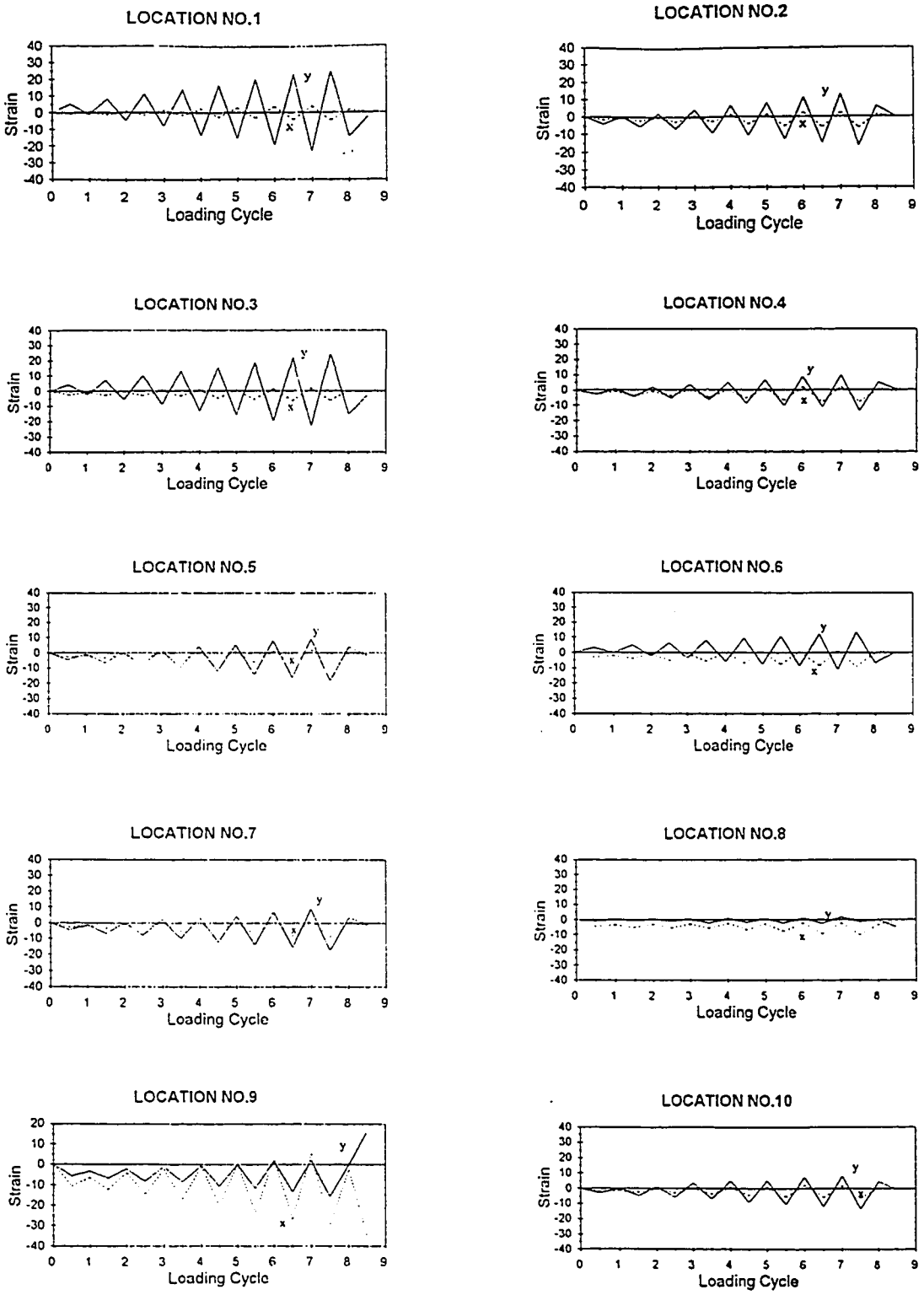

Figure 6.7 Strain variation at different locations in the second test (strain × 10^6)

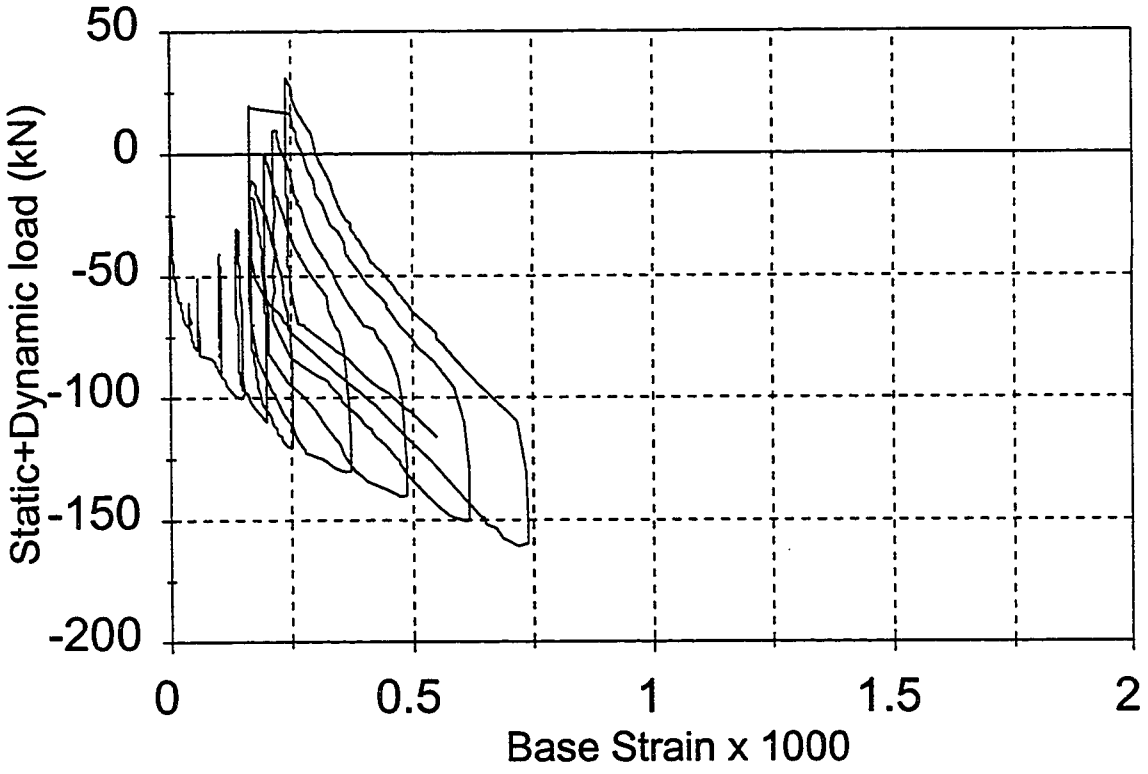

Figure 6.8 Variation of base strain in the third test

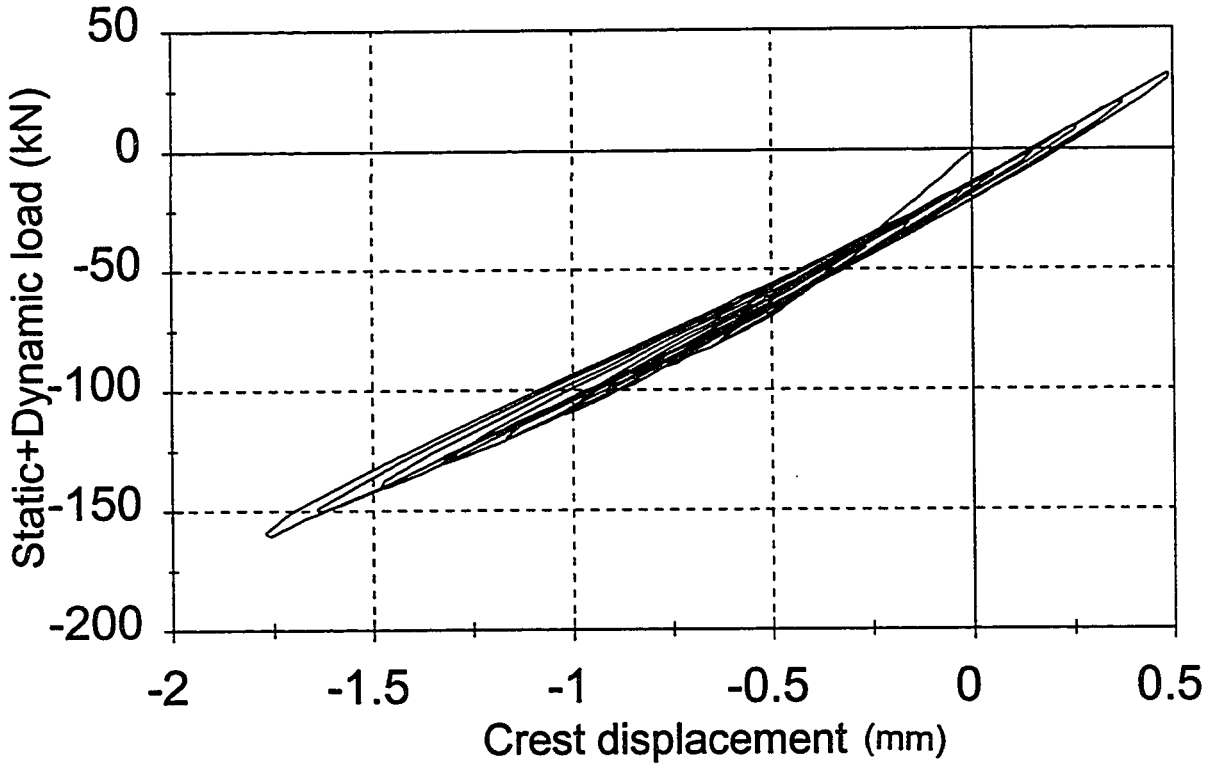

Figure 6.9 Crest displacement in the third test

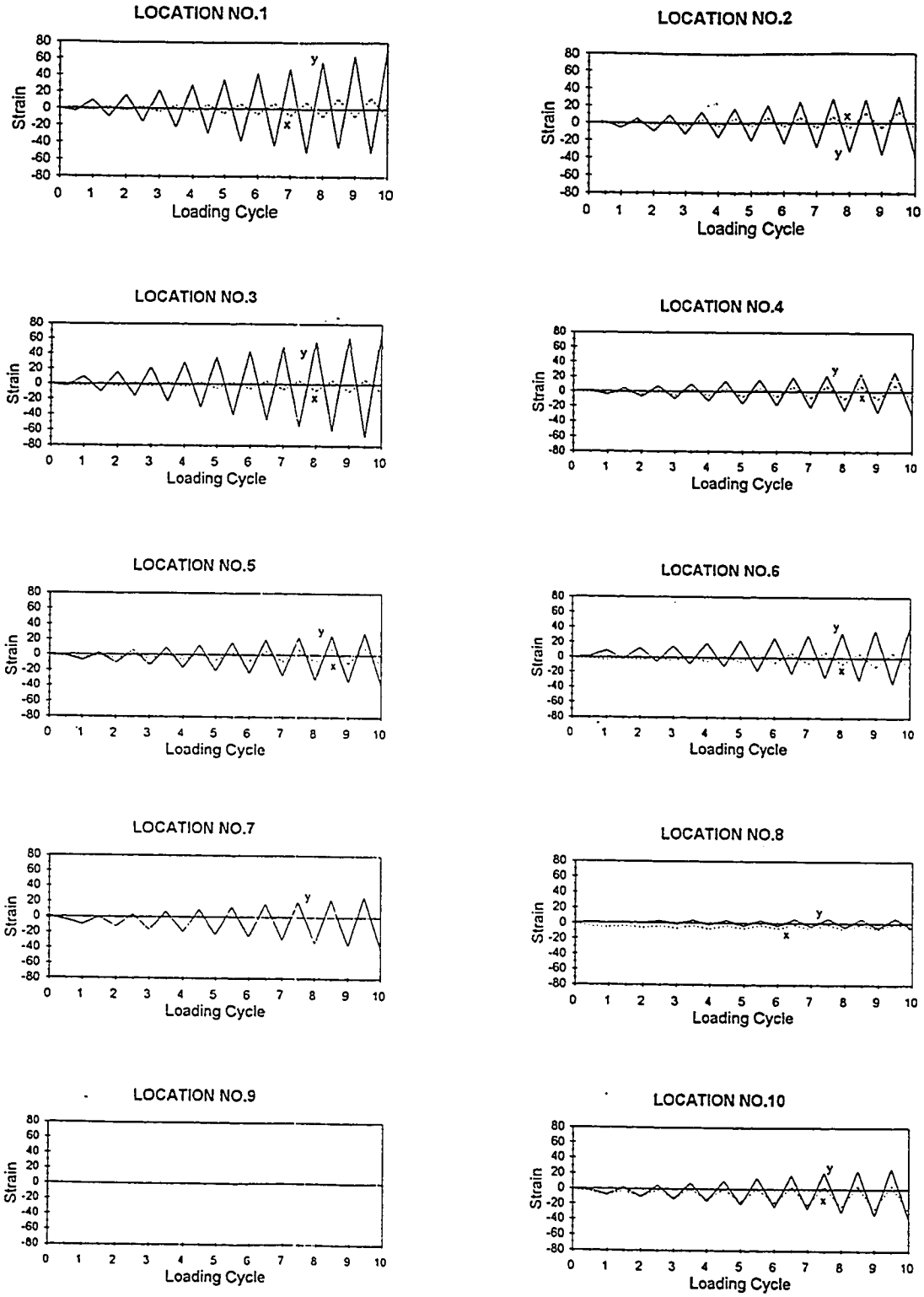

Figure 6.10 Strain variation at different locations in the third test (strain × 10^6)

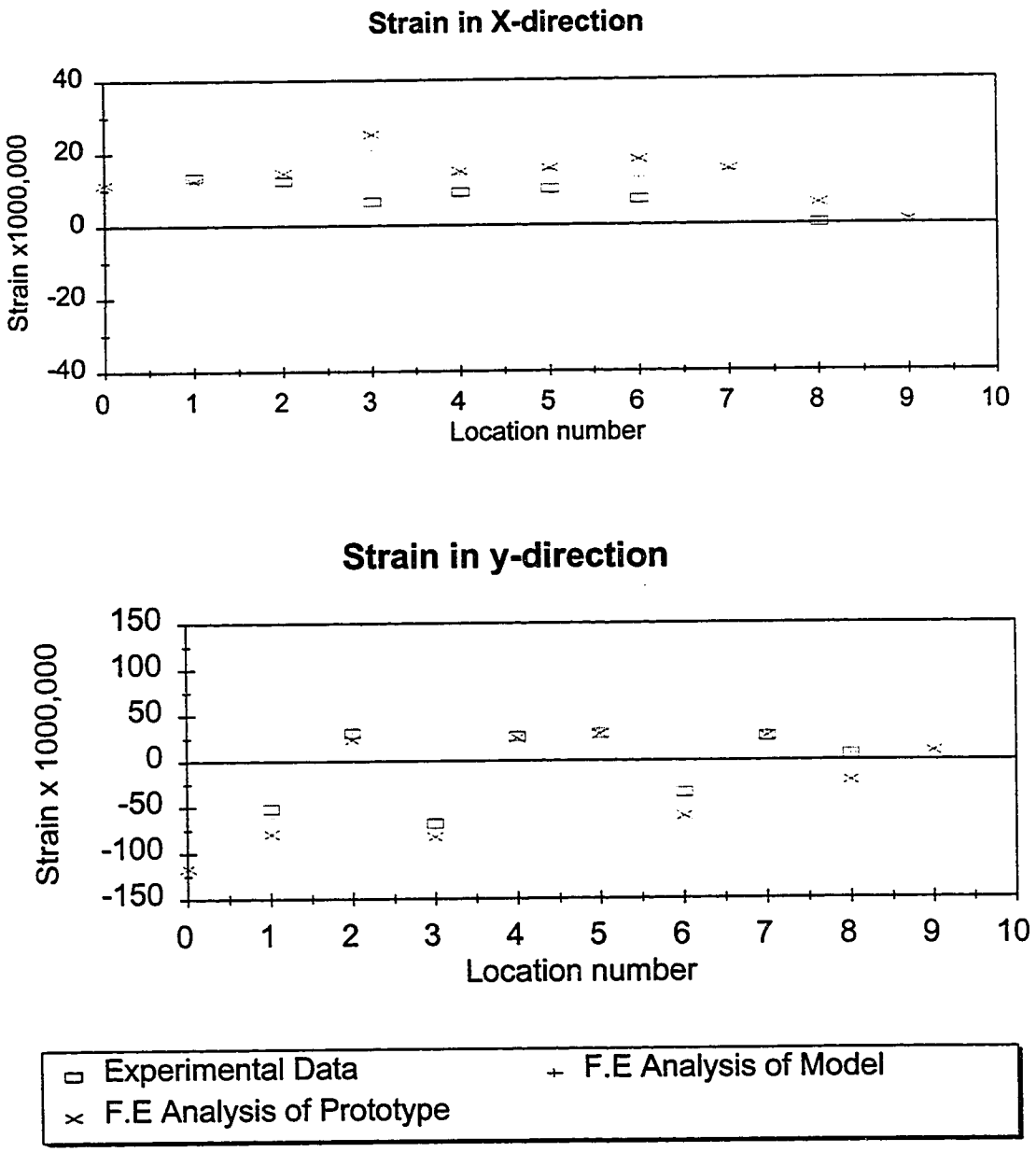

Figure 6.11 Comparison of strains obtained from experiment and finite element analysis static load=-70 kN, dynamic load=100 kN

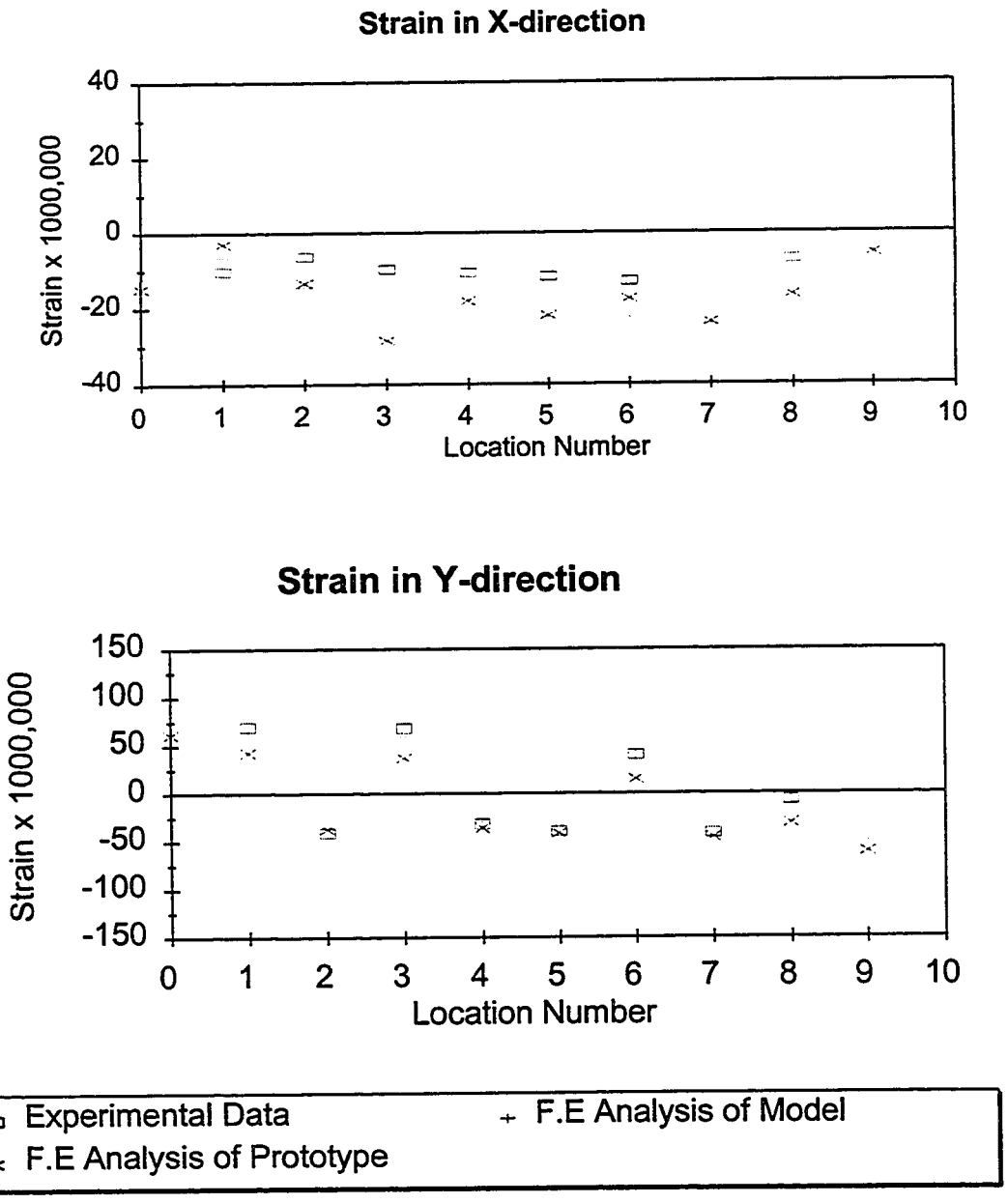

Figure 6.12 Comparison of strains obtained from experiment and finite element analysis static load=-70 kN, dynamic load=-100 kN

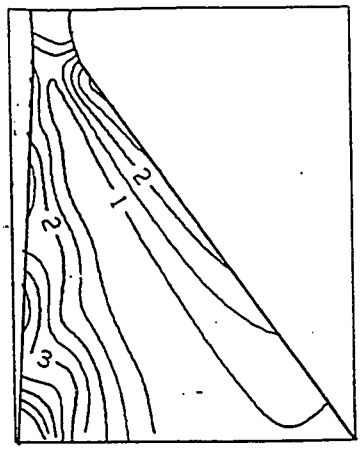

a) Model dam

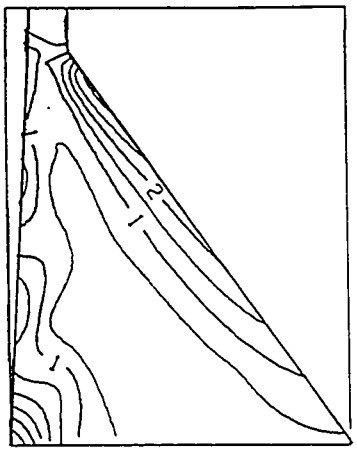

b) Prototype

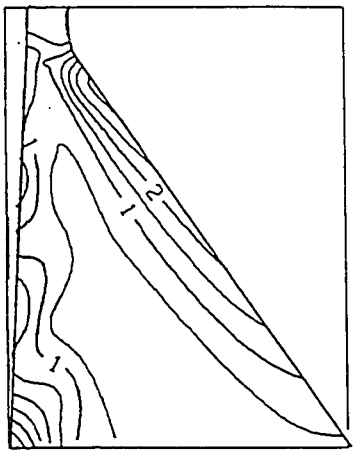

c) Model dam with correction for gravity effect

Figure 6.13 Maximum principal tensile stress contours obtained from finite element analysis using proposed experimental approach, MPa
static load=-70 kN, dynamic load= ±100 kN

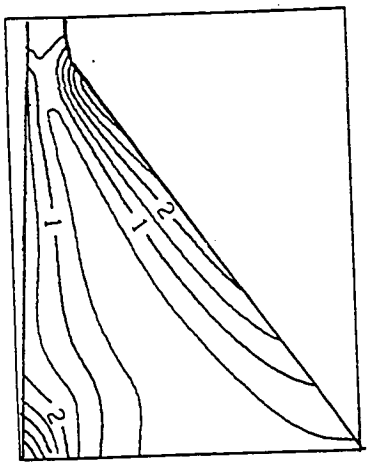

Figure 6.14 Maximum principal tensile stress contours (MPa) obtained from dynamic analysis of the prototype under the Taft earthquake ground motion scaled to PGA of 0.242 g, (Hydrostatic pressure=0.69735 full hydrostatic pressure)

CHAPTER SEVEN

CONCLUSIONS AND RECOMMENDATIONS

7.1 INTRODUCTION

A study was conducted to investigate the dam-reservoir interaction effect on the linear and nonlinear seismic response of concrete gravity dams. A mathematical approach has been developed for the time domain solution of the coupled dam-reservoir interaction problem which can be implemented in the nonlinear seismic analysis of concrete gravity dams. The developed approach is applicable when the effect of the travelling seismic waves on the dynamic response of the dams is taken into account. An experimental study of small-scale models of concrete gravity dams was conducted. The dam reservoir interaction in terms of hydrostatic, hydrodynamic and seismic loads were simulated using a mechanical loading system.

7.2 CONCLUSIONS

The following conclusions can be reached based on the numerical analysis and the experimental work conducted in this research program.

- The proposed method of partitioned solution, namely the staggered solution procedure is found to be accurate when compared with the existing frequency domain analytical solution. The proposed staggered method requires no iterations and is less time consuming than the other classes of solution for the coupled field problem. The method is convenient and easy to apply in the nonlinear seismic analysis of concrete dams.

- The dynamic response of concrete gravity dams to earthquake ground motion can be significantly influenced by the effect of the travelling seismic excitation waves. Nonuniform ground motion may result in higher response for the horizontal earthquake component than in the case of uniform ground motion. The earthquake wave velocity is an important factor that affects the response parameters significantly. The inclusion of nonuniform earthquake excitations is necessary in the calculation of the hydrodynamic pressure distribution and therefore on the dam crest displacement. Due to limited speed of the travelling seismic wave, the assumption of uniform earthquake ground motion may not be realistic.

  The direction of the earthquake wave propagation in the horizontal direction has a noticeable effect on dam response. A seismic wave propagating from the reservoir's far boundary toward the dam may have more effect on the dam response than a seismic wave travelling in the opposite direction. The response parameters due to the vertical earthquake excitation are not sensitive to the direction of the wave propagation.

- The nonlinear seismic fracture response analysis of concrete gravity dams that include dam-reservoir interaction gives a crack pattern that is close to the observed damage to the Sefid-rud dam during the 1990 Manjil earthquake. The predicted crack pattern is different from that of the case when the dam-reservoir interaction is approximated using the added mass approach. It is concluded that proper modelling of the dam-reservoir interaction is important in the nonlinear response analysis of concrete gravity dams.

- From the experimental study of small scale dam models, it is concluded that the hydrostatic, hydrodynamic and seismic loads can be simulated using the proposed mechanical loading system.

  It is found that approximating the reservoir forces on the dam by four concentrated loads provides a reasonably accurate experimental representation of the dam-reservoir interaction effect. Strains measured during the testing of the model with the same material properties as the prototype, are found to be in good agreement with strains calculated using the finite element approach. The stress distribution at the top part of the dam model with the gravity load scaling correction is found to be in close agreement with the stress distribution in the prototype of the same material properties.

  The proposed experimental technique has the potential for being used to model and test the top part of the dam only as well as the comparative testing of models of dams with different structural characteristics such as original and

rehabilitated dams. It may be also used to validate some of the assumptions adopted in the formulation of the dynamic analysis solutions for the response of dam-reservoir systems.

7.3 RECOMMENDATIONS

Base on the experience gained from the dam-reservoir interaction study, the followings are recommendations for future work:

- The proposed staggered solution method can be applied to the 3 dimensional dam-reservoir interaction problem.

- The effect of travelling seismic waves can be investigated using different earthquake ground motions. The effect of different configurations of the reservoir can be studied. Various reservoir geometries can be investigated such as rectangular or triangular reservoirs with different slopes of the far end.

  The effect of nonuniform earthquake motion on the three-dimensional analysis of the dynamic response of the dam-reservoir system can be investigated. The variation of the earthquake components in all directions can be included in the dynamic response of the dam.

- Finite element stress type analyses based on G_f - type smeared crack model are useful in identifying the crack profile. However the post cracking behaviour is not well represented because a closed crack cannot slide. Moreover, small displacement theory is used. Dynamic instability of dams is induced by large displacements. A separate dynamic stability analysis recognizing the cracked components as rigid bodies (or elastic bodies) with appropriate interface constitutive model (e.g. Mohr-Coulomb for sliding) is needed to asses the dynamic stability of cracked gravity dams. Due to the limitations of the constitutive model used, the magnitude of the sliding displacement cannot be determined.

  A Smeared crack model based on nonlinear fracture mechanics crack propagation criterion needs to be developed to study the three dimensional cracking of dams. The validity of the model can be checked using damage data obtained from the Sefid-rud dam during the 1990 Manjil earthquake (Iran).

- Experimental work on the dynamic testing of dam-reservoir systems is extremely difficult. It is acknowledged that model shake table testing lacks the appropriate representation of the dam-reservoir interaction. In most of the experimental studies, water was taken to be incompressible and the material of the dam model did not meet the corresponding properties of the prototype material. Therefore, the results of the tests cannot be considered to provide a good indication of crack profile in concrete gravity dams. There is a need to develop the proposed experimental technique to take advantage of the distorted modelling approach. Developments may be in the direction

of pseudo-dynamic loading and the modelling and testing of the top part of the dam only.

REFERENCES

Aviles, J. and Sanchez-Sesma, F. (1989), "Water pressures on rigid gravity dams with finite reservoir during earthquakes", Earthquake Engineering and Structural Dynamics, Vol. 18, pp. 527-537.

Ayari, M. and Saouma, V. E. (1990), "A fracture mechanics based seismic analysis of concrete gravity dams using discrete cracks", Engineering Fracture Mechanics, Vol. 35, No. 1/2/3, pp. 587-598.

Bakhtin, B.M. and Dumenko, V.I. (1979). "Seismic stability of a concrete gravity dam having a light weight profile". Translated from Gidrotekhnicheskoe Stroitel'stro, No. 5, 17-21.

Barrett, P., Foadian, H. and Rashid, R. (1991), "Effect of cracking on damping of concrete dams", Lifeline Earthquake Engineering, Edited by Cassaro, M. A., ASCE, Monograph No.4.

Baumber, T. A. and Ghobarah, A. (1995), "Response of concrete gravity dam with finite reservoir to earthquake ground motion", Proceedings of the 7th Canadian Conference on

Earthquake Engineering, Montreal, Canada, pp. 349-356.

Bazant, P. and Oh, B. H. (1983),"Crack band theory for fracture of concrete", Materials & Structures, Vol. 16, No. 93, pp. 155-177.

Bhattacharjee S. S. and Léger, P. (1992), "Concrete constitutive models for nonlinear seismic analysis of concrete gravity dams– state-of-the-art", Canadian Journal of Civil Engineering, Vol. 19, pp. 492-509.

Bhattacharjee S. S. and Léger, P. (1993), "Seismic cracking and energy dissipation in concrete gravity dams", Earthquake Engineering and Structural Dynamics, Vol. 22, pp. 991-1007.

Bhattacharjee S. S. and Léger, P. (1994), "Application of NLFM models to predict cracking in concrete gravity dams", Journal of Structural Engineering, ASCE, Vol. 120, No. 4, pp. 1255-1271.

Bolzon, G., Cocchetti, G., Maier, G., Novati, G. and Giuseppetti, G. (1994), "Boundary element and finite element fracture analysis of dams by the cohesive crack model: A comparative study". Dam Fracture and Damage, edited by: Bourdarot, E., Mazars, J. and Saouma, V. C. Proceedings of the International Workshop on Dam Fracture and Damage, Chambery, France.

Borst, R. and Nauta, P. (1985), "Non-orthogonal cracks in a smeared finite element model", Engineering Computations, Vol 2, pp. 35-46.

Bruhwiler, E. and Wittmann, F. H. (1990), "Failure of dam concrete subjected to seismic loading conditions", Engineering Fracture Mechanics, Vol. 35, No.1/2/3, pp. 565-571.

Chopra, A. K. (1967), "Hydrodynamic Pressures on Dams during Earthquakes", Journal of Engineering Mechanics Division, ASCE 93 No. EM6, pp. 205-223.

Chopra, A. K. (1987), "Earthquake analysis, design, and safety evaluation of concrete dams", Proceedings of the Fifth Canadian Conference on Earthquake Engineering, Ottawa, Canada, 6-8 July, pp. 39-62.

Dam Safety Guidelines, (1996), Canadian Dam Safety Association, South Edmonton, Postal Station, Edmonton, Alberta, Canada, T6E 4X7.

Dancygier, A. N. (1995). "Qualitative evaluation of effect of gravity on small-scale modelling". Journal of Engineering Mechanics, ASCE, Vol. 121, No. 7, 773-778.

Donlon, W.P. (1989). "Experimental investigation of the nonlinear seismic response of concrete gravity dams." Earthquake Engineering Research Laboratory, Report No. EERL 89-01, California Institute of Technology, Pasadena, California.

Donlon, W.P. and Hall, J.F. (1991). " Shaking table study of concrete gravity dam monolith." Earthquake Engineering and Structural Dynamic, Vol. 20, 769-786.

El-Aidi, B. and Hall, J. F. (1989a), "Non-linear earthquake response of concrete gravity dams, Part 1: Modelling", Earthquake Engineering and Structural Dynamics, Vol. 18, pp. 837-851.

El-Aidi, B. and Hall, J. F. (1989b), "Non-linear earthquake response of concrete gravity dams, Part 2: Behaviour", Earthquake Engineering and Structural Dynamics, Vol. 18, pp. 853-865.

Felippa, C.A. and Park, K. C., (1980), "Staggered transient analysis procedures for coupled mechanical systems: Formulation", Computer Methods in Applied Mechanics and Engineering, Vol. 24, pp. 61-111.

Feltrin, G. Wepf, D. and Bachmann, H. (1990), "Seismic cracking of concrete gravity dams", Dam Engineering, Vol. I, Issue 4, pp. 279-289.

Fenves, G. and Chopra, A. K. (1984a), " EAGD-84 A computer program for earthquake analysis of concrete gravity dams", Earthquake Engineering Research Center, Report No. UCB/EERC-84/11, University of California, Berkeley, CA.

Fenves, G. and Chopra, A.K. (1984b), "Earthquake analysis and response of concrete gravity dams", Earthquake Engineering Research Center, Report No. UCB/EERC-84/10, University of California, Berkeley, CA.

Fenves, G. and Chopra, A. K. (1985). " Simplified Earthquake analysis of concrete gravity dams: separate hydrodynamic and foundation interaction effects." Journal of Structural Engineering, ASCE, Vol. 111, No. 6, 715-756.

Fenves, G. and Chopra, A. K. (1986). "Simplified analysis for earthquake resistant design of concrete gravity dams." Earthquake Engineering Research Center, Report No. UCB/EERC-85/10, University of California, Berkeley, California,

Fenves, G. and Chopra, A. K. (1987)." Simplified Earthquake analysis of concrete gravity dams." Journal of Structural Engineering, ASCE, Vol. 113, No. 8, 1688-1708.

Fenves, G., Mojtahedi, S. and Reimer, R. B. (1992), "Parameter study of joint opening effects on earthquake response of arch dams", Earthquake Engineering Research Center, University of California, Berkeley, Report No. UCB/EERC-92/05, April 1992, Berkeley, California.

Fenves, G. and Vargas-Loli, M. (1988), " Nonlinear dynamic analysis of fluid-structure systems", Journal of Engineering Mechanics, ASCE, Vol. 114, No. 2, pp. 219-240.

Filiatrault, A., Léger, P. and Tinawi, R. (1994),"On the computation of seismic energy in inelastic structures", Engineering Structures, Vol. 16, pp.425-436.

Flores Victoria, A., Herrera, I. and Lozano, C. (1969), "Hydrodynamic pressures generated by vertical earthquake component", Proceedings of the Fourth World Conference on Earthquake Engineering, Santiago, Chile, Vol. II, B-4, January 13-18, pp. 25-36.

Ghaemian, M. and Ghobarah, A. (1997), "Seismic response of the Sefid-rud concrete buttress dam" European Earthquake Engineering, Vol. XI, No. 1., pp. 3-15.

Ghrib, F. and Tinawi, R. (1995a), "An application of damage mechanics for seismic analysis of concrete gravity dams", Earthquake Engineering and Structural Dynamics, Vol. 24, pp. 157-173.

Ghrib, F. and Tinawi, R. (1995b), "Nonlinear behaviour of concrete dams using damage mechanics", Journal of Engineering Mechanics, ASCE, Vol. 121, No. 4, pp. 513-527.

Gutidze, P.A. (1985). "Model investigations of seismic action on the concrete arch dam of the Inguri Hydroelectrical Station." Translated from Gidrotekhnicheskoe Stroitel'stro, No. 11, 26-30.

Hall, J.F. and Chopra, A.K. (1979), "A transmitting boundary for analysis of hydrodynamic

pressures in bounded domain", ASCE-EMD, Third Annual Meeting, Austin, Texas, Sept. 17-19, pp. 475-478.

Hall, J.F. and Chopra, A.K. (1982), "Two-dimensional dynamic analysis of concrete gravity and embankment dams including hydrodynamic effects", Earthquake Engineering and Structural Dynamics, Vol. 10, pp. 305-332.

Hanna, Y. G., and Humar, J. L. (1982), "Boundary Element Analysis of Fluid Domain", Journal of Engineering Mechanics division, ASCE 108, No. EM2, pp. 436-450.

Hilber, H. M. and Hughes, T. J. R. (1978), "Collocation, dissipation and overshoot for time integration schemes in structural dynamics", Earthquake Engineering and Structural Dynamics, Vol. 6, pp. 99-117.

Hilber, H. M., Hughes, T. J. R. and Taylor, R. T. (1977), "Improved numerical dissipation for time integration algorithms in structural dynamics', Earthquake Engineering and Structural Dynamics, Vol. 5, pp. 283-292.

Huang, M. (1995), "New developments in numerical analysis of dynamic and static soil problems", Ph.D. Thesis, University of Wales Swansea, Department of Civil Engineering, C/Ph/185.

Hughes, T. J. R. (1987), "The Finite Element Method, Linear static and dynamic analysis", Prentice-Hall, Inc., Englewood Cliffs, New Jersey.

Humar, J. and Roufaiel, M. (1983), "Finite Element Analysis of Reservoir Vibration", Journal of Engineering Mechanics Division, ASCE, Vol.109, No.1, pp. 215-230.

Kojic, S. B. and Trifunac, M. D. (1991a), "Earthquake stresses in Arch dams. I: Theory and antiplane excitation", Journal of Engineering Mechanics Division, ASCE, Vol. 117, pp. 532-552.

Kojic, S. B. and Trifunac, M. D. (1991b), "Earthquake stresses in Arch dams. II: Excitation by SV-,P-, and Rayleigh waves", Journal of Engineering Mechanics Division, ASCE, Vol. 117, pp. 553-574.

Kuo, J. S-H. (1982), "Joint opening nonlinear mechanism: interface smeared crack model", Earthquake Engineering Research Center, University of California, Berkeley, California, Report No. UCB/EERC-82/10, April 1982.

Léger, P. and Bhattacharjee S. S. (1992), "Reduced frequency-independent models for seismic analysis of concrete gravity dam", Computers & Structures, Vol. 44, No. 6, pp. 1381-1387.

Léger, P. and Bhattacharjee S. S. (1994), "Energy concepts in seismic fracture analysis of concrete gravity dams", Dam Fracture and Damage, Edited by Bourdarot, E., Mazars, J. and Saouma, V., Proceedings of the International Workshop on Dam Fracture and Damage, Chambery, France, 16-18 March 1994.

Léger, P. and Bhattacharjee S. S. (1995), "Seismic fracture analysis of concrete gravity dams", Canadian Journal of Civil Engineering, Vol. 22, No. 1, pp. 196-201

Léger, P. and Leclerc, M. (1996), "Evaluation of earthquake ground motions to predict cracking response of gravity dams", Engineering Structures, Vol. 18, No. 3, pp. 227-239.

Lyatkher, V.M. and Kaptsan, A.D. and Semenov, I.V. (1977). "Seismic stability of the Toktogul dam." Translated from Gidrotekhnicheskoe Stroitel'stro, No. 5, 8-14.

Mir, R. Z. and Taylor, C. A. (1995). "An experimental investigation into earthquake-induced failure of medium to low height concrete gravity dams." Earthquake Engineering and Structural Dynamics, Vol. 24, 373-393.

Mir, R. Z. and Taylor, C. A. (1996). "An investigation into the base sliding response of rigid concrete gravity dams to dynamic loading." Earthquake Engineering and Structural Dynamics, Vol. 25, 79-98.

Mlakar, P. F. (1987), "Nonlinear response of concrete gravity dams to strong earthquake-induced ground motion", Computers & Structures, Vol. 26, No. ½, pp. 165-173.

Niwa, A. and Clough, R.W. (1980). "Shaking table research on concrete dam models." Earthquake Engineering Research Center, Report No. UCB/EERC-80/05. University of California, Berkeley, California.

Norman, C.D. (1986). "Dynamic Failure tests and analysis of a model concrete dam." Department of the Army, Waterways Experiment Station, Corps of Engineers, Technical report SL-86-33, Vicksburg, Mississippi.

Nowak, P. S. and Hall, J. F. (1990), "Arch dam response to nonuniform seismic input", Journal of Engineering Mechanics Division, ASCE, Vol. 116, pp. 125-139.

Oberti,G. and Lauletta, E. (1960). "Dynamic tests on models of structures." Proceeding of the Second World Conference on Earthquake Engineering, Tokyo, Vol. 2, 947-960.

Oberti,G. and Lauletta, E. (1967). "Structural models for the study of dam earthquake resistance." Proceedings of the Ninth Congress on Large Dams, Istanbul, Turkey, 431-442.

Park, K. C. (1980), "Partitioned transient analysis procedures for coupled-field problems: Stability analysis", Journal of Applied Mechanics, ASCE, Vol. 47, pp. 370-376.

Park, K. C. and Felippa, C. A. (1980), "Partitioned transient analysis procedures for coupled-field problems: Accuracy analysis", Journal of Applied Mechanics, ASCE, Vol. 47, pp. 919-926.

Park, K. C. and Felippa, C. A. (1984), "Recent Developments in coupled field analysis methods", Chapter 11 of Numerical Methods in Coupled Systems, Edited by Lewis, R. W., Bettes, P. and Hinton, E, John Wiley & Sons.

Paul, D. K., Zienkiewicz, O. C. and Hinton, E. (1981), "Transient dynamic analysis of reservoir-dam interaction using staggered solution schemes", Numerical Methods for Coupled Problems, Edited by Hinton, E., Bettes, P. and Lewis, R. W., Pineridge Press, Swansea.

Paultre, P. and Proulx, J. (1995), "Large scale dynamic tests", Proceedings of the 7th Canadian Conference on Earthquake Engineering, Montreal, Canada, pp. 665-672.

Pekau, O. A. and Batta, V. (1991), "Seismic crack propagation in concrete gravity dams", Proceedings of the 6th Canadian Conference on Earthquake Engineering, Toronto, pp. 197-204.

Pekau, O. A., Chuhan, Z. and Lingming, F. (1991), "Seismic fracture analysis of concrete gravity dams", Earthquake Engineering and Structural Dynamics, Vol. 20, pp. 335-354.

Pekau, O. A., Lingming, F. and Chuhan, Z. (1995), "Seismic fracture of Koyna dam : case study", Earthquake Engineering and Structural Dynamics, Vol. 24, pp. 15-33.

Pellegrini, R., Imperato, L., Torda, M., Ferrara, G., Mazza, G. and Morabito, P. (1994), "Physical and mathematical models for the study of crack activation in concrete dams". Dam Fracture and Damage, edited by: Bourdarot, E., Mazars, J. and Saouma, V. C., Proceedings of the International Workshop on Dam Fracture and Damage, Chambery, France.

Plizzari, G. A., Saouma, V. C. and Waggoner, F. A. (1994), "Experimental study of concrete gravity dams in a centrifuge", Dam Fracture and Damage, edited by: Bourdarot, E., Mazars, J. and Saouma, V. C. Proceedings of the International Workshop on Dam Fracture and Damage, Chambery, France.

Ramadan, O. and Novak, M. (1992), "Dam response to spatially variable seismic ground motions- Part I: Analytical model; Part II: Parametric study", Geotechnical Research Center, Faculty of Engineering Science, The University of Western Ontario, London, Canada, Report No. GEOT-14-92, October 1992.

Raphael J.M. (1963), "Properties of plaster celite mixtures for models", Symposium on concrete dams models, Lisbon, Portugal, Paper No.15, 1-30.

Rea, D., Liaw, C-Y. and Chopra, A. K. (1975) ,"Mathematical models for the dynamic

analysis of concrete gravity dams", Earthquake Engineering and Structural Dynamics, Vol. 3, pp. 249-258.

Renzi, R., Ferrara, G. and Mazza, G., (1994), "Cracking in a concrete gravity dam: A centrifugal investigation". Dam Fracture and Damage, edited by: Bourdarot, E., Mazars, J. and Saouma, V. C. Proceedings of the International Workshop on Dam Fracture and Damage, Chambery, France.

Rescher, O. (1990), "Importance of cracking in concrete dams", Engineering Fracture Mechanics, Vol. 35, No.1/2/3, pp. 503-524.

Saouma, V. E. and Broz, J. J. and Boggs, H. L. (1991), "In situ field testing for fracture properties of dam concrete", Journal of Materials in Civil Engineering, Vol. 3, No. 3, pp. 219-234.

Shames, I.H. (1982) Mechanics of fluids". Second edition, McGraw-Hill International, NewYork.

Sharan, S. (1985a), "Finite Element Analysis of Unbounded and Incompressible Fluid Domains", International Journal for Numerical Methods in Engineering, Vol. 21, pp. 1659-1669.

Sharan, S. (1985b), "Finite Element Modelling of Infinite Reservoirs", Journal of Engineering Mechanics Divisions ASCE, Vol. 111, No. 12, pp. 1457-1469.

Sharan, S. (1986), "Modelling of radiation damping in fluids by finite elements", International Journal for Numerical Methods in Engineering, Vol. 23, pp. 945-957.

Sharan, S. (1987), "Time-Domain Analysis of Infinite Fluid Vibration", International Journal for Numerical Methods in Engineering, Vol. 24, pp. 945-958.

Singhal, A. C. (1991), "Comparison of computer codes for seismic analysis of dams", Computers & Structures, Vol. 38, No. 1, pp. 107-112.

Skrikerud, P. and Bachmann, H. (1986), "Discrete crack modelling for dynamically loaded, unreinforced concrete structures", Earthquake Engineering and Structural Dynamics, Vol. 14, pp. 297-315.

Tinawi, R. and Guizani, L. (1994), "Formulation of hydrodynamic pressures in cracks due to earthquakes in concrete dams", Earthquake Engineering and Structural Dynamics, Vol. 23, pp. 669-715.

Tsai, C. S. and Lee, G. C. (1990), " Method for transient analysis of three dimensional dam-reservoir interaction", Journal of Engineering Mechanics Division, ASCE, Vol. 116, pp.

2151-2172.

Uang, C. and Bertero, V. V. (1990) ,"Evaluation of seismic energy in structures", Earthquake Engineering and Structural Dynamics, Vol. 19, pp. 77-90.

Valente, S., Barpi, F., Ferrara,G. And Giuseppetti, G. (1994), "Numerical simulation of centrifuge tests on prenotched gravity dam model", Dam Fracture and Damage, Edited by: Bourdarot, E., Mazars, J. And Saouma, V. C., Proceedings of the International Workshop on Dam Fracture and Damage, Chambery, France, 16-18 March, 1994.

Wepf, D., Feltrin, G. and Bachmann, H. (1993), "Influence of time-domain dam-reservoir interaction on cracking of concrete gravity dams", Earthquake Engineering and Structural Dynamics, Vol. 22, pp. 573-582.

Westergaard, H. M. (1933), "Water Pressures on Dams During Earthquakes", Transactions, ASCE, Vol. 98, pp. 418-433.

Wood, W. L. (1990), "Practical Time-Stepping Schemes", Clarendon Press, Oxford.

Yang, R., Tsai, C. S. and Lee, G. C. (1991), "Time domain analyses of dam-reservoir system, II: substructure method", Journal of Engineering Mechanics, ASCE 117, No. 9, pp. 2007-2026.

Yang, R., Tsai, C. S. and Lee, G. C. (1993), "Explicit time-domain transmitting boundary for dam-reservoir interaction analysis", International Journal for Numerical Methods in Engineering, Vol. 136, pp. 1789-1804.

Yoshida, T. and Baba, K. (1965), "Dynamic response of dams", Proceeding of the Third World Conference on Earthquake Engineering, Auckland, New Zealand, Vol. II, pp. 748-764.

Zienkiewicz, O. C. (1984), "Coupled problems and their numerical solution", Chapter one Numerical Methods in Coupled Systems, Edited by Lewis, R. W., Bettes, P. and Hinton, E, John Wiley & Sons.

Zienkiewicz, O. C. and Chan, A. H. C. (1989), "Coupled problems and their numerical solution", Chapter four, Advances in Computational Nonlinear Mechanics, Edited by Doltsinis, I. St., Springer-Verlag, Wien- New York.

Zienkiewicz, O. C. and Newton, R. E. (1969), "Coupled vibrations of a structure submerged in a compressible fluid", Proceeding of the Symposium on Finite Element Techniques held at the Institute Für Statiund, University of Stutgart, Germany, June 10-12, pp. 359-379.

Zienkiewicz, O. C. and Taylor, R. L. (1989), "Finite Element Method", 4th Edition, Volume 2, McGraw Hill Book Company, London.